

University of Central Lancashire

***Equine Spermatogenesis:
Meiotic Chromosome Behavior and
Recombination***

By

Ayman Ismail Al-Jaru

A thesis submitted in partial fulfillment for the requirements for the degree of Doctor of Philosophy at the University of Central Lancashire

September 2010

DECLARATION

I declare that while registered as a candidate for the research degree, I have not been a registered candidate or enrolled student for another award of the university or other academic or professional institution.

Signed ----- Date-----

Ayman I. Al-Jaru

Abstract

Studying the spermatogenesis of horse is beneficial for the horse industry by identifying the causes of chromosomal abnormalities, which cause embryonic loss, congenital abnormalities and infertility. Little is known about the spermatogenesis in horse. This is the first report that investigates the horse spermatogenesis in detail, particularly metaphase I (MI) and prophase I (PI) stages of the first meiotic division.

Meiotic recombination is considered to be the major outcome of meiosis. It is essential for proper chromosome segregation and formation of normal haploid gametes. Analysis of recombination frequency and distribution are crucial for genomic and association studies. Any alteration of the recombination frequency and positioning can cause non-disjunction and generation of aneuploidy.

The frequency and distribution of chiasmata were estimated at MI chromosomes from fourteen fertile stallions. The average frequency of autosomal chiasmata was 49.45 ± 2.07 , corresponding to a genetic length of 2,472.5 cM. All autosomal bivalents had at least one chiasma. The majority of chromosomes have one or two chiasmata, which are mostly distally localized. The frequency and the distribution as well as the genetic length of chiasmata were also estimated for the first time in eight different individual autosomes.

Immunofluorescent localization was used to characterize the early stages of the first meiotic division as well as to examine the frequency and the distribution of DNA mismatch repair protein MutL Homologous Protein 1 (MLH1) foci on synaptonemal complexes (SCs) from sex fertile stallions. The mean frequency of autosomal recombination foci was 50.11 ± 2.35 . All autosomal bivalents had at least one recombination focus. In general, foci were located near the distal ends with some foci interstitially distributed. The distribution of MLH1 foci indicated positive interference; however, foci were very close to one another in rare instances. The average SCs relative length was highly correlated with the average number of MLH1 foci. MLH1 have been proposed to mark crossover sites at PI since the frequency and distribution of MLH1 foci closely correspond to the frequency and distribution of chiasmata on MI chromosomes.

Spermatozoa viability, which include spermatozoa head and tail membrane integrity, acrosomal integrity and mitochondrial function assessment are the main sperm analysis parameters considered in this thesis to evaluate the stallion fertility using epididymal collected semen samples. The mean percentage of spermatozoa with viable heads and tails, using Chicago sky blue stain, was 81.26 ± 5.06 . FITC-*Pisum sativum agglutinin* (FITC-PSA) and MitoTracer green were used successfully to assess the spermatozoal acrosomal status as well as the mitochondrial function, respectively. The mean percentage of spermatozoa with integrated acrosome was 93.85 ± 1.9 , while for functional mitochondria was 95.63 ± 1.63 .

In conclusion, this finding is the cornerstone to understanding the genetic basis of normal horse spermatogenesis. Simultaneous assessment of different functional sperm parameters as well as investigating the synapsis and recombination frequency and distribution, at PI or MI, would assist with predictions of stallion fertility prior to breeding. In addition, this study will enable investigators to use linkage analysis in identifying and localising different genetic loci associated with specific traits.

*To God
For Giving Me Great Parents*

*To My Parents
For Encouraging Me to Overcome All The
Difficulties*

*To My Wife
For Her Support and Love*

*To My Family and Friends
For Their Help*

I am Grateful To All of You

Acknowledgment

All thanks are due to Allah, the creator, who has power over all things.

There are a number of people who supported me during my research project. I would like to express my deepest and profound acknowledgement to His Highness Sheikh Mohammed Bin Rashid for his financial support to conduct this project. I would like to thank Dr Ali Ridah, administrative director of CVRL, for approving my PhD and supporting me during my study with which I could not achieve my PhD.

I would like to thank my supervisor Dr William Goodwin who has provided me with guidance and advice throughout the course of my PhD project. I am greatly indebted to my supervisor Dr Kamal Kazanahdari, Head of MBG lab, for his continuous and generous suggestions, encouragement and endless patience throughout this project. Also I would like to thank Dr. Julian Skidmore for revision of the thesis and offering her valuable comments that enriched this work. Many thanks go to Professor Jaipaul Singh for his advice and valuable help.

I would like to thank Dr Ulli Wernarry, scientific director of CVRL, for his support and help. Also I would like to express my appreciation for Dr Morgane Schambourg, Sharjah Equine Hospital and Mr Abdullah Al Mutari, Administrative director of Dubai Equine Hospital, for supplying me with horse testicular samples.

Special acknowledgement is owed to a number of friends and colleagues in the CVRL, particularly MBG lab, who have supported me especially Faysal Abdelshakur, Rana El-Nabulsi, Motasem Ismail, Mai Shihadah, Dr Osman Jafer and Shazia Salim. I would like to extend my thanks to other colleagues in MBG lab Noushad Karuvantevida, Fazle Ali, Fatima Abidi, Fatima Hakimuddin, Lalie Detal, Husna Maliakkal, Ramida Moossa, Li Changlu, Xin Huang and Wenhai Lee for their kindness and friendly understanding. Errol Bagaipo and Sajid Iqbal have also added to the luster of this manuscript by providing their experience in statistical analysis, revising the print quality and cooperation.

Many thanks go to my best friends, Ayman Eideh and Zaid Abu Rubaiha, for their support and encouragement.

Very big thanks go to my family. I am forever indebted to my parents and my wife for their love, support and encouragement. Thanks are also due to my brothers, and sisters for their inspiration

Finally, I sincerely apologize for any unintended omissions.

Table of Content

DECLARATION	I
ABSTRACT	II
ACKNOWLEDGMENT	V
TABLE OF CONTENT	VIII
LIST OF FIGURES	X
LIST OF TABLES	XIII
CHAPTER 1	1
INTRODUCTION	1
1.1. BACKGROUND	1
1.2. SPERMATOOZOA FORMATION.....	4
1.2.1. Spermatogoniogenesis	6
1.2.2. Spermatogenesis	6
1.2.3. Spermiogenesis	7
1.2.4. Efficiency of Spermatogenesis.....	8
1.3. MEIOSIS	9
1.3.1. Prophase I (PI)	10
1.3.1.1. Homologous Pairing.....	11
1.3.1.2. Synaptonemal Complex	13
1.3.1.3. Factors influence homologue recognition and initiation of pairing	16
1.3.1.3.1. Chromatin Organisation	16
1.3.1.3.2. Repeated DNA Sequences	17
1.3.1.4. Recombination	19
1.3.1.4.1. Double Strand Breaks (DSBs).....	20
1.3.1.4.2. Recombination Nodules	25
1.3.1.4.3. Recombination Frequency and Distribution.....	27
1.3.1.5. Chromosome Synapsis	29
1.3.2. Metaphase I (MI)	31
1.3.2.1. Chiasmata.....	32
1.3.3. Anaphase I (AI) and Telophase I (TI)	33
1.3.4. Meiotic Division II	34
1.3.5. Meiotic Checkpoint	35
CHAPTER 2	43
METAPHASE I: CHROMOSOME CONFIGURATION, CHIASMATA DISTRIBUTION AND FREQUENCY	43
2.1. INTRODUCTION	43
2.2. MATERIALS AND METHODS	45
2.2.1. Materials.....	45
2.1.1.1. Mouse material.....	45
2.1.1.2. Equine material	45
2.2.2. Methods.....	45
2.2.2.1. Testicular Gross Examination	45
2.2.2.2. Meiotic Analysis Methods.....	45
2.2.2.3. Direct Microscopic Examination.....	46
2.2.2.4. Air Dry Technique (Metaphase I)	46
2.2.2.5. Meiotic Chromosomes Individual Identification	46
2.2.2.6. Statistical Analysis	48
2.3. RESULT	49
2.3.1. Mouse testicular samples	49

2.3.2. <i>Horse testicular samples</i>	51
2.3.2.1. Gross and Direct microscopic examination.....	51
2.3.2.2. Air dry technique (MI).....	52
2.3.2.2.3. Spermatogenesis cell stages.....	52
2.3.2.2.2. Chiasmata frequency and distribution.....	60
2.3.2.3. Chiasmata Distribution on 8 Different Horse Chromosomes.....	67
2.4. DISCUSSION.....	76
CHAPTER 3.....	82
PROPHASE I: HOMOLOGOUS PAIRING AND RECOMBINATION FREQUENCY.....	82
3.1. INTRODUCTION.....	82
3.2. MATERIALS AND METHODS.....	84
3.2.1. <i>Surface Spreading Technique (Prophase I)</i>	84
3.2.1.1. Lipsol spreading for equine meiotic chromosomes.....	84
3.2.1.2. Sucrose spreading for equine meiotic chromosomes.....	84
3.2.1.3. Electron Microscopy Spreading for Meiotic Chromosomes.....	85
3.2.2. <i>Silver Staining</i>	85
3.2.3. <i>Immunostaining of Meiotic Spreads</i>	86
3.2.4. <i>Localization of MLH1 foci to synaptonemal complex</i>	86
3.2.5. <i>Statistical Analysis:</i>	87
3.3. RESULTS:.....	87
3.3.1. <i>Mouse prophase I sub-stages</i>	87
3.3.2. <i>Horse prophase I sub-stages</i>	89
3.3.3. <i>Light and electron microscopy spreading for prophase I</i>	93
3.3.4. <i>MLH1 Foci frequency and distribution</i>	98
3.3.5. <i>Localization of MLH1 foci to synaptonemal complex</i>	109
3.4. DISCUSSION.....	112
CHAPTER 4.....	118
VIABILITY OF STALLION SPERMATOZOA.....	118
4.1. INTRODUCTION.....	118
4.2. MATERIALS AND METHODS.....	121
4.2.1. <i>Spermatozoa Viability Test</i>	121
4.2.2. <i>Assessment of Spermatozoa: Acrosome Integrity</i>	121
4.2.3. <i>Assessment of Spermatozoa: Mitochondrial Function</i>	122
4.2.4. <i>Statistical Analysis</i>	122
4.3. RESULTS.....	123
4.3.1. <i>Sperm viability</i>	123
4.3.2. <i>Spermatozoa Acrosome Integrity</i>	130
4.3.3. <i>Spermatozoa Mitochondrial Function</i>	134
4.4. DISCUSSION.....	137
CHAPTER 5.....	141
GENERAL DISCUSSION.....	141
REFERENCES.....	148
APPENDICES.....	169

List of Figures

Chapter 1

Figure 1.1: Standard karyotype for the horse male	3
Figure 1.2: Section of stallion germinal epithelium in the seminiferous tubule.....	5
Figure 1.3: Diagram of synaptonemal complex (SC).....	14
Figure 1.4: Molecular events of DSB repair model of meiotic recombination.....	24

Chapter 2

Figure 2.1: Primary spermatocytes (MI) preparations from normal mice.....	49
Figure 2.2: Primary spermatocyte diakinesis preparation from normal mouse male.....	49
Figure 2.3: Spermatogonial metaphase from normal mouse male preparation.....	50
Figure 2.4: Different primary spermatocyte metaphase I (MI) preparations from different normal stallions.....	53
Figure 2.5: Different primary spermatocyte metaphase preparations from normal stallions.....	54
Figure 2.6: Different primary spermatocyte diakinesis preparations from 4 different normal stallions.....	55
Figure 2.7: Second meiotic metaphase (MII) preparations from 4 different normal stallions.....	56
Figure 2.8: Pre-meiotic mitotic metaphase (spermatogonial metaphase) preparations from 4 different normal stallions.....	57
Figure 2.9: Prophase I (PI) preparations from 4 different normal stallions.....	58
Figure 2.10 Sertoli cells with from 3 different stallions.....	59
Figure 2.11: Autosomal bivalents frequency with 1-4 chiasmata among 14 stallions.....	66
Figure 2.12: Subsequent FISH analysis for chromosome 10.....	68
Figure 2.13: Subsequent FISH analysis for chromosome 6.....	69
Figure 2.14: Subsequent FISH analysis for chromosome 6 and 31.....	70

Figure 2.15: Subsequent FISH analysis for chromosome 10 and 13.....	71
Figure 2.16: Chiasmata frequency in 8 chromosomes (2, 6, 10, 13, 15, 24, 26 and 31) among 5 stallions.....	75

Chapter 3

Figure 3.1: Surface spread mice spermatocytes labeled with anti-SCP3 (green) and anti-CREST (blue).....	88
Figure 3.2: Surface spread mouse spermatocytes labeled with anti-SCP3 (green)....	88
Figure 3.3: Surface spread of horse spermatocytes labeled with anti-SCP3 (red).....	90
Figure 3.4: Surface spread of horse spermatocytes labeled with anti-SCP3 (red). Zygotene stage nuclei in which the lateral elements are partially synapse.....	91
Figure 3.5: Surface spread of horse spermatocytes labeled with anti-SCP3 (red). Pachytene stage in which the two lateral are fully synpse.....	92
Figure 3.6: Light microscopy for meiotic prophase I of silver-stained preparations of stallion spermatocytes.....	94
Figure 3.7: An EM surface spread preparation of fully paired horse male pachytene nucleus.....	95
Figure 3.8: Another example of EM surface spread preparation of fully paired horse male pachytene nucleus.....	96
Figure 3.9: An EM surface spread preparation of different stages of PI horse male.....	97
Figure 3.10: SC spreading from horse spermatocytes at pachytene stage labelled with anti-SCP3 antibody (red) and anti-MLH1 antibody (green).....	100
Figure 3.11: SC spreading from horse spermatocytes at pachytene stage labelled with anti-SCP3 antibody (red) and anti-MLH1 antibody (green).....	101
Figure 3.12: Autosomal bivalents frequency with 1-4 MLH1 foci among 6 stallions.....	108
Figure 3.13: Correlation between the average SCs relative length and the average number of MLH1 foci.....	111

Chapter 4

Figure 4.1: Stallion spermatozoa stained with Chicago sky blue staining	124
Figure 4.2: Stallion spermatozoa stained with Chicago sky blue staining to visualise morphological abnormalities.....	125
Figure 4.3: Fluorescence microscopy method. Stallion spermatozoa labelled with acrosomal stain (FITC-PSA).....	131
Figure 4.4: Fluorescent microscopy method: Morphological abnormalities.....	132
Figure 4.5: Fluorescence microscopy method to analyze stallion spermatozoa labelled with mitochondria stain (MitoTracer Green) and DNA stain (Hoechst 33342).....	135

List of Tables

Chapter 2

Table 2.1: Probes for different horse chromosome.....	48
Table 2.2: Descriptions of materials used in this study.....	51
Table 2.3a: Autosomal bivalent frequency with 1 chiasma among 14 stallions.....	61
Table 2.3b: ANOVA table for autosomal bivalent frequency with 1 chiasma among 14 stallions.....	61
Table 2.4a: Autosomal bivalent frequency with 2 chiasmata among 14 stallions...	62
Table 2.4b: ANOVA table for autosomal bivalent frequency with 2 chiasmata among 14 stallions.....	62
Table 2.5a: Autosomal bivalent frequency with 3 chiasmata among 14 stallions...	63
Table 2.5b: ANOVA table for autosomal bivalent frequency with 3 chiasmata among 14 stallions.....	63
Table 2.6a: Autosomal bivalent frequency with 4 chiasmata among 14 stallions...	64
Table 2.6b: ANOVA table for autosomal bivalent frequency with 4 chiasmata among 14 stallions.....	64
Table 2.7a: Chiasmata frequency in autosomal bivalents per cell among 14 stallions.....	65
Table 2.7b: ANOVA table for chiasmata frequency in autosomal bivalents per cell among 14 stallions.....	65
Table 2.8a: Chiasmata frequency in chromosome 2 among 5 stallions.....	72
Table 2.8b: ANOVA table for chiasmata frequency in chromosome 2 among 5 stallions.....	72
Table 2.9a: Chiasmata frequency in chromosome 13 among 5 stallions.....	73
Table 2.9b: ANOVA table for chiasmata frequency in chromosome 13 among 5 stallions.....	73
Table 2.10a: Chiasmata frequency in chromosome 24 among 5 stallions.....	74
Table 2.10b: ANOVA table for chiasmata frequency in chromosome 24 among 5 stallions.....	74
Table 2.11: Chiasmata frequency in 8 individual chromosomes (2, 6, 10, 13, 15, 24, 26 and 31) among 5 stallions.....	75

Table 2.12: Average chiasmata frequency per cell for different species.....	80
Table 2.13: Mean chiasmata number in human males reported from different studies.....	80
Table 2.14: Chiasmata frequency and the genetic length of 8 individual chromosomes (2, 6, 10, 13, 15, 24, 26 and 31) among 5 stallions.....	81

Chapter 3

Table 3.1a: Autosomal SCs frequency with one MLH1 focus among 6 stallions...	102
Table 3.1b: ANOVA table for autosomal SCs frequency with one MLH1 focus among 6 stallions.....	102
Table 3.2a: Autosomal SCs frequency with two MLH1 foci among 6 stallions....	103
Table 3.2b: ANOVA table for autosomal SCs frequency with two MLH1 foci among 6 stallions.....	103
Table 3.3a: Autosomal SCs frequency with three MLH1 foci among 6 stallions...	104
Table 3.3b: ANOVA table for autosomal SCs frequency with three MLH1 foci among 6 stallions.....	104
Table 3.4a: Autosomal SCs frequency with four MLH1 foci among 6 stallions...	105
Table 3.4b: ANOVA table for autosomal SCs frequency with four MLH1 foci among 6 stallions.....	105
Table 3.5a: MLH1 foci frequency in autosomal SCs per cell among 6 stallions....	106
Table 3.5b: ANOVA table for MLH1 foci frequency in autosomal SCs per cell among 6 stallions.....	106
Table 3.6a: MLH1 foci frequency in autosomal SCs per cell among 6 stallions....	107
Table 3.6b: ANOVA table for MLH1 focus frequency in autosomal SCs per cell among 6 stallions.....	107
Table 3.7: Average absolute and relative lengths of stallion autosomal SCs.....	110
Table 3.8: The minimum absolute and relative distances between any two MLH1 foci among SCs with 4, 3 and 2 foci.....	111
Table 3.9: Average MLH1 frequency per spermatocyte for different species.....	117

Chapter 4

Table 4.1a: Viability test of spermatozoa with live heads and tails among 13 stallions.....	126
Table 4.1b: ANOVA test for viability of spermatozoa with live heads and tails among 13 stallions.....	126
Table 4.2a: Viability test of spermatozoa with dead heads and tails among 13 stallions.....	127
Table 4.2b: ANOVA test for viability of spermatozoa with dead heads and tails among 13 stallions.....	127
Table 4.3a: Viability test of spermatozoa with dead heads and live tails among 13 stallions.....	128
Table 4.3b: ANOVA test for viability of spermatozoa with dead heads and live tails among 13 stallions.....	128
Table 4.4a: Viability test of spermatozoa with dead heads and live tails among 13 stallions.....	129
Table 4.4b: ANOVA test for viability of spermatozoa with dead heads and live tails among 13 stallions.....	129
Table 4.5a: Acrosome integrity test of spermatozoa with intact acrosome among 8 stallions.....	133
Table 4.5b: ANOVA test for acrosome integrity test of spermatozoa with intact acrosome among 8 stallions.....	133
Table 4.6a: Mitochondrial function test of spermatozoa with functional mitochondria among 8 stallions.....	136
Table 4.6b: ANOVA test for mitochondrial function test of spermatozoa with functional mitochondria among 8 stallions.....	136

Chapter 1

Introduction

1.1. Background

The horse, as we know today, is the result of evolutionary changes over many years. The first evidence for the existence of the horse is found in North America from where it is believed to migrate to the rest of the world such as Europe, Asia and Africa (Morel, 1999). Horses were domesticated first in the areas of China and Mesopotamia (Morel, 1999) and belong to one species, *Equus caballus* (Evans, 1992) that has different breeds, a few of which are: Thoroughbred, Arabian, Andalusian, Akhal-teke, Quarterhorse, Icelandic Pony and Standardbred.

The horse has played a key role in the history of man and civilizations by providing a means for transportation and service of utility (Russell, 2007). The first breeding, in the Near East about 3500 years ago, began when man discovered that he could influence the characteristics of any offspring by selecting appropriate stallions and mares; this led to development of animals suitable for different needs. Selective breeding of horses then became more widespread in various parts of the world. Selective breeding changed at the beginning of the last century from selecting for power and transport to focus on the selection of traits suitable for sport and leisure, such as hunting, racing and riding (Morel, 1999).

Horse management from an early age is important to minimize any risk of injury and to protect its well being and reproductive potential. A stallion with a desirable trait can sire many foals in a single year and the demand is very high especially for a horse with a good performing record or conformation characteristics (Morel, 1999). Thus, early detection of horse fertility problems can allow management changes, such as managing the frequency of breeding and/or increasing the frequency of examinations of the mares so they are bred only once close to ovulation thereby prolonging the fertility of stallions (Samper, 2009).

1.1.1. Basic Horse Genetics

The standard domestic horse karyotype was agreed in 1989 at the Second International Conference for Standardization of Domestic Animal Karyotypes. The domestic horse has 31 autosomal chromosome pairs, in addition to sex chromosomes, X and Y. Among the 31 autosomal chromosome pairs, 13 are metacentric or submetacentric, and 18 are acrocentric. For the sex chromosomes, the X chromosome is the second largest metacentric while the Y chromosome is one of the smallest acrocentric chromosomes (Evans, 1992; Bowling *et al.*, 1997) (Figure 1.1).

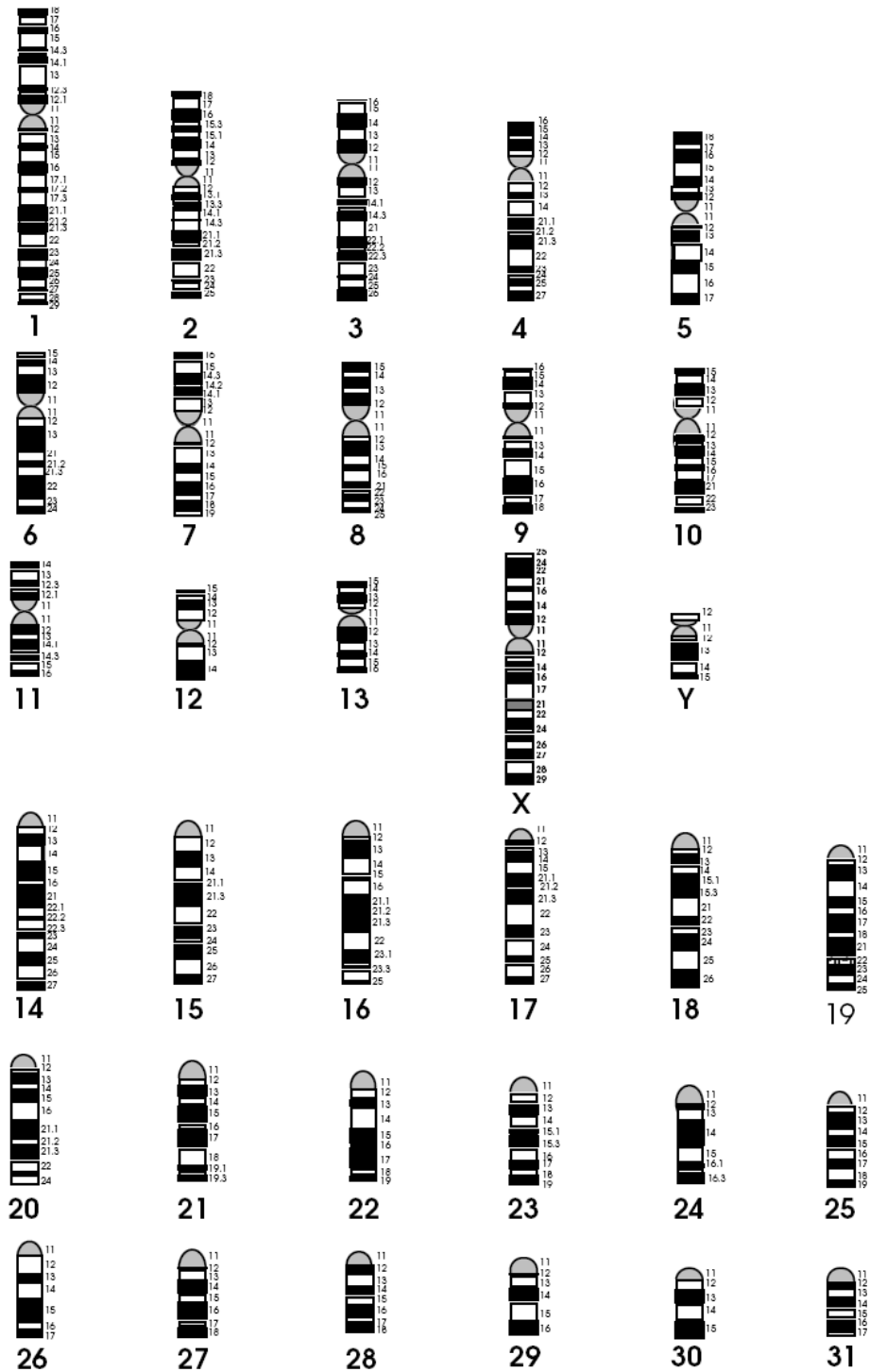


Figure 1.1: Standard karyotype for the horse male as defined by the International System for Cytogenetic Nomenclature of the Domestic Horse (ISCNH 1997).

1.2. Spermatozoa formation

Spermatozoa formation occurs in the testis in the seminiferous epithelium. It begins at puberty, after a long preparatory period, and continues throughout life until old age, the products of which are the mature germ cells, namely spermatozoa (Holstein *et al.*, 2003). The ultimate purpose of this process is to generate a vehicle for the transmission of the paternal genome into the female gamete, the oocyte, at fertilization. Each species of animal has specific sperm morphology varying in the shape, size and density of the nucleus (de Jonge & Barratt, 2006).

Spermatozoa formation starts with the mitotic division of spermatogonia during which DNA replicates and cell division results in a continuous source of cells for sperm production through meiosis. The subsequent meiotic divisions consist of two successive cell divisions of spermatocytes, following one round of DNA replication, giving rise to four haploid cells, spermatids (Bruce *et al.*, 1994).

Spermatozoa formation is a complex process that is regulated by many genes. Some of these genes are located on the Y chromosome while the rest are located on autosomes (Seshagiri, 2001). Three major stages of spermatozoa formation are: spermatogoniogenesis, spermatogenesis and spermiogenesis (Figure 1.2).

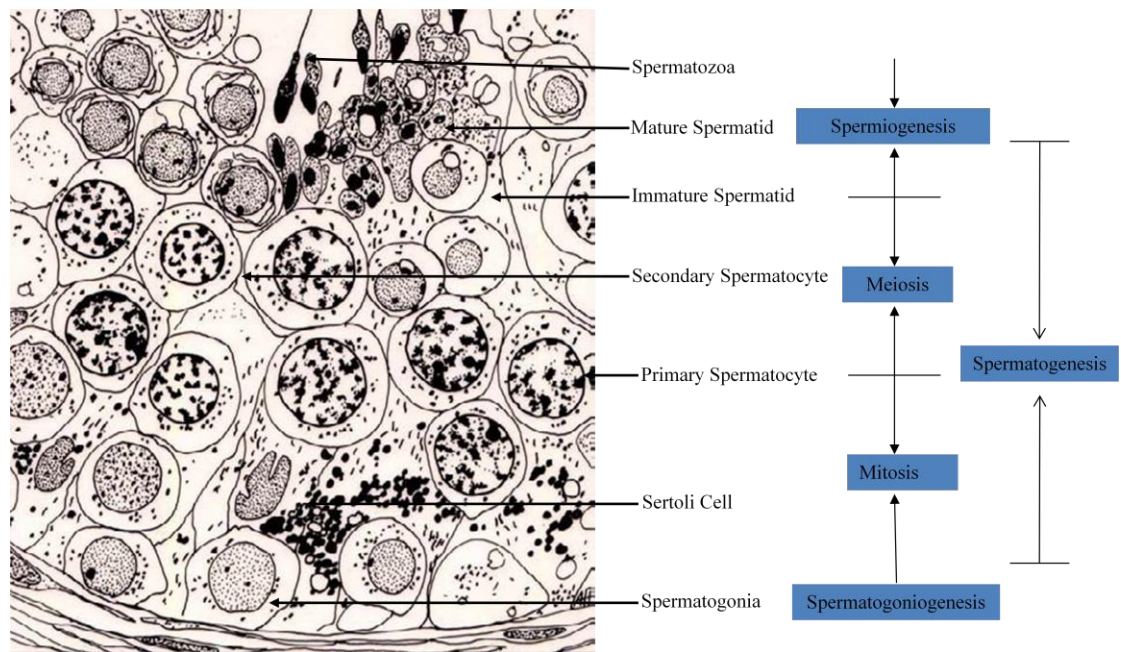


Figure 1.2: Section of stallion germinal epithelium in the seminiferous tubule showing different stages of spermatozoa formation process. Spermatogonia, primary spermatocytes, secondary spermatocytes, and spermatids develop in the space between two or more Sertoli cells. Modified from (Holstein *et al.*, 2003).

1.2.1. Spermatogoniogenesis

Spermatogonia are the germ cells that lead to the production of spermatozoa. The two distinct fates for a spermatogonium are either: a) it undergoes mitosis to duplicate itself (A_0) to maintain a progenitor population that is capable of continuing the spermatogenic lineage, or b) it undergoes mitosis to produce daughter cells which are committed to give rise to primary spermatocytes that differentiate into spermatozoa (Samper, 2009; De Jonge & Barratt, 2006). Spermatogonia multiply continuously at regular intervals by mitosis, but the dividing cells are usually incomplete since the daughter cells remain interconnected by cytoplasmic bridges (Holstein *et al.*, 2003). Uncommitted A_1 -spermatogonia divide to form either two new uncommitted A_1 -spermatogonia or two cells that are joined by an intercellular bridge that continues to divide to form a chain of eight jointed cells. Most A_1 -spermatogonia divide to form differentiated A_2 -spermatogonia that are functionally different from A_1 -spermatogonia. A_2 -spermatogonia can divide to form further differentiated A_3 -spermatogonia that divide to form B_1 -spermatogonia, which are morphologically different and can further divide to form B_2 -spermatogonia. These in turn divide to produce primary spermatocytes (Mckinnon & Voss, 1992).

Sertoli cells serve a number of functions during spermatogenesis as they support the developing gametes by secreting different substances and hormones that control spermatogenesis, as well as phagocytose residual left overs from spermatogenesis. In the absence of spermatogonia, no spermatogenesis can take place and the germinal epithelium would only consist of Sertoli cells. Spermatogonia may be absent from birth, a condition called congenital Sertoli cell-only syndrome, or destroyed by different agents, such as x-radiation, which result in acquired Sertoli cell-only syndrome (Holstein *et al.*, 2003).

1.2.2. Spermatogenesis

B_2 -spermatogonia divide by mitosis at regular intervals to produce primary spermatocytes, which are the largest germ cells of the germinal epithelium. Primary spermatocytes, in turn, divide during the first division of meiosis to produce spherical secondary spermatocytes that will divide throughout the second meiotic division,

without DNA replication, to produce spermatids which have a characteristic elongated cellular shape and condensed nucleus (Samper, 2009; Holstein *et al.*, 2003).

1.2.3. Spermiogenesis

Spermiogenesis refers to the process of dramatic differentiation and maturation of spermatids, which includes mainly cell morphology and size, into mature spermatozoa that are released from the seminiferous epithelium. Spermatids are non-motile and round specialized cells whereas spermatozoa are motile, elongated and have specialized components and surface molecules (Holstein *et al.*, 2003).

To achieve the motility that is needed for the primary function of fertilizing an oocyte, the spermatozoon must lose most of its organelles (such as endoplasmic reticulum and lysosomes which are unnecessary for the task of delivering the DNA to the egg) and most of its cytoplasmic volume (Bruce *et al.*, 1994). Anatomically, stallion spermatozoa consist of 3 regions (Ramalho-Santos *et al.*, 2007):

- The head, which contains a condensed haploid nucleus and the acrosome which is the anterior part of the head that contains several enzymes necessary for penetrating into the zona pellucida of oocyte.
- The mid-piece, which contains many mitochondria that can power the flagellum by providing the spermatozoon with the energy needed for its movement.
- The tail (or flagellum), which is composed of an axoneme consisting of two central singlet microtubules surrounded by nine evenly spaced microtubule doublets that are responsible for sperm motility.

Based on the biogenesis of individual sperm accessory structures and progression of sperm nuclear condensation, spermiogenesis can be divided into three different processes (De Jonge & Barratt, 2006):

- Super condensation of the nuclear chromatin to about one tenth of the volume of an immature spermatid (Holstein *et al.*, 2003). Nuclear hypercondensation and sperm head shaping are achieved by the removal of histones and their replacement with protamines (de Jonge & Barratt, 2006). Testis-specific histone and histone binding variants expressed specifically during meiosis participate in nucleosome formation and chromatin remodeling (Drabent *et*

al., 1991, 1993, 1996; Koppel *et al.*, 1994; Wolfe & Grimes, 1999). It has been proposed that the high condensation of chromatin protects the paternal genome from environmental stress during transport in the male and female reproductive tract. It is confirmed, in men as well as in horses, that with reduced chromatin integrity normal fertilization is possible, but impaired embryo development follows (Samper J, 2009).

- Formation of the enzyme filled acrosome cap by the Golgi apparatus (Holstein *et al.*, 2003).
- Development of flagellum structures which are in contact with the nucleus.

The mature spermatids are delivered from the germinal epithelium to the lumen of the seminiferous tubule by a complex process, called spermiation, which is managed by the Sertoli cells (Holstein *et al.*, 2003). The fully differentiated spermatozoa detach from each other and from the surface of seminiferous epithelium, become free cells, and travel through the lumen of the seminiferous tubule (de Jonge & Barratt, 2006). The different processes of spermatozoa maturation, such as surface and membrane differentiation, take place after they have been released (Holstein *et al.*, 2003). The cytoplasmic lobe is shed in the form of the residual body, which is phagocytosed by Sertoli cells, leaving a minute remnant of a spermatid cytoplasm (de Jonge & Barratt, 2006). Spermatozoa acquire their mobility during their transport throughout the epididymal ducts (Holstein *et al.*, 2003).

1.2.4. Efficiency of Spermatogenesis

Continuous production of spermatozoa is maintained throughout the reproductive lifespan. Such massive proliferation and differentiation requires a certain degree of quality control that may be assured by programmed cell death or apoptosis (de Jonge & Barratt, 2006). For quality management, spermatogenesis is a process of little efficiency with a high number of germ cell being lost during spermatogenesis, mostly due to malformation. Many germinal cells die during the process of spermatogenesis and are rapidly phagocytosed by Sertoli cells (Mckinnon & Voss, 1992). In humans about 75% of the developed germ cells are lost by degeneration or apoptosis and more than half of the remaining are deformed, thus, only 12% of the product has

reproductive potential. However, spermatogenetic efficiency is lower in humans than in other animals (Holstein *et al.*, 2003).

The number of Sertoli cells in the testis is the best indicator of spermatogenic efficiency: the more Sertoli cells a testis contains, the more spermatozoa that testis can produce (Segatelli *et al.*, 2004). In bulls, a direct relationship is found between the number of Sertoli cells in the testis and the daily spermatozoa production by that testis (Mckinnon & Voss, 1992). Each Sertoli cell can support a limited number of germ cells and the number of Sertoli cells per testis and the maximum numbers of germinal cells per Sertoli cell are species-specific (Mckinnon & Voss, 1992, Segatelli *et al.*, 2004). It was presumed that any alteration in spermatogenesis in post-pubertal animals would change the ratio of germ cells to Sertoli cells (Jones & Berndtson, 1986). The mean spermatid-Sertoli cell ratio is 3-4 for human germinal epithelium, versus 12 in rats (Holstein *et al.*, 2003).

Spermatogenesis, as a whole, can be disturbed at every level. Different factors reduce or destroy the spermatogenesis activity, such as environmental factors, diseases, different nutritive substances, therapeutics, drugs, hormones and their metabolites toxic substances, X-radiation or simple increased temperature. If the germinal cells, spermatogonia, survive these factors then spermatogenesis may be resumed (Holstein *et al.*, 2003).

1.3. Meiosis

Meiosis is a complex process, which takes place in virtually all sexually reproducing eukaryotes to generate haploid cells as well as generate genetic diversity, and therefore help the survival of species or generation of new species. It is conserved throughout evolution with marked differences between sexes and species. Genetic variation occurs through random fertilization, crossing over and random segregation and this variation is the basis for natural selection and evolution (Critchlow *et al.*, 2004; Maguire, 1992).

Meiosis is more complex than mitosis and has a greater degree of genetic control. It consists of unique structures and events at each phase of the cell process (Chaganti *et al.*, 1980; Uhlmann, 2001; Wolgemuth *et al.*, 2002; Nasmyth, 2002; Critchlow *et al.*,

2004). In mitosis, DNA replication and chromosome compaction are followed by segregation of sister chromatids, thus restoring the initial genetic makeup in each daughter cell; however, meiosis yields haploid cells (Kleckner, 1996). The fusion of two gametes to form a zygote restores the normal chromosome complement, rather than doubling it. In meiosis replication of the DNA takes place in interphase and is followed by two cycles of nuclear division, in the first division, called meiotic division I, homologous chromosomes separate and in the second division, meiotic division II, the sister chromatids separate (Bruce *et al.*, 1994; Critchlow *et al.*, 2004). Meiotic division II, which is also known as equational division, resembles mitosis in that sister chromatids segregate; however, in meiotic division I, which is also known as reductional division, sister chromatids remain associated with each other so one chromosome moves to one cell and its homologue moves to the other cell (Roeder, 1997).

As in mitosis these divisions are sub-divided into the Prophase, Metaphase, Anaphase and Telophase stages, thus a full meiotic process includes two of each of these stages.

Meiotic Division I

1.3.1. Prophase I (PI)

Meiosis is dominated by prophase of the first meiotic division (PI), which can occupy 90% or more of the total meiotic duration (Parvinen *et al.*, 1991; Cobb & Handel, 1998; Critchlow *et al.*, 2004). Homologous chromosome pairing, synapsing and recombination are three different coordinated events that occur during prophase I (Jordan, 2006).

Prophase I events are divided into substages based on changes in chromosome morphology and their pairing behaviour during synapsis (Roeder, 1997). It starts with the leptotene stage in the basal compartment of the germinal epithelium and thereafter the spermatocytes reach the adluminal compartment, meiosis I continues through the prophase stage, with zygotene, pachytene and diplotene (Holstein *et al.*, 2003).

1.3.1.1. Homologous Pairing

Chromosome pairing is a mechanism that brings homologous chromosomes together into tightly synapsed pairs. Such pairing is essential for successful meiosis; generally only paired homologs can recombine, crossover and form the required configuration for correct segregation into haploid sets (Cook, 1997). It is thought that any homologous chromosome segment should undergo pairing during the pairing phase and homologous chromosomes pair up precisely along their length, thus failure to carry out this step can result in chromosome mal-segregation, at later stages of meiosis, that could lead to meiotic arrest (Critchlow *et al.*, 2004; Villagómez & Pinton, 2008).

Meiotic chromosome pairing at PI involves three successive developmental stages: 1) homologue recognition, in which the chromosomes are pulled from their scattered locations towards each other, 2) presynaptic alignment, which is assumed to be the first physical connection between the homologous chromosomes and 3) intimate synapsis. Chromosomes search out their homologues during meiotic leptotene to establish a connection that sometimes results in gene conversion, this in turn promotes initiation of synapsis (von Wettstein *et al.*, 1984; Kleckner, 1996).

Co-localization of the homologous chromosomes is a crucial step in the even distribution of genetic material between daughter cells (Barlow & Hultèn, 1998). Several intensive studies explored different hypothesis or models of initiation of homologous chromosome pairing; however, no clear picture of this process has yet emerged. It is thought that there are several different pairing mechanisms and different organisms react differently with each mechanism, also pairing is a multi-step and usually a multi-path process (Roeder, 1997; Schwazacher, 2003).

Earlier studies revealed that the nuclear envelope is involved in initiation of homologous pairing. In many organisms, such as man and mouse, the subtelomeric regions of chromosomes are observed at the leptotene stage to be attached to the inner nuclear membrane and form a cluster structure known as a bouquet that facilitates the first alignment and pairing of homologues at their connection point to the inner nuclear membrane (Comings & Okada, 1972; Scherthan *et al.*, 1996). The telomeres first attach to the restricted site on the nuclear envelope and then move to a common clustered location along the envelope, which is next to the spindle pole body (SPB) in

yeast and the centrosome in mammals. This brings homologous chromosomes into close proximity, which results in numerous potential encounters among the homologues and thereby facilitates homology testing at different pairing sites.

It is suggested that chromosome pairing occurs transiently during leptotene whilst the telomeres are moving towards each other and the telomere movement is thought to be mediated by microtubules (Scherthan *et al.*, 1996; Schwazacher, 2003; Turner, 2007). Mutations in Ndj1p, telomeric-associated protein, that seems to be required for bouquet formation and telomere attachment, disrupt bouquet formation and homologous pairing in budding yeast (Trelles-Sticken *et al.*, 2000; Turner, 2007). Other proteins, such as Taz1 from fission yeast, Bqt1 and Bqt2 from *Schizosaccharomyces pombe*, have been identified and characterized to mediate telomere clustering and association with SPB (Chikashige *et al.*, 2006). Correct telomere positioning and bouquet formation facilitates alignment and pairing of homologues, this is a prerequisite for meiotic recombination. Bouquet dissolution seems to be dependent on completion of recombination (Sideraki and Tarsounas, 2007).

Other studies showed that pairing is initiated in several scattered sites (Moses, 1968); however, contrary to this observation, studies in yeast suggested that homologous pairing was initiated very early before condensation of chromosomes and most likely during the pre-meiotic interphase (Kleckner, 1996). Early meiotic pairing may involve the formation of reversible and unstable interactions between intact DNA duplexes which could be sufficient for homologous alignment since they are held together at multiple sites along their length (Kleckner & Weiner, 1993). In some organisms, such as *S. Pombe*, pre-meiotic pairing of homologues is observed near the centromere (Scherthan *et al.*, 1994; Jordan, 2006). Pre-meiotic pairing is not conserved since it is not observed in mammals and other organisms such as *Saccharomyces cerevisiae* (Weiner & Kleckner, 1994).

Several genetic and cytogenetical studies indicate that pairing sites in many species are numerous and uniformly distributed along the chromosomes in meiotic prophase and most or all chromosomal segments are capable of pairing (Vincent & Jones, 1993; Roeder, 1997). However, there are certain organisms, such as *Caenorhabditis elegans* and *Drosophila melanogaster*, in which only particular sites on chromosomes, called pairing centres, can initiate homologous pairing. In *C. elegans* these sites are referred

to as a homologue recognition region (HRR) and are located at one end of the chromosome (Zetka & Rose 1995). The HRR initiates homologue pairing since it acts as a binding site for a protein complex that is involved in homology searching, as well as initiating and stabilizing pairing of homologous chromosomes (Roeder, 1997, Jordan, 2006).

Two proteins, SNM (stromalin in meiosis) and MNM (modifier of *mdg4* in meiosis), were reported to be localized to the XY pairing centre in *D. melanogaster* and are required for stabilizing initial pairing of homologous chromosomes. MNM is also localized on autosomes as multiple spots within the chromatin that disappeared by anaphase I (Thomas *et al.*, 2005).

Studies in *S. cerevisiae* suggested that initiation of homologous chromosome pairing prevents meiotic nuclear division until all chromosomes are fully paired. This triggers certain checkpoints such as the Tam1/ndj1 protein that is localised at the end of the meiotic chromosomes (Chua & Roeder, 1997; Roeder, 1997).

In most organisms, synapsis between homologous chromosomes requires the presence of a meiosis-specific proteinaceous structure termed the synaptonemal complex (SC; Roeder, 1997).

1.3.1.2. Synaptonemal Complex

The synaptonemal complex (SC) is a protein lattice that resembles railroad tracks and connects paired maternal and paternal homologous chromosomes in most meiotic systems. The SC was named and discovered in the spermatocyte of crayfish by Moses (1956a). Subsequently, it has been found in the spermatocytes of a variety of animals including: cat, mouse and pigeon (Fawcett, 1956); grasshopper and salamander (Moses, 1956b); rat, fish and spider (Sotelo & Trujillo-Cenoz, 1958); and pulmonate snail (Roth, 1960). The SC has long been viewed as being essential for crossing over; however, recombination has now been shown to be initiated before the formation of the SC and there are some studies that have revealed the absence of SC in certain species (e.g. *S. pombe* and *Aspergillus nidulans*) even though normal crossing over occurs (Egel-Mitani *et al.*, 1982; Bahler *et al.*, 1993; Munz, 1994; Schwazacher, 2003). It is considered that the SC may be important in maturation of crossovers into

chiasmata, chromatin cohesion and crossover interference (Moens, 1994; Schwazacher, 2003).

The SC structure is composed of microfibrillae which are arranged to form two lateral elements (LEs) that are separated from each other by a uniform distance, which varies slightly between species but usually ranges between 100-300 nm, and one central element (CE; Schwazacher, 2003). The LE consists of an outer lamina and a thinner, less electron-dense inner lamina. The CE is apparently formed by the overlapping microfibrillar stretching from the inner laminae of the two LEs toward the centre of SC known as transverse filaments (TF). Many of these filaments transverse from one LE to the other, whereas others terminate at the CE (Figure 1.3; Roeder, 1997). However, new findings in mice suggesting that SC is a quadripartite structure and CE represents a distinct structure after isolating a novel protein within the central element (Hamer *et al.*, 2006; Turner, 2007).

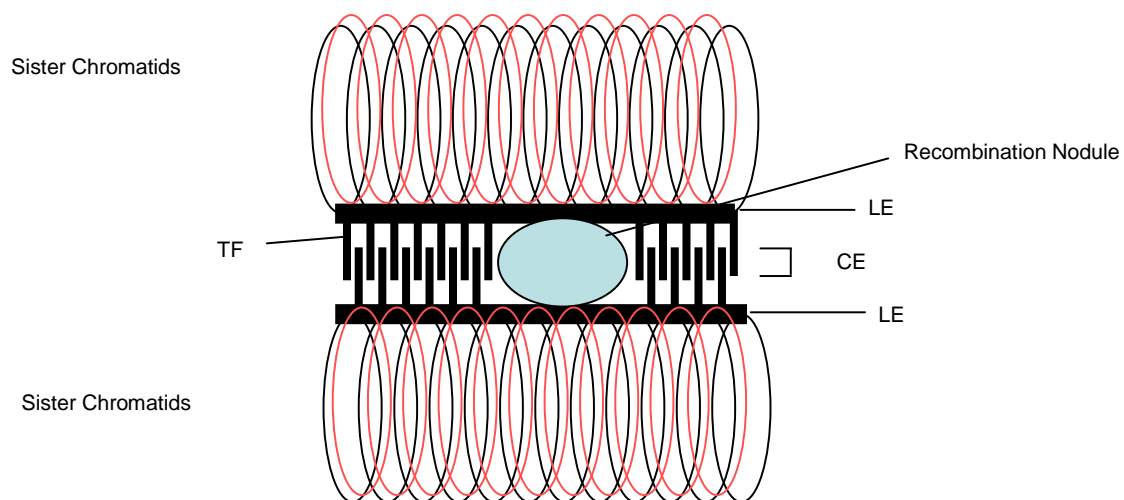


Figure 1.3: Diagram of synaptonemal complex (SC). Lateral elements (LE) of homologous chromosomes align and synapse together via a meshwork of transverse filaments (TF). The overlapping of the TFs forms the central element (CE). The recombination nodules are constructed on the central element. Modified from (Roeder, 1997).

SC assembly can be divided into three major stages which are used to classify the PI substages: 1) During the leptotene stage, the first stage of prophase I, the two sister chromatids of a single chromosome develop an axial element (AE) (Roeder, 1997). 2) During zygotene, TF start connecting the axial elements of the two homologs after its

polymerization at distinct loci. 3) During pachytene the SC is completely assembled, comprising two LE, which is referred previously to AE, and CE (Lynn *et al.*, 2007). Moses (1968) pointed out a reduction of AEs and an increase of LEs as meiosis proceeds through zygotene (when synapsis starts for a very small stretch, usually at the telomeric regions, and the AEs are transformed to the LEs of the SC) to pachytene (when synapsis is completed and the SC consists of LEs and a CE). The SC then breaks down at diplotene stage of prophase I, preferentially at the centromerical terminal segments and the bivalents are obviously more relaxed and longer than those observed at the pachytene. The CE disappears first while the LEs remain briefly along the homologs before they disintegrate (Moses, 1968; Villagómez & Pinton, 2008).

Genes that encode the TFs, such as ZIP1 gene in *S. cerevisiae*, the SCP1 gene in rats, SYCP1 in mice and Syn1 homologs of SCP1 in hamsters and humans, have been cloned (Roeder, 1997). These genes are expressed specifically in meiotic prophase cells and these proteins localized to synapsed chromosomes but not to AEs. The size of the proteins in these genes range from 875 to 997 amino acids, with 74% to 93% of mammalian protein identity (Sym *et al.*, 1993; Dobson *et al.*, 1994). Based on SYCP1 sequences in mice and by using gold labelled antibodies against the C and N terminal coupled with electron microscopy, the C terminal region has been located to the edge of the LE, while the N terminal region localized to the CE. The N termini of SYCP1 molecules can interact with each other (Costa and Cooke, 2007). Three new proteins, SYCE1, SYCE2 and TEX12 were identified as part of mouse CE components and they interact with the N terminus of SYCP1 and between themselves. These proteins are delocalized in the absence of SYCP1 (Costa *et al.*, 2005; Hamer *et al.*, 2006).

Different components of the LEs, such as Cor1 protein of hamsters and homologous SCP3 proteins of rats, have been characterized. Cor1 and SCP3 are phosphoproteins that extent of phosphorylation changes and their size is around 250 amino acids that localized to unsynapsed AEs as well as the mature LEs (Dobson *et al.*, 1994; Lammers *et al.*, 1994). Cor1 and SCP3 are thought to play a role in meiotic chromosome segregation due to their localization pattern. They remain associated with the cores of the chromosomes from diplotene to metaphase I and then accumulate near the centromeres by anaphase I and finally dissociate from the centromeres at anaphase II (Roeder, 1997). Red1 is another example of *S. cerevisiae*

meiosis-specific protein that is associated with AEs and mature SC LEs (Smith & Roeder, 1997).

SC proteins in general show low conservation and sequence homology (Schwazacher, 2003). In different studies, several SC protein components have been isolated and various important meiotic structures have been identified by the use of immunofluorescence. Antibodies against SC components, such as TEs (SCP1) or LEs (SCP3), serve as valuable tools in investigating the structure of SC since they can be used to visualize the SC under a fluorescent microscope (Sun *et al.*, 2004). Antibodies against SC components of related species show limited cross reaction; however, no cross reactions have been reported between vertebrates, invertebrates, fungi and plants (Schwazacher, 2003).

1.3.1.3. Factors influencing homologue recognition and initiation of pairing

Different factors, such as chromosome morphology, chromatin condensation pattern, proteins bound to DNA and specific sequence distribution, in addition to DNA-DNA interaction, are involved directly or indirectly in homologue recognition and initiation of pairing (Sybenga, 1999; Schwazacher, 2003).

1.3.1.3.1. Chromatin Organisation

Genome size has a major effect on chromosome organization and chromatin packaging as well as on the distribution of genes and repeated sequences that influence homologous pairing and recombination (Schwazacher, 2003). Each pair of sister chromatids forms a single linear array of loops connected at their bases by an axial element (AE), which lies on the same side of this axis (Kleckner, 1996). The average size of the chromatin loops are species-specific and range from 0.5 μm in *S. cerevisiae* to 14 μm in grasshoppers (Moens & Pearlman, 1988). It has been postulated that there are specialized DNA sequences that associate with the meiotic chromosome core and regulate the loop size. In one study in rats, when the SC was treated with DNase, the DNA fragments were found to contain dinucleotide repeats with GT motif and retroelement-related repetitive sequences such as short

interspersed sequence elements (SINE) and long interspersed sequence elements (LINE) (Pearlman *et al.*, 1992). The loop size near the telomeres was two to three times smaller than in the interstitial regions, which was attributed by the chromosomal position, not the DNA sequence, since inserting the telomeric sequence in the interstitial regions did not affect the packaging ratio (Heng *et al.*, 1996). In humans, the telomeric region is seen tightly associated with the SCs compared with the centromeric region (Barlow & Hultèn, 1996). Each chromosome in a haploid set has a unique array of loops of transcription units and therefore, homologues share similar arrays (Cook, 1997).

The rate of meiotic recombination is inversely correlated to the chromatin packaging density. For example the average recombination rate in yeast is 300 times more than in humans since the amount of DNA per unit length of SC in humans is 25 times more than yeast. However, if we introduce human DNA into yeast, it will adopt the same packaging and recombination rate of yeast (Loidl *et al.*, 1995).

1.3.1.3.2. Repeated DNA Sequences

Repeated sequences might aid the first homologous recognition (Roeder, 1997). Telomeres and centromeres are two examples of repeated sequences.

Telomeres

Telomeres are essential for genomic stability through protecting the chromosome ends from degradation. Their dysfunction, shortening or loss of telomeric capping, is associated with genetic instability and implicated in aging and cancer (Sideraki and Tarsounas, 2007). During early meiosis telomeres play an important role in homologous pairing since bouquet formation depends on telomere attachment and movement to the inner nuclear membrane and cluster surrounding the centrosome in mammals (Scherthan *et al.*, 1996). Bouquet assembly occurs at the leptotene-zygotene transition, while telomeres remain attached to the nuclear membrane from leptotene to late pachytene (Sideraki and Tarsounas, 2007). There are short subtelomeric repeats that are chromosome-specific and their distribution could be important for homologous recognition. This repeat, (TTAGGG)ⁿ in mammals, which varies in length from 10 kb in human to >40 kb in mouse, and (TTTAGGG)ⁿ in most plants, is highly conserved and repeated hundreds of times at the telomeres (Fuchs *et al.*, 1995;

Zakian, 1995; Kilian *et al.*, 1995). The telomeres end with single-strand 150 nucleotides called 3' overhang that acts as a substrate for telomerase, which has reverse transcriptase activity to extend the G-rich strand of the telomere. This can prevent gradual loss of DNA sequences from chromosome ends after replication (Sideraki and Tarsounas, 2007). Mice with telomerase deficiency have short telomeres which result in chromosomes end-to-end fusion and cell death as well as infertility problems (Herrera *et al.*, 1999). Telomerase may act in the germ line since its activity was detected in testes and ovaries, but not in mature sperm or oocytes; however, the sperm telomeres are significantly longer than those of somatic cells (Wright *et al.*, 1996 Sideraki and Tarsounas, 2007). Telomeres elongation may occur before and after meiosis since the telomerase activity peaks in pre-leptotene and spermatid cells of adult mouse testis using *in situ* TRAP assay (Sideraki and Tarsounas, 2007). It is thought that homologous recombination can protect the telomeres from damage during meiosis through remodelling the telomeric DNA into t-loop structure (Griffith *et al.*, 1999).

Centromeres

Eukaryotic centromeres are responsible for sister chromatid cohesion, attachment to the spindle, and correct chromosomes alignment on the metaphase plate in order to allow proper segregation at the anaphase stage. The centromere of many species contains highly repetitive sequences which are known as tandem satellite repeats and retroelement-like components (Schwazacher, 2003). For example in humans, the tandem α -satellite repeats, which constitute about 0.3% of the human genome, play a major role in chromosome segregation and centromere function and show a chromosome-specific pattern of sequence variants (Willard, 1985). These variants, in addition to different DNA binding proteins such as histone H3 and CENP-A, are thought to be involved in homologous recognition (Schwazacher, 2003). Studies in *S. cerevisiae* and female *D. melanogaster* show that pairing at the centromeric region plays an important role in homologous pairing and are also required for correct segregation in the case of achiasmata chromosomes (Karpen *et al.*, 1996; Kemp *et al.*, 2004).

1.3.1.4. Recombination

Meiotic recombination is the molecular process by which new combinations of the genetic material are generated and is considered to be the major outcome of meiosis (Heyer & Kohli, 1994). Recombination is essential for meiotic chromosome segregation and the formation of normal haploid gametes (Hassold *et al.*, 2000). Recombination frequency and distribution are useful for genomic and association studies (Heyer & Kohli, 1994) and it is also important in providing a pathway for the repair of damaged DNA. Recombination processes may lead to oncogene activation or loss of tumor suppressor genes, which are important steps in carcinogenesis (Heyer & Kohli, 1994). For example, mutation in BRCA2 gene, which is a tumor suppressor gene, causes predisposition to breast and ovarian cancer (Li & Heyer, 2008). In general, it is considered that the reduction of frequency and alterations in the positioning of recombination are risk factors for non-disjunction and generation of aneuploidy (Lamb *et al.*, 1997).

The process of chiasma formation, crossing over and recombination during meiosis is a dynamic one, and can vary even within the same species and race. Variation is seen between males and females, between individuals with normal and those with structurally rearranged karyotypes, and even between individuals with normal karyotypes (Hultèn, 1994).

Two different approaches have been introduced to determine the genome-wide patterns of recombination: 1) Direct cytogenetic approach, in which recombination can be determined by analyzing the number of chiasmata and location on each chromosome in gametes. 2) Indirect conventional genetic linkage analysis of pedigrees. Genetic markers are used to produce recombination maps of chromosome segments, which can then be linked to estimate the recombination frequencies for specific chromosome (Sun *et al.*, 2004; Hassold *et al.*, 2004). The second approach has two limitations. First, it needs three well-characterized generation families. Second, only one-half of all recombinations can be detected since this approach relies on the analysis of haploid products rather than meiotic cells (Lynn *et al.*, 2002).

Meiotic recombination is initiated by the formation of double strand breakage (DSB), which is repaired during homologous chromosome recombination (Borde, 2007). Chromosome segregation requires two processes in most organisms. Firstly, the

chromosomes are broken (at interphase stage) by DSBs, and rejoined with some of the breakage–reunion events that occur between homologs leading to recombinant products (During Prophase I), which can be visualized by light microscopy at Metaphase I stage as chiasmata. Secondly, synapsis and recombination between homologs are facilitated and formed by the SC (Figure 1.4) (Hassold *et al.*, 2000).

1.3.1.4.1. Double Strand Breaks (DSBs)

It is thought that recombination is initiated by double-strand breaks (DSBs) as the frequency and the distributions of the DSBs are correlated consistent with the meiotic recombination (Roeder, 1997). In general, the double strand cleaves first followed by exonuclease digestion in which 5' strand termini are rapidly resected, while leaving 3' strand tails suitable to invade an uncut homologous duplex. This followed by branch migration forms double Holliday junctions, which connect the homologues at the DNA level, resulting in crossover or non-crossover products (Kleckner, 1996).

There are many remarkably conserved features of meiosis between different organisms. Meiotic specific DSB differ from most DSB, which occur either after drug treatment, irradiation or during replication, in that it is repaired by homologous recombination (Borde, 2007). Repairing of these DSBs by recombination generates recombinant molecules that could be either crossover (reciprocal exchanges) or non-crossover (gene conversion; Baudate and Massy, 2007). Meiotic specific DSBs have been demonstrated in yeast but there is evidence that the DSBs model can be applied to different species. With the use of insertional mutagenesis, whole genome sequencing, knock-out mutants and different screening methods, numerous yeast homologues genes have been identified in different multicellular organisms such as *C. elegans*, *D. melanogaster*, mouse and human (Roeder, 1997, Schwazacher, 2003). More than 200 genes specific for meiosis and gametogenesis have been identified (Schwazacher, 2003). Yeast artifact chromosomes carrying human DNA inserts exhibit characteristics of meiotic DSB patterns (Klein *et al.*, 1996). DSB repair model has been demonstrated physically that can be divided into the following 4 different steps (Figure 1.4):

1) Initiation of DSBs by double-strand break formation:

The Spo11 protein, which is purified from a DNA-protein complex and is widely conserved, has been shown to be required for the initiation of meiotic recombination in yeast and possibly in most, if not all, organisms such as mouse and man (Klapholz *et al.*, 1985). Protein sequence analysis showed that Spo11 contains several motifs which are homologous to Top6A, the catalytic subunit of an archaeobacterial type II topoisomerase that mediates a reversible DNA break, which is necessary in the absence of a suitable homologue (Roeder, 1997; Schwazacher, 2003). Once breaks are formed, Spo11 becomes linked covalently to the 5' end of the DSBs, forming a Spo11p-DNA intermediate, which is then removed before break resection and strand invasion can take place (Schwazacher, 2003; Turner, 2007). Spo11 is also required during leptotene for centromere pairing of homologous chromosomes (Tsubouchi & Roeder, 2005). It was observed that homologous chromosomes pairing is absent in *S. cerevisiae* Spo11 null mutants (Cha *et al.*, 2000). Also different studies in different organisms indicated that DSBs are not only initiated before SC formation, but are required for homology searches and SC formations since the Spo11 mutants do not have SCs (Schwazacher, 2003). The *S. pombe* rec12 gene is a homologue of the *S. cerevisiae* Spo11 gene (Lin & Smith, 1994).

2) Exonuclease resection to produce recombinogenic 3'-OH tails:

The two 5' ends of the break undergo resection to yield long 3'-OH single stranded overhang tails, approximately 600 nucleotides in length, that can invade a homologous duplex. Different studies showed that three genes, RAD50, MRE11, and Xrs2, are required for the formation and processing of meiotic DSBs since they mediate resection in addition to cleavage through their exonuclease activity. Mutations in these genes lead to failure in resection of cleaved DNA molecule by 5'-to-3' exonuclease activity that leads to an absence of meiotic recombination in yeast (Borde, 2007; Alani *et al.*, 1990; McKee & Kleckner, 1997; Lynn *et al.*, 2007). RAD50 belongs to a family of chromosome condensation and segregation proteins that include Smc1 and Smc2. RAD50 can also bind the DNA and it contains an ATP-binding motif and two coiled-coil domains that are separated by a spacer (Kleckner, 1996); however, COM1/SAE2 is required specifically for resection. COM1/SAE2 protein, after conjunction with the RAD50/MRE11/Xrs2 complex, could remove the 5'-attached Spo11 protein together with a short 15-30 bp DNA oligonucleotide,

through its nuclease activity, away from the break site to allow the resection to proceed (Keeney *et al.*, 1997; Turner, 2007). In human hypomorphic mutations, which are partial loss of gene function, in MRE11 causes genetic instability disorder called ataxia like disorder (ATLD) including radiation sensitivity and chromosome instability (Borde, 2007). The *S. pombe* RAD32 gene is homologous to the *S. cerevisiae* MRE11 gene (Tavassoli *et al.*, 1995) whereas the *Escherichia coli* SbcC and SbcD share similarity with RAD50 and MRE11 respectively (Sharples & Leach, 1995). Also RAD50 and MRE11 homologs have been found in humans as part of a larger protein complex with elevated levels of RAD50 transcript in testis (Dolganov *et al.*, 1996). EXO1 is another example, in budding yeast and mice, of an exonuclease enzyme that generates 3'-ended-single-stranded DNA (Morin *et al.*, 2008).

3) Strand Invasion and Double Holliday Junctions Formation:

Four different yeast enzymes, RAD51, RAD55, RAD57, and DMC1, are thought to be involved in the invasion of single strand tails into uncut DNA homologous duplex, and mutation of these genes can lead to failure in repairing the resected DSBs (Bishop *et al.*, 1992; Shinohara *et al.*; 1992; Schwacha & Kleckner, 1997). RAD51 protein, was co-localized with LE in yeast, human and mouse from early leptotene to pachytene, and is stimulated by a heterodimer of RAD55 and RAD57 to promote strand exchange (Bishop, 1994; Barlow *et al.*, 1997; Sung, 1997). The number of RAD51/DMC1 foci decreases from zygotene to early pachytene and disappears at the middle of pachytene in mouse and human spermatocytes and oocytes, which reflects the progression of the repair events (Moen *et al.*, 2002, Baudat and Massy, 2007). RAD51 is also proposed to have a role in the homology search during chromosome pairing. RAD51 bring the broken DNA molecule into close proximity with its uncut homologous partner (Schwazacher, 2003; Turner, 2007).

The consequences of strand invasion and DSB repair processes is the formation of two Holliday junctions, one on each side of the strand exchange region, which are visualized by their distinctive pattern of migration on two-dimensional gels after *in-vivo* crosslinking (Smith, & Nicolas, 1998). The double Holliday junction can be resolved as either reciprocal recombination, known as crossover, or gene conversion, which is known as non-crossover (Gilberston and Stahl, 1996; Schwazacher, 2003). If the resolution of the junction occurred in opposite directions, crossover will result. Crossovers and non-crossovers are completed at the end of pachytene, immediately

before or concomitant with SC disappearance (Kleckner, 1996). However, studies in yeast show that crossover and non-crossover events may result from two different pathways. In human, the conversion tract size in crossover events, 500 bp, is longer than that for non-crossover events, 50 bp to 300 bp, in addition to the fact that MLH1 and MLH3 were found to be required for crossover but not for non-crossover formation (Jeffreys and May, 2004). Crossovers, which are dependent on DMC1, are formed by resolution of the intermediates of Holiday junctions; however, non-crossovers are resolved by a second mechanism known as synthesis dependent strand annealing (Hunter & Kleckner, 2001). Non-crossovers are poorly documented in mammalian genomes since they are difficult to estimate. Most of the data comes from molecular analysis that depends on the presence of polymorphic markers (Baudat and de Massy, 2007). Mammalian MSH4/5, unlike in *S. cerevisiae*, seem to be not exclusively involved in crossover formation and MLH1 and 3 are specifically required for crossover pathway, not for non-crossover events. Mice MSH4/5 might participate in non-crossover regulation (Baudat and de Massy, 2007). Mammalian non-crossover could be important in homologous chromosome pairing through contributing to bringing chromosome axes together (Baudat and de Massy, 2007).

4) Mismatch Repair:

DNA mismatch repair is one of the important systems that can recognize and repair DNA damage and errors, such as insertion, deletion and mis-incorporation of bases that can arise during DNA replication and recombination. Three bacterial MutS homologous proteins, MSH2, MSH3, and MSH6, and two MutL homologous proteins, PMS1 and MLH1, are shown to be required for mismatch repair in yeast. First, a heterodimer of MSH2 and either MSH3 or MSH6 recognizes the mismatch, followed by binding of another heterodimer of PMS1 and MLH1 (Marsischky *et al.*, 1996; Prolla *et al.*, 1994). The MLH1 mutant cells arrest in pachytene and are deficient in chiasmata (Smith, & Nicolas, 1998). In studies of male mice with a targeted disruption of the MLH1 gene, meiotic crossing over was eliminated and most chromosomes were present as univalents during meiosis I, causing the arrest of spermatocytes at this stage (Hassold *et al.*, 2000).

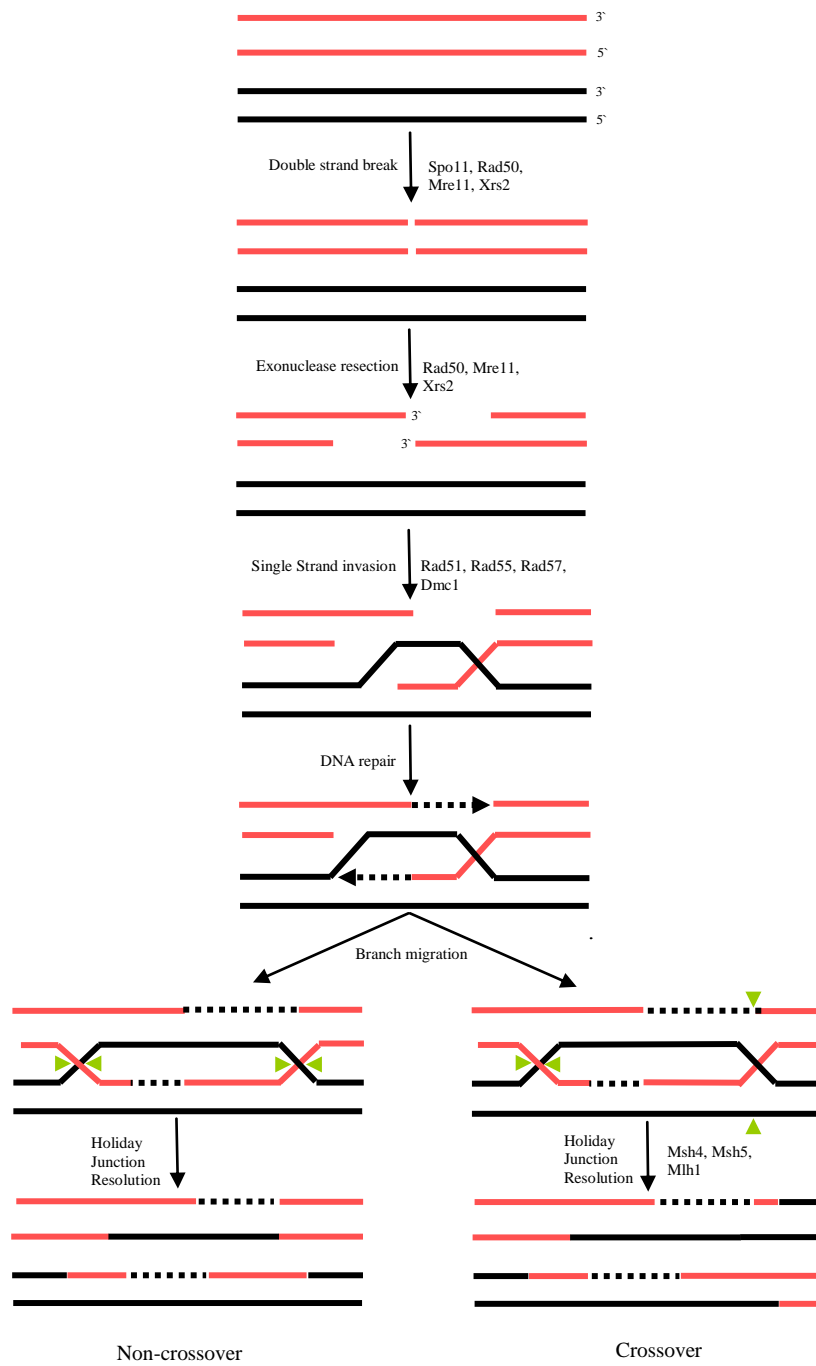


Figure 1.4: Molecular events of DSB repair model of meiotic recombination. Text near arrows describes the events. Green arrow heads point out positions of cuts at Holliday junctions. Modified from (Roeder, 1997).

1.3.1.4.2. Recombination Nodules

Recombination nodules (RN) are electron-dense spherical structures about 100 nm in diameter located at discrete intervals along the SC. RN's were first described by Carpenter (1975) in *D. melanogaster* oocytes as transient structures. They are the sites of meiotic recombination that associate with SC during zygotene and pachytene. The molecular basis for these structures is not fully characterized; however, they are thought to be protein complexes acting at the sites of breakage/processing of recombinational events (Critchlo *et al.*, 2004). RNs are so small and they can be directly observed only by electron microscopy (EM) utilizing three-dimensional (3-D) reconstruction of serial-sectioned nuclei, which is technically difficult and labour intensive (Carpenter, 1975). Two types of nodule are thought to exist, early and late nodules that can differ from one another in timing, shape, size, relative numbers, staining characteristics, and protein components.

The early nodules (ENs), present during leptotene or zygotene, are numerous and present on unsynapsed AE and briefly on the newly formed SC with random distribution. ENs sometimes differ in shape and it is thought that these nodules may be involved in recognition and alignment of homologous chromosomes. They also mark the sites of all strand exchange reactions since they are often found at AE convergence sites. These sites are thought to represent homologous regions on synapsing chromosomes and the initial step in SC formation, as well as the sites of recombination related protein (Carpenter, 1975; Albini & Jones, 1987; Roeder, 1997; Anderson & Stack, 2002). For example, in mice, 200 to 400 DSBs are formed during leptotene; however, only around 23 of them proceed to form crossovers (Turner, 2007).

In yeast, two RecA-like proteins, DMC1 and RAD51, are thought to be the components of ENs that are present at the same time as DSBs and disappear as chromosomes synapse (Bishop, 1994; Roeder, 1997). In different organisms – such as mice, human and chicken, yeast – RAD51 homologous genes have been identified and localized on chromosomes during the zygotene stage by electron microscopy using antibodies tagged with gold. However, in some organisms, the RAD51 protein does not dissociate from synapsed chromosome (Ashley *et al.*, 1995; Moens *et al.*, 1997; Roeder, 1997).

Late nodules (LNs) are fewer in number and are distributed non-randomly on the fully synapsed SC. They are observed associated with the CE of the SC from early pachytene through to early diplotene. LNs are more regular in size and shape as well as tending to stain more darkly than ENs (Anderson *et al.*, 1997). LNs presumably represent the sites where crossing over forms since non-crossovers have no cytogenetical correlate after mid-pachytene, (Kleckner, 1996). There is an excellent correlation between the number and distribution of LNs and the number and distribution of crossovers or chiasmata in several species (Hassold *et al.*, 2000). However, there are some exceptional cases in some plant species, such as *Allium fistulosum*, that show fewer RNs than the number of chiasmata, which may be due to technical losses and/or the fact that RNs are transient structures (Jones & Albin, 1988; Hassold *et al.*, 2000).

Due to the difficulty in visualizing RNs in mammals, relatively little effort has been made to characterize them. However, with the development of immunolocalization methodologies, it has become possible to determine whether the distribution of any of the recombinogenic proteins is consistent with that predicted for RNs (Hassold *et al.*, 2000). In yeast, different protein components of LNs have been identified such as MutS homologue MSH4, MSH5 and MLH1 that localize to discrete spots on chromosomes predominantly during the pachytene. Mutations of these proteins show reduced crossing over (Hollingsworth *et al.*, 1995; Hunter & Borts, 1997; Roeder, 1997).

For example, different studies have demonstrated that application of anti-MLH1 to SC preparations at pachytene stage show a labelling pattern consisting of distinct foci that allow precise localization of the sites of crossovers in germ cells in both mouse (Baker *et al.*, 1996) and human spermatocytes and oocytes (Barlow & Hultèn 1998; Lynn *et al.* 2002; Tease *et al.* 2002). The number and location of the MLH1 foci closely agrees with that expected of a molecule that marks the site of recombination and chiasmata (Hassold *et al.*, 2000; Sun *et al.*, 2004). Thus, it seems likely that MLH1 foci mark the sites of the LNs and that MLH1 is an appropriate marker for chiasma formation. Therefore, it becomes possible to generate chromosome specific and genome-wide genetic maps by studying the localization of MLH1 (Hassold *et al.*, 2004).

Several intensive studies explore different hypothesis of the relationship between early and late RNs. One idea is that most of ENs are lost by mid pachytene stage and some of them become LNs since some recombination proteins other than RAD51 and DMC1, such as RAD50, MRE1, BLM, MSH4, and MSH5, are components of LNs and have been localized during early prophase I in yeast, mice and maize (Stack & Anderson, 1986; Bishop, 1994; Moens *et al.*, 2002). It is thought that ENs in some organisms that associate first with the SC, usually in distal regions, have a higher likelihood to become LNs than later associate ones which are usually proximal (Anderson & Stack, 2005). Also, there is strong evidence that most of non-crossover breaks are resolved as gene conversion events (Turner, 2007). However, other researchers have proposed that early and late nodules are separate entities in which ENs are responsible for gene conversion, while LNs are responsible for crossovers (Carpenter, 2003; Anderson & Stack, 2005). In yeast, the ZMM protein family (ZIP1, ZIP2, ZIP3, ZIP4, MSH4, MSH5, MER3) plays an important role in crossovers formation and assembly of the SC central element. ZMM proteins have also identified in animals and plants. ZMM proteins are important for the formation of more than 80% of yeast crossovers since mutations in any one result in losing most of crossovers without affecting non-crossovers events. However these proteins may be important for non-crossovers formation in other species like mice. Different studies suggested that ZMM proteins may be required early and possibly before the completion of stable strand exchange, may involve in strand invasion (Lynn *et al.*, 2007).

1.3.1.4.3. Recombination Frequency and Distribution

Recombination frequency can vary from one region to another and is not uniformly distributed throughout the genome, or even within a single chromosome (Roeder, 1997). Recombinations are not randomly distributed, but there are regions in which the frequency of recombination occurs more often than the average for the overall genome. These regions known as recombination hot spots, and correlate correspond to the sites of DSBs in yeast, and occur mostly in the regions that contain transcription promoters and the nuclease-hypersensitive sites such as DNase I and micrococcal nuclease (MNase); however, not all chromatin hypersensitive sites are DSB sites (White *et al.*, 1992; Xu & Kleckner, 1995; Smith, & Nicolas, 1998). In general, recombination hot spots correspond to GC high and certain transcriptional regions

which may be due to lower chromatin condensation of these regions. Studying high resolution mapping reveals that hot spot regions do not occur at a specific sequence but instead are scattered (Xu & Kleckner, 1995). Recombination hotspots consist of regions that are 1 kb to 2 kb wide, where recombinations are clustered - the average spacing between them is 50 to 100 kb in human and mouse. An estimated 25,000 to 50,000 hot spots are present in the human genome (Myers *et al.*, 2005). Some hot spots however have been found in coding sequences or at the junctions of artificial inserts (Bullard *et al.*, 1996). In *S. cerevisiae*, it is thought that hypersensitivity to MNase increases specifically at hot spots during early prophase and before DSBs form, this may be due to the assembly of a pre-initiating recombination complex at these sites which is necessary to provide a substrate to the DSB nuclease (Lichten & Goldman, 1995). Different studies show that most crossover hot spots are also non-crossover hotspots, suggesting that the same genomic regions can lead to both crossover or non-crossover events (Jeffreys and May, 2004). The ratio of crossover and non-crossover differs from one hot spot to another (Holloway *et al.*, 2006). Moreover, non-crossovers are usually clustered at the center of the crossover hot spots (Jefferys and May, 2004). Cold spots or the regions with low frequency of recombinations are found near centromeres and telomeres (Gerton *et al.*, 2000).

Chromatin, chromosome and genome structure also play an important role in regulating recombination (Froenicke *et al.* 2002; Sun *et al.*, 2004). Anderson and Stack (2002) have shown that in most organisms the number of recombinations correlates with total SC length at the pachytene stage and gene number, rather than total genome size. In general, recombination frequencies in euchromatin that contains genes are greater than in heterochromatin that contains a high proportion of repeated sequences (Schwazacher, 2003). Kong *et al.* (2002) reported that the intensity of G-band staining is inversely related to the recombination frequency in humans. Thus, chromosomes with the highest proportions of G bands should have shorter SCs and decreased levels of recombination than would be expected from their mitotic chromosome length. In contrast, in other organisms, such as *C. elegans*, recombination occurs preferentially in gene poor regions (Barnes *et al.*, 1995). In male humans and mice, recombination occurs at higher than average frequencies near telomeres (Ashley, 1994). Tapper *et al.* (2002) reported that CT/CA repeats that are associated with recombination are largely subtelomeric in human chromosome 21,

whereas in chromosome 22 they are widely distributed offering a greater chance for double recombination events. The pseudoautosomal region is a special recombination hot spot between X and Y chromosomes in male mammals (Rappold, 1993). Furthermore, if a single gene is inserted in an ectopic location of one yeast chromosome, it will strongly induce a recombination between that ectopic sequence and its normal chromosome counterpart. This is known as ectopic recombination (Lichten *et al.*, 1987).

In most organisms, small chromosomes recombine more per unit of physical distance than large chromosomes. If any chromosome is cut into two smaller chromosomes, the number of recombinations will increase (Kaback *et al.*, 1992). In human, the largest chromosome differs 5-fold in length from the smallest one; however, both chromosomes require at least one crossover to segregate efficiently (Tease *et al.*, 2002; Lynn *et al.*, 2007).

The positions of recombinations are not random, and they rarely occur close to each other. It is hypothesized that the formation of one recombination in a given chromosome region reduces the possibility of additional crossovers through transmitting an inhibitory signal to nearby potential sites of recombination (Egel, 1995; Sun *et al.*, 2004). The mechanism controlling crossover interference is not understood; however, it is thought that SC plays an important role in signal transmission since mutation in yeast *zip1*, which is transverse filaments of SC, eliminates the recombination interference (Sym & Roeder, 1994). Also some organisms, such as *S. pombe* and *A. nidulans*, do not exhibit interference since they fail to make SC (Egel-Mitani *et al.*, 1982; Bahler *et al.*, 1993). Also, male sex chromosomes (XY) do not have a homologous region except short pseudoautosomal, which is likely to be the place of XY DSB and meiotic recombination (Baudat and de Massy, 2007).

1.3.1.5. Chromosome Synapsis

Different analyses in yeast indicate that recombination and synapsis are concurrent events (Schwacha & Kleckner, 1994; Roeder, 1997). DSBs appear early in prophase and disappear in zygotene when synapsis initiates whereas mature recombinations are

produced at the end of pachytene. Formation and correction of the recombination intermediates are required to promote chromosome synapsis in all studied organisms except *C. elegans* and *Drosophila* (Borde, 2007). Defects in PMS2, MSH4 and MSH5 mice genes participate in recombination, resulting in abnormal chromosome synapsis (Baker *et al.*, 1995; Kneitz *et al.*, 2000; Mahadevaiah *et al.*, 2001).

Synapsis initiate at a few sites along the chromosome in most organisms. There is general correspondence between pairing initiation patterns and chiasma distribution and the regions of chromosomes that synapse first. Usually sub-telomeric regions tend to be where most chiasmata are found (Jones, 1984). Different cytological studies have demonstrated that synapsis initiates at the sites of recombination. Homologous chromosomes are held together at multiple sites known as axial association before the formation of SC and it is hypothesized that these connections serves as sites for initiation of synapsis, since different studies indicated that ZIP2 protein, which localizes to axial associations, is required for the initiation of synapsis (Albini & Jones, 1987; Rockmill *et al.*, 1995; Roeder, 1997). Synapsis initiates at discrete loci known as synaptic initiation complexes (SIC) which contains ZIP2, ZIP3, and ZIP4 proteins and shows the same genetic distribution as crossovers (Tsubouchi *et al.*, 2006; Costa and Cooke, 2007). In many organisms, the frequency of the synapsis sites are more than the frequency of crossovers and in some organisms the synapsis is initiated predominantly near the chromosome end while crossovers are not distally localized (Roeder, 1997). Some of these observations could be due to some synapsis initiation that is accompanied by non-reciprocal recombination (Ashley, 1994; Roeder, 1997). Analysis of the distribution of synapsis initiation in humans suggests that they are located near the subtelomeric regions, which correlates with the crossover distribution (Brown *et al.*, 2005). However, synapsis in some organisms such as *Drosophila* females, are not initiated at the recombination sites since mutations in two genes, W68 and mei-P22, eliminate the recombination, but do not have any effect on synapsis (McKim *et al.*, 1998). *C. elegans* is another exceptional case in which chromosomes synapse normally in a Spo11 mutant and this organism have a set of proteins, HIM-8, ZIM-1, ZIM-2 and ZIM-3, which interact with a chromosome-specific pairing centres to mediate pairing of specific chromosomes (Phillips and Dernburg, 2006).

Synapsis and recombination of homologous chromosomes are accompanied by chromosome conformation changes (Kelly and Aramayo, 2007). The sex chromosomes (X and Y) pair only at pseudoautosomal region (PAR) and the unpaired regions of the X and Y undergo transcriptional inactivation (Holmes and Cohen, 2007). Meiotic Sex Chromosome Inactivation (MSCI), which refers to the transcriptional silencing of the X chromosome in males in different species, forms a heterochromatic sex chromosomes during pachytene, and is an example of chromosome conformation changes (Kelly and Aramayo, 2007). Different phosphorylated proteins, such as H2AX, BRCA1 and MAELSTROM, have been isolated and localized around the X and Y chromosomes (Turner *et al.*, 2004; Costa *et al.*, 2006). Silencing also occurs for autosomes with no homologous partners which therefore fail to synapse. Thus, in general, chromosomes or regions without homologous partners are subjected to silencing during meiotic PI. Meiotic Silencing of Unsynapsed Chromatin (MSUC) is a conserved mechanism that silences any unsynapsed chromosome (Kelly and Aramayo, 2007). Recent studies show that MSCI accompanied with massive replacement of histone variant, H3.1 and H3.2, with H3.3, especially in XY (van de Heijden *et al.*, 2007). The main functions of meiotic silencing are genome defence to preserve their integrity, evolution and speciation (Kelly and Aramayo, 2007). The genes that are required for spermatogenesis are poorly represented on the X chromosome in mammals and worms. In species exhibiting MSCI, it seems heavily biased towards moving genes required for spermatogenesis from the X chromosome to autosomes (Kelly and Aramayo, 2007).

1.3.2. Metaphase I (MI)

Metaphase I is much shorter in duration and complexity than PI. During Metaphase I, the nuclear envelope is completely disrupted and the homologous chromosomes are held together and aligned on the equatorial plate with the kinetochores being the point of attachment to the spindles. Each pair of sister chromatids are present as a unit with both sister kinetochores facing the same direction, mono-orientation, resulting in pulling both sister chromatids of a homologue to the same pole at anaphase I (Nicklas *et al.*, 1997; Critchlow *et al.*, 2004).

During prometaphase, homologues attached to spindle microtubules of the same or opposite pole. For stable homologue configuration, the attachment should occur from opposite poles; however, if the attachment occurs from the same pole, the homologs dissociate and try again. The chromosomes proper orientation depends on tension that results from pulling the homologs toward opposite poles and the resistance of this pulling by chiasmata (Roeder, 1997).

1.3.2.1. Chiasmata

Chiasma is the site of crossing over between two non-sister chromatids that can be visualized at MI by cytogenetic techniques. The chiasmata play an important role in holding homologous chromosomes together after relaxation of synapsis and dissolution of the SC that occurs at the transition from pachytene to deplotene, in such a way that allows proper orientation of the maternal and paternal chromosome bivalent on metaphase I and during the next phase, Anaphase I, when they get separated (Moens *et al.*, 1987; Anderson & Stack, 2005; Barlow & Hultèn, 1998). It counteracts the spindle microtubules pulling forces to ensure a proper alignment of the bivalents in metaphase plate before their segregation (Turner, 2007). Chiasmata are cytological evidence of crossover events (Barlow & Hultèn, 1998). Failure of chiasma formation causes maternal and paternal homologous chromosomes to become disoriented leading to random segregation, and daughter cells may then receive maternal, paternal, both or none of these chromosomes (Hassold & Hunt, 2001).

Several studies explore different models of how chiasma holds homologous chromosomes together. One model hypothesis is that homologous chromosomes are held together at the chiasmata, since sister chromatids are glued together at distal region of chiasmata. Whereas another model suggests that homologs are held together by chiasma binding proteins (Roeder, 1997). However, studies in different organisms, such as humans, yeast and fruit flies, suggest that distal crossovers are less effective and less stable in proper disjunction than proximal ones, which supports the view that chiasma function depends on the sister chromatid cohesion (Koehler *et al.*, 1996; Lamb *et al.*, 1996; Ross *et al.*, 1996). Cohesion protein is important in stabilizing

chiasmata, so chromosome attachment until anaphase I (Costa and Cooke, 2007). In *Drosophila*, ORD is an important gene for meiotic sister chromatid cohesion and defects in this gene lead to segregation of sister chromatids before MI (Bickel *et al.*, 1997). SMC1 and REC8 are examples of mice cohesion proteins. SMC1 β knockout mice show increase in univalents and reduction in recombination (Costa and Cooke, 2007).

In different species, chiasmata have some tendency to sex-specific positioning along the chromosome. For example, chiasmata accumulated more often near the ends of chromosomes in human males than females, which occupy preferential positions slightly more interstitially (Hultèn *et al.*, 2005). However, the chiasma frequency in the grasshopper (*Eyprepocnemis plorans*) is lower in females compared with males, and females also have fewer proximal but more interstitial and distal chiasmata (Cano *et al.*, 1987). Chiasma formation is a dynamic process, varying somewhat between chromosomes and cells but there is surprisingly little variation in the pattern of chiasma frequency and their distribution along the lengths of individual chromosomes in normal fertile human males (Baker *et al.*, 1976).

1.3.3. Anaphase I (AI) and Telophase I (TI)

Anaphase I (AI) is a very rapid process, as evidenced by the absence of any AI spermatocytes in preparations from human testicular biopsy samples (Kleckner, 1996). At AI, the physical connections between homologs breaks down, while the sister chromatids connection at the centromere remains.

A gametocyte passing through anaphase I (AI) and Telophase I (TI) is expected to give rise to two daughter cells, containing the haploid chromosome number (Alberts *et al.*, 1994).

Proper segregation of homologous chromosomes depends on crossing over to establish chiasmata and the placement of genetic exchanges along the chromosomes length. Mis-located or absence of exchanges increases the chance of meiotic non-disjunction in most organisms (Hassold *et al.*, 2004). In fertile males at least one chiasma per chromosome is required to secure proper segregation at AI (Anderson & Stack, 2005).

Some chromosomes in certain organisms, such as *Drosophila* chromosome 4, do not recombine. Different studies suggest that Nod protein, which is a plus-end directed microtubule motor, plays an important role in achiasmata chromosome segregation (Hawley & Theukauf, 1993; Roeder, 1997). Nod is a DNA binding protein that is found along the length of all chromosomes at prometaphase, which can direct movement toward the metaphase plate and away from spindle poles (Afshar *et al.*, 1995). Nod protein can compensate for the absence of chiasmata by pushing the achiasmata chromosomes toward each other and the microtubule motor activity of this protein can provide a force that counterbalances the poleward forces (Theukauf & Hawley, 1992).

1.3.4. Meiotic Division II

At metaphase II (MII), as in mitosis, the sister chromatids are bi-oriented and sister kinetochores face the opposite direction. This will allow segregation of one chromatid per daughter cell during anaphase II (AII). The chromatids of individual MII chromosomes of spermatocytes are slightly separated and loosely coiled and have a tendency to hook into each other, which makes the chromosome investigation at MII problematic (Hultèn *et al.*, 2005).

Chromosome segregation efficacy at AI can be estimated by chromosome analysis of cells at MII. In human males, the analysis of MII indicates that AI mal-segregation is rare. The aneuploidy rate in human spermatocytes at MII is estimated to be less than 0.5-1% and the chromosome analysis of the mature sperm shows that around 2-3% of them are aneuploid with slightly increased rates in chromosomes 21, 22 and XY (Hultèn *et al.*, 2005). However, oocyte MII chromosomes are more condensed and therefore female mal-segregation is very common. Different studies estimated that aneuploidy and mal-segregation rates in human oocytes are around 15-20%, and there is a direct correlation between advanced maternal age and increased aneuploidy frequency, with an increased rate in smaller chromosomes (in particular trisomy 21) than larger ones (Hultèn *et al.*, 2005; Pellestor *et al.*, 2005). Different studies demonstrated that chromosome non-disjunction is not only caused by low frequency of exchange but also by the site of exchange. For example in yeast, distal exchanges

are less effective since they are perhaps more susceptible to premature disassembly resulting from a loss of sister cohesion (Bascom-Slack, 1997)

Meiotic sister chromatid cohesion is released first along the chromosome arms at AI; however, the cohesion near the centromeres is maintained until AII when individual chromatids segregate (Miyazaki & Orr-Weaver, 1994; Kleckner, 1996). In *Drosophila*, mei-S332 is an example of a protein that ensures the cohesion at the centromeric regions of chromosomes. This protein appears and associates with the centromeres during late prophase I and disappears at AII. Mutation of this gene leads to random segregation of the sister chromatids at AII (Kerrebrock *et al.*, 1995).

1.3.5. Meiotic Checkpoint

All meiosis processes have to be carefully coordinated. If any one goes wrong, the cell generally will be eliminated to prevent the generation of abnormal daughter cells (Turner, 2007). In order to ensure success of meiosis division, two different checkpoints have been identified that control the division. Firstly, the recombination checkpoint that ensures that recombination intermediates have been resolved before the cells exit pachytene. Different checkpoint proteins, such as PI3-like checkpoint kinase family (ATM, ATR in yeast), have been isolated. They are chromosome-associated signal transduction kinases that phosphorylate an array of recombination and repair proteins that serve to facilitate protein-protein interactions (Matsuoka *et al.*, 2007). Mutation of different genes that confer defects in recombination, such as ZIP1, DMC1, SAE3 genes in yeast, ATM gene in mice and mei-41 gene in *Drosophila*, leads to arrest of the cells at pachytene stage (Carpenter, 1979; Bishop *et al.*, 1992; Sym *et al.*, 1993; McKee & Kleckner, 1997; Xu *et al.*, 1995). However, there is no checkpoint to ensure the initiation of recombination since mutations that affect DSB formation in yeast do not prevent meiotic cycle progression and result in massive chromosome mal-segregation (Klapholz *et al.*, 1985; Alani *et al.*, 1990; Smith, & Nicolas, 1998).

The second checkpoint is the metaphase checkpoint that ensures all homologs have been properly oriented on the spindle before the cells exit metaphase I. The presence of unpaired chromosomes in male mice leads to arrest of the cell at metaphase I;

however, the female mice oocytes will complete the first meiotic division. This suggests that male and female meiosis have different cell cycle control such that females have less efficient mechanisms for monitoring meiotic chromosome behaviour (Hunt *et al.*, 1995). In human females, this mal-segregation results in aneuploidy that could lead to a variety of birth defects and miscarriages (Hassold *et al.*, 1996).

1.4. Testicular Development and Spermatogenesis in Horse

Normally the testes descend into a scrotum from last month of gestation to the first 10 days postpartum; however, there is some cases in which the testes descend into the inguinal region for some time. Failure of the testes to descend leads to a condition called cryptorchidism which could be unilateral (most common in horses) or bilateral. This condition can be treated either by hormonal therapy, such as Luteinizing hormone (LH) or human chorionic gonadotropin (hCG) in which the timing of the therapy is important especially for unilateral condition, or surgical therapy (Samper, 2009). Rotation of one or both testes, up to 180 degrees, is another condition that affects stallions and it is often transient and more common in certain breeds such as Welsh pony stallions (Samper, 2009).

The seminiferous epithelium has a unique architecture that cares for different developmental stages of germ cells, namely spermatogonia, primary spermatocytes, secondary spermatocytes and spermatids, from basal membrane towards the lumen of the seminiferous tubule, respectively (Holstein *et al.*, 2003). In newborn mammals, we can only find Sertoli cells, spermatogonia and preleptotene spermatocytes. However, in pre-puberty and adult testis, advanced leptotene, zygotene, pachytene and diplotene spermatocytes and spermatids appear (de Jonge & Barratt, 2006).

At birth, stallion testis contains few functional leydig cells and only indifferent supporting cells and gonocytes (progenitors of spermatogonia and Sertoli cells). The stallion then enters the infertile stage of its life that continues through ≥ 6 months but after this, he enters the pre-pubertal stage when changes are initiated (Mckinnon & Voss, 1992). The timing of this stage differs among stallions and might be influenced by breed and season of birth.

Puberty starts when the stallion is capable of reproduction (production of first spermatozoa). The increased production of gonadotropic hormones induces a massive mitotic proliferation of A-type spermatogonia into B-type spermatogonia competent to enter meiosis (de Jonge & Barratt, 2006). With some stallions, puberty starts at 14 months of age but it is two to four years after puberty that they achieve sexual maturity with maximum reproductive capacity. The population of equine Sertoli cells increases until 4-5 years of age and fluctuates with seasons; however, the adult equine testes have only a limited capacity to alter the ratio of Sertoli cells to germ cells (Jones & Berndtson, 1986). For most stallions, no change in daily sperm production occurs between 4 and 20 years of age, with adult stallions producing billions of spermatozoa daily. It is estimated that the two testes produce about 70,000 spermatozoa each second during the breeding season (Mckinnon & Voss, 1992).

Daily sperm production (DSP) in horses is affected by season. It declines during the non-breeding season and averages 50% in stallions between 6 to 20 years old (6.40 vs 3.19 billion spermatozoa daily). This could be due to testicular weight decreasing in the non-breeding season, in addition to environmental factors such as day length or temperature, drugs or unknown factors can lead to increased degeneration of germ cells (Jonson, 1991; Mckinnon & Voss, 1992). The seasonal differences in number of spermatogonia are greater than seasonal differences in sperm production. There are also seasonal differences in the given spermatogonial subtypes that degenerate as there is a greater yield early and a reduced yield late in spermatogenesis during the breeding season (Jonson, 1991). Maximum DSP occurs in May and June and minimum production occurs in July and August (Mckinnon & Voss, 1992). Testicular size may differ greatly among stallions, depending on breed, season, age and reproductive status, and is correlated to spermatozoa production rate (Mckinnon & Voss, 1992; Samper, 2009). As in most species, testicular parenchymal weight correlates with DSP, which is a useful predictor of a stallion's breeding potential, and can be measured in most stallions. The DSP in stallions is estimated to be around 18-20 million sperm per gram of testicular parenchyma. The testicular size measurement can be assessed by either caliper or ultrasonographic measurement (Samper, 2009).

The duration of spermatogenesis is about 57 days in stallions according to Amann (1981) and Johnson (1990), although others have been reported it to be 55 days (Swierstra *et al.*, 1975) and it is not influenced by season. This process takes 72 days

for humans, 61 days for bulls and 60 days for rats (Mckinnon & Voss, 1992). The duration of spermatogenesis in stallion (57 days) represents three phases: spermatogoniogenesis (19.4 days), meiosis (19.4 days), and spermiogenesis (18.6 days; Mckinnon & Voss, 1992). Swierstra *et al.* (1975) concluded that the duration of one cycle of seminiferous epithelium was 12.2 days, which means that at any given area within the seminiferous epithelium the same cellular stage is repeated every 12.2 days. Because total duration of spermatogenesis is apparently 4.7 cycles of the seminiferous epithelium (12.2 days), spermatogenesis requires about 57 days in stallions. Using information on relative frequency for each stage and data for the duration of the cycle of the seminiferous epithelium, the life span of each stage has been calculated. The life spans of primary spermatocytes, secondary spermatocytes, and spermatids are reported as 18.7, 0.7, and 18.6 days, respectively. Knowledge of the time required to produce a spermatozoon is essential for understanding the recovery time after trauma to the testis or drug injection (Mckinnon & Voss, 1992; Holstein, 2003).

The spermatogenic cycle progression is not synchronized along the length of the seminiferous tubule, but it is distributed in distinct waves in a loop. This leads to an even distribution of all spermatogenic stages throughout the epithelium, which enables a stable and an uninterrupted daily spermatozoa output (de Jonge & Barratt, 2006). Spermiation, the process of releasing the spermatozoa into the seminiferous tubular lumen, occurs at approximately 12-day intervals, which is known as one cycle of seminiferous epithelium. Following spermiation, the sperm are transported into the rete testis, which are extensively branched and fuses with efferent tubules that finally fuse with epididymal duct (Samper, 2009). As the sperm are transported, they undergo a number of physiologic and morphologic maturational changes such as capacity for motility, DNA stabilization, acrosomal membrane alteration and metabolic changes (Samper, 2009).

1.5. Genetic Basis of Horse Infertility

Cytogenetic errors during male meiosis can be responsible for the birth of a child with abnormal karyotype or spontaneous abortion and stillbirth. It is evident that the abnormal chromosomes behaviour during meiosis is the major underlying reason for

infertility (Menchini *et al.*, 1981; Koulischer *et al.*, 1982; Egozcue *et al.*, 1983; Braekeleer *et al.*, 1991). In humans an estimated 20% of male infertility problems can be explained by abnormalities in mitotic and/or meiotic chromosomes (Braekeleer *et al.*, 1991). In cattle, an azoospermic bull carrier of a reciprocal translocation (rcp 8;13) showed meiotic arrest in 61.2% of cells. Reciprocal translocations usually produce a lot of unbalanced sperm frequency, which depend on the structure of the translocation (Villagómez & Pinton, 2008).

When meiosis goes wrong it can lead to severe fertility problems, most commonly through non-disjunction of chromosomes resulting in aneuploidy, which is the leading cause of pregnancy loss and mental retardation in humans (Critchlow *et al.*, 2004). In addition, many defects in meiosis can cause apoptotic spermatocytes or megalospermatocytes (Holstein *et al.*, 2003).

Infertility could be either primary or secondary. Primary infertility is in the case of no pregnancy; however, secondary infertility is where there has been a pregnancy regardless of the outcome (Seshagiri, 2001). The causes of the infertility can be traced by either male or female factors in addition to idiopathic condition (Seshagiri, 2001).

It is believed that most of the non-obstructive azoospermia can be explained on a genetic basis (Hargreave, 2000). It is hypothesized that many of idiopathic non-obstructive cases are due to abnormalities in pairing/synapsis and/or recombination at meiosis I that subsequently can result in meiotic arrest or abnormalities in chromosome segregation or non-disjunction (Bascom-Slack *et al.*, 1997).

Chromosomal aberrations in horses can cause congenital abnormalities, embryonic loss and infertility (Lear & Bailey, 2008). Chromosomal abnormalities are well documented in mares but less known in stallions (Morel, 1999). Some abnormalities are associated with mares infertility such as Turners syndrome, a female with a single X chromosome (63XO), mosaic chromosomal configuration (63XO:64XX) and quarter/deletion (64XY; Morel, 1999). Bugno and colleagues (2000) found that 2% of 500 randomly selected mares and stallions from different breeds had a chromosomal abnormality and 3.7% of the 272 mares had chromosomal abnormalities and mainly sex chromosomes including one mare with Turners syndrome monosomy (63XO) and seven with mosaicism (63XO:64XX; Lear and Bailey, 2008).

Some reports describe the chromosomal abnormalities in stallions as different forms of sex chromosome mosaicism such as (63XO:64XY; 64XX:64XY; etc). Mäkinen and colleagues (2000) reported Klinefelter syndrome (65XXY) in French Trotter stallions with normal sexual behavior but azoospermia and small soft testes and small penis, in addition to a mosaic form (64XY:65XXY) in a standardbred trotter with azoospermia and normal testes (Lear and Bailey, 2008). The mosaic form of Y chromosome disomy (63X:65XY) was reported in a few horses and the histological examination of the inguinal gonads showed seminal hypoplasia with no mature spermatogonia and hypertrophy of the Leydig cells (Paget *et al.*, 2001). Other autosomal trisomy, such as trisomy 28 (colt with small stature and azospermia) or trisomy 23 (colt with multiple developmental defects), can be explained by abnormalities in meiosis particularly chromosomal non-disjunction (Lear and Bailey, 2008). It is hypothesised that trisomy involving larger chromosomes may cause a severe disorder such as early embryonic loss (Lear and Bailey, 2008).

Besides numerical abnormalities of sex chromosome in horses, structural abnormalities like sex-reversal syndromes (64XY or 64XX) that are due to mutations, deletions or duplications in genes especially in the SRY region on the Y chromosome and androgen receptor proteins (testicular feminization or androgen insensitivity syndrome) on the X chromosome (Xq), may also lead to phenotypic reproductive disorder. Horses with these abnormalities are phenotypic females but genotypic male (64XY) (Lear and Bailey, 2008). The XX-sex-reversal horses are suspected to be inherited as autosomal recessive disorder. Female horses with this abnormalities exhibit different male-like phenotypes such as small penis, testes but azoospermia or some internal or external organs such as ovarian tissue (Buen *et al.*, 2000). Moreover, some translocation, such as (64XY;t(1;30)), reduce the stallion fertility but revealed normal phenotype (Long, 1996).

Furthermore, other autosomal abnormalities, such as deletion in q arm of horse chromosome 13 (64XY;del(13)(qter)), can exhibit infertile stallions with abnormal spermatozoa and poor motility (Lear and Bailey, 2008).

It is believed that most Y chromosome genes are involved in sexual differentiation. Thus any defect in these genes will lead to phenotypic abnormalities unless there are any autosomal homologous genes (Seshagiri, 2001).

1.6. Importance of the study

Spermatogenesis abnormalities can cause significant economic loss for horse breeders due to production losses as well as the cost of care for the stallion, mare and foal. Thus, knowledge of testicular function and understanding the normal stallion spermatogenesis, particularly meiotic division, as well as developing an accurate method for assessing spermatogenesis are important for the industry. It will place the equine practitioners, who are involved with the care of breeding stallions, and the clinician in a better position to monitor the health and reproductive status of the stallions and avoid actions that may interfere with normal testicular function as well as recognize possible origins of any alterations in spermatozoa production.

1.7. Project Aims

Most of our understanding of detailed pathways of meiotic recombination has come from studies of lower eukaryotes. However, over the past few years meiosis has increasingly become the focus of genetic, molecular and biochemical studies. Genes encoding different structural components of meiotic chromosomes and recombination enzymes have been cloned and sequenced. Several components of the mammalian meiotic recombination pathway have been identified and new molecular and cytological approaches for analysis of mammalian meiosis have been developed; however, surprisingly little is known about meiotic processes in horses (Hassold *et al.*, 2000). Areas such as homologous chromosomes pairing, crossing over, metaphase chromosome configuration and segregation have not been explored in detail in the horse. Consequently, little is known about the overall number and location of meiotic exchanges in individual germ cells.

Therefore, the main aims of this project are to explore equine spermatogenesis with emphasis on meiosis, particularly Prophase I (PI) and Metaphase I (MI). This study can provide an insight into fertility problems in horses and will be invaluable for horse breeders.

Specific Aims:

1. To study the meiotic homologous chromosome pairing, chiasmata distribution and frequency as well as chromosome configuration and segregation during meiosis I division.
2. To investigate the homologous pairing during prophase I using FISH to identify different homologous chromosomes on surface spread nuclei and estimate the recombination frequency using immunocytochemistry to localize different meiotic recombination proteins to PI preparation.
3. To determine the viability of stallion sperm by investigating its nuclei, mitochondria, flagella tail and acrosome integrity.

Chapter 2

Metaphase I: Chromosome Configuration, Chiasmata Distribution and Frequency

2.1. Introduction

Meiosis I is the process during which genetic content of a diploid somatic precursor cell reduces to a haploid gametic content with the diploid genetic content restored after fusion of gametes (Barlow and Hultèn, 1998). It is a complex process during which homologous chromosomes pair and synapse enabling the exchange the genetic material during meiotic recombination (Judis *et al.*, 2004). The physical location of meiotic crossing over can be visualized as chiasmata at metaphase I (Jones, 1984; Anderson *et al.*, 1998). Crossovers are not evenly distributed among the chromosomes or their length. Ordinarily, each bivalent has at least one obligatory crossover and additional events are proportional to different factors, such as chromosome length and interference (Kaback *et al.*, 1992; Anderson *et al.*, 1998). Recombination occurs mainly in euchromatin, gene rich regions, and the occurrence of one exchange in one region reduces the likelihood of another nearby (Anderson *et al.*, 1998).

The cytogenetical or diakinesis approach is a classical method that based on recording the numbers and locations of chiasmata at either deplotene, in which the chromosomes are twisted and difficult to distinguish, or diakinesis/metaphase I (MI) stages, in which the chromosomes are contracted (Laurie and Hultèn, 1985; Barlow and Hultèn, 1998; Sun *et al.*, 2006). These investigations provide an unique insight information on the chiasmata distribution and frequency as well as chromosomal configuration in different organisms providing a tool to estimate the genetic map interval.

Individual chromosome identification is more difficult at meiosis than mitosis since at meiosis the chromosome configurations are more complex and centromeres more difficult to visualize than during mitosis (Saadallah and Hultèn, 1983). Therefore, in order to utilize MI karyotyping, fluorescence *in situ* hybridisation (FISH), using chromosome specific fluorescently labelled probe, can be applied after a cytogenetic MI assay, to identify individual chromosomes, which permits the analysis of recombination frequencies and distributions for each specific pair of chromosomes. There have been few studies on these combined assays. Hultèn and colleagues have reported the chiasmata frequency in human individual chromosomes in seven infertile men and localized the chiasmata in one fertile and one infertile individual (Hultèn, 1974; Laurie and Hultèn, 1985a.; Laurie and Hultèn, 1985b).

In this chapter, Optimization of the air dry technique was carried out and used to investigate the chiasmata distribution and frequency as well as chromosomal configuration during metaphase I. Moreover, for the first time, recombination maps were constructed for eight different stallion autosomes at MI using the FISH technique.

2.2. Materials and Methods

2.2.1. Materials

2.1.1.1. Mouse material

Two testicular samples were obtained from adult male mice from the animal house of the Central Veterinary Research Laboratory, Dubai, UAE. The animals were sacrificed by cervical dislocation, and the testes were immediately dissected and processed, as described below. These samples were used to practice the techniques.

2.1.1.2. Equine material

Twenty-four stallion testis samples were obtained from Dubai Equine Hospital, Dubai, and Sharjah Equine Hospital, Sharjah, UAE. Testicular materials were obtained after surgical castration under full or local anesthesia.

2.2.2. Methods

2.2.2.1. Testicular Gross Examination

All castrated stallion testicular samples were examined before processing for normal size (80 mm to 140 mm in length by 50 mm to 80 mm in width) and weight (approximately 150 g to 300 g) and appearance according to Amann R.P description.

2.2.2.2. Meiotic Analysis Methods

A small piece of tissue, around 1 cm³, was minced in Ham F10 media (Invitrogene, UK) within 30 min of collection. Cells were squeezed out using two sharp curved forceps and the cell suspension was divided into four parts for different purposes namely: direct microscopic examination, air dry technique (to study metaphase I, anaphase I, metaphase II and pre-meiotic metaphase), surface spreading technique (to study prophase I), and storage in 10% glycerol at -80 °C for future use.

2.2.2.3. Direct Microscopic Examination

Cells, from the cell suspension, were diluted 1:3 using normal saline (0.9% w/v NaCl) and one drop was placed on a clean slide. The slides were examined under light microscope for the presence and motility of the spermatozoa.

2.2.2.4. Air Dry Technique (Metaphase I)

Fresh material, within 30 min of castration, was used for this part of the study. One to two ml of cell suspension was transferred to a 15 ml falcon tube. Twelve ml of freshly prepared, pre-warmed (37 °C) 1% tri sodium citrate (hypotonic solution) was added to the cell suspension drop by drop as the cell suspension was gently mixed.

Optimization was carried out by incubating at different temperatures (37 °C and room temperature) and timings (10, 15, 20, 25, 30, and 35 min). The best conditions to get good-quality of MI cells were either 37 °C for 20 min or room temperature for 25 min. At the end of hypotonic treatment, 1 ml of cold fixative (3:1 v/v methanol:acetic acid) was added and the cell suspension was centrifuged at 400xg for 10 min after which the supernatant, which contained most of the spermatozoa, was discarded. The pellet was resuspended in fresh fixative and left on ice for 15 min. The fixative was changed three to four times at 15 min intervals and cells were resuspended in an appropriated volume (around 5 ml) of fixative. The slides were stained in Giemsa stain (Merck, Germany) (1:20 v/v Giemsa:phosphate buffer) at pH 6.8 for 2 min and examined under the light microscope for the presence of metaphase I and II cells as well as premeiotic mitotic spermatogonia metaphase.

The number of configurations and chiasma at metaphase I were counted in 1,107 cells from fourteen stallions and the average number of different chiasma/ta per bivalent as well as the total chiasmata per cell was calculated.

2.2.2.5. Meiotic Chromosomes Individual Identification

Fluorescent *In Situ* Hybridization (FISH) technique was used to identify 8 different chromosomes (chromosomes 2, 6, 10, 13, 15, 24, 26 and 31). The metaphase I cells from 5 different horses were scored for chiasmata frequency and distribution and the coordinates noted for subsequent FISH analyses. For FISH, slides were Giemsa

destained by soaking in fixative (3:1 methanol:acetic acid) for 5 min followed by methanol for 5 min before air-dried. Slides were dehydrated with serial alcohol (70%, 90% and 100% ethanol) 5 min each. A 15 µl of probe cocktail containing indirectly labeled DNA probes specific for chromosomes 2, 6, 10, 13, 15, 24, 26 and 31 (Table 2.1) (a gift from Terje Raudsepp, Texas A & M University, Texas, USA) and hybridization buffer (Chrombios, Germany) was overlaid on the slides. A coverslip was placed on each slide, and sealed with rubber cement. Slides were placed on an 85 °C hot plate for 6 min and incubated overnight at 37 °C in a humidified chamber. Slides were then washed 2 times in 2X SSC solution, containing 50% formamide (Q-Biogene, USA), for 5 min at 45 °C, soaked in 2X SSC for 5 min at 45 °C followed by 2 washes with 4X SSC containing 0.1% Tween 20, for 5 min (first time at 45 °C and second time at room temperature). After blocking by soaking in 4X SSC solution, containing 5% non-fat dry milk, at room temperature for 5 min, slides were incubated with 100 µl streptavidin-FITC and anti-DIG TRITC cocktail and incubated at 37 °C in humidified chamber for 30 min. The slides were washed 3 times with 4X SSC solution, containing 0.1% Tween 20, with constant agitation, at room temperature for 10 min each time. After the slides were air-dried, antifade with DAPI (Vectashield, Germany) was applied to the slides. In order to analyse the slides, bivalents were relocated using the images generated for the previous chiasmata analysis; labeled bivalents were visualized using an Olympus BX61 fluorescence microscope (Olympus, Japan). Images were captured using Applied Imaging Cytovision 3.1 software (Applied Imaging, UK). Chiasmata localization and frequencies for the 8 chromosomes was carried out.

Table 2.1: Probes for different horse chromosome

^a Horse chromosome	Gene/marker symbol	Cytogenetic location	Label/Color
2	PNOC	2q13	DIG/TRITC
6	NINJ2	6q12-q13	BIO/FITC
10	PREP	10q17	BIO/FITC
13	ATP8VOC	13q15-16	BIO/FITC
15	LTBP1	15q24	DIG/TRITC
24	CHGA	24q16.2-16.3	DIG/TRITC
26	ROBO2	26q14	DIG/TRITC
31	MAP3K4	31q13	BIO/FITC

^a DNA probes are a gift from Terje Raudsepp, Texas A & M University, Texas, USA

2.2.2.6. Statistical Analysis

The descriptive and inferential statistics were applied through SPSS (version 16) and using the statistical software in the Excel package (Version 2007, Microsoft Corporation, Redmond, WA, USA). The statistics used were F statistics (ANOVA) to test the viability and variability across horses. In all cases, significance level was set at $P < 0.05$.

2.3. Results

2.3.1. Mouse testicular samples

Mouse samples were used to practise the techniques which resulted in good-quality meiotic preparations and chromosome configurations (Figure 2.1). Nineteen autosomal bivalents and XY bivalent were observed with different configurations such as rod, ring and cross shape and each bivalent has at least one chiasma. Eight MI cells from two mice were scored for the chiasmata frequency and the genome wide chiasmata distribution per cell ranged from 21 to 27.

Different stages of meiosis were observed such as primary spermatocyte diakenesis in which the chromosomes repel each other (Figure 2.2) and premeiotic mitotic metaphase (spermatogonial metaphase) that have 40 chromosomes, in which the chromosomes are shorter than normal mitotic chromosomes (Figure 2.3).

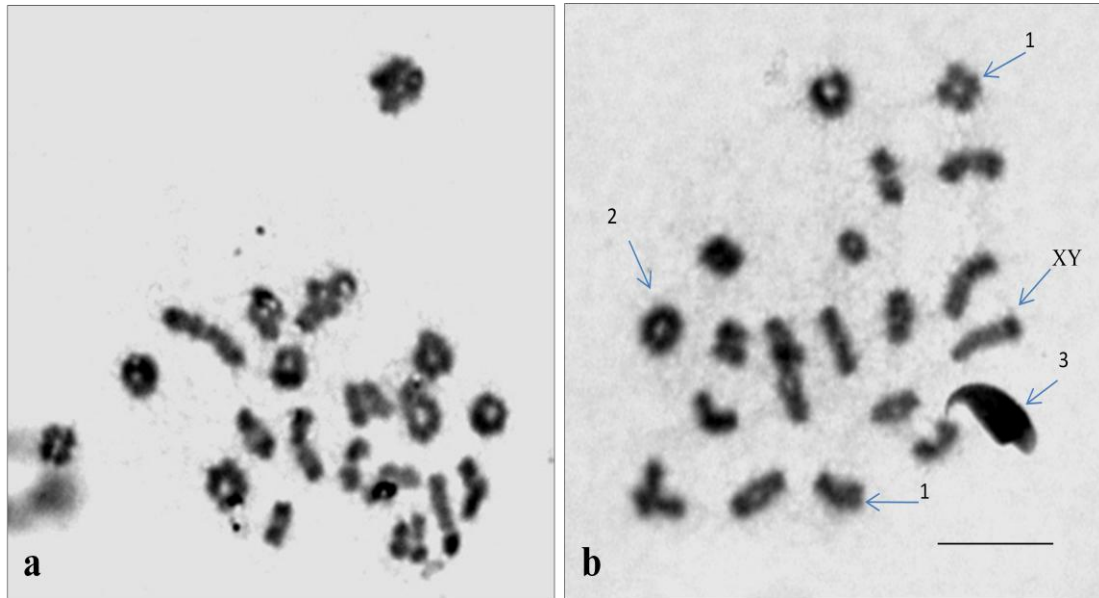


Figure 2.1 Primary spermatocytes (MI) preparations from normal mice. (a & b) different MI from 2 different mice with 19 autosomal bivalents and an XY bivalent. Bivalents forming different configurations such as: (1) Rod or cross shape bivalent with 1 chiasma. (2) Ring shape bivalent with 2 chiasmata. (3) spermatozoa head (hook-shaped) and XY bivalent is clear with 1 chiasma and rod shape. Giemsa stain. Scale bar—10 μ m.

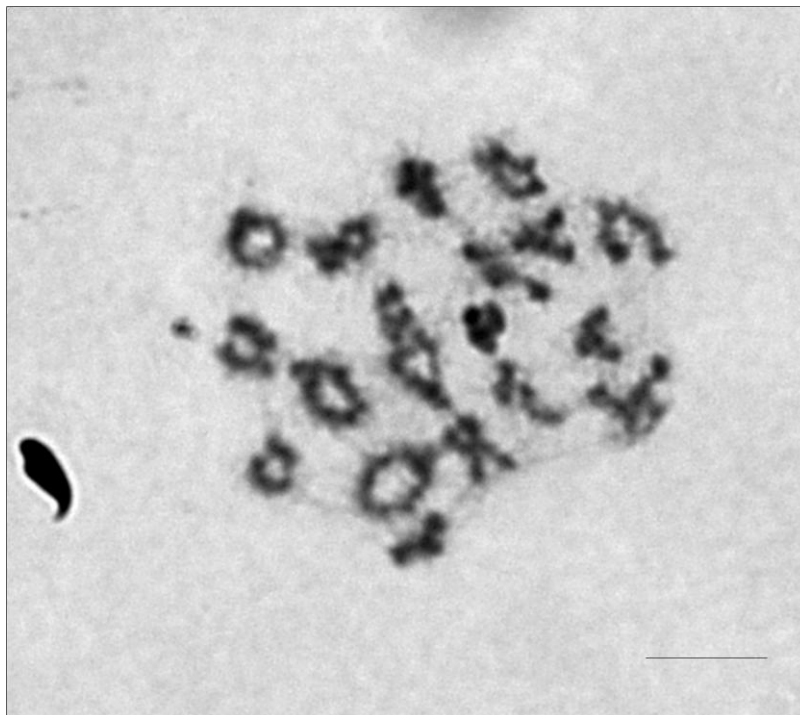


Figure 2.2 Primary spermatocyte diakinesis preparation from normal mouse male. Twenty homologous chromosomes repel from each other. Giemsa stain. Scale bar—10 μ m.

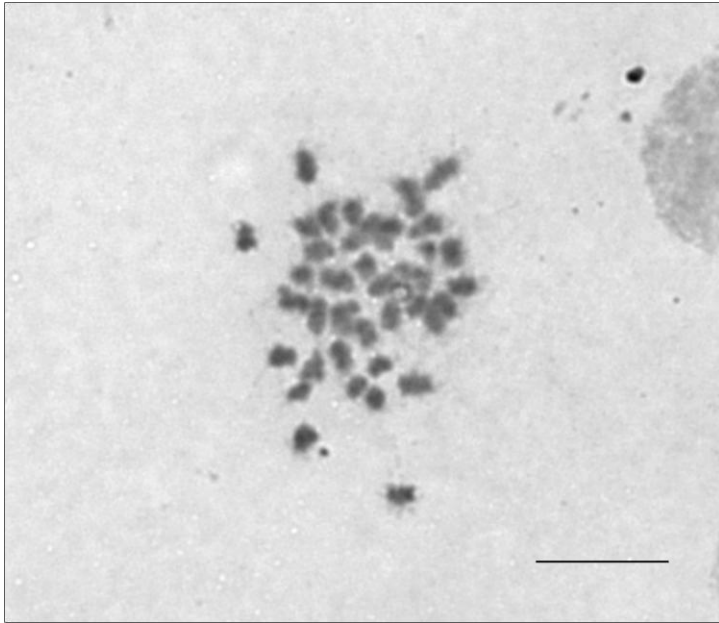


Figure 2.3 Spermatogonial metaphase from normal mouse male preparation. Forty individual small chromosomes can be seen. Giemsa stain. Scale bar—10 μ m.

2.3.2. Horse testicular samples

2.3.2.1. Gross and Direct microscopic examination

All stallion testicular samples show normal size and appearance (Table 2.2). Direct microscopic examination of the cell suspension revealed horse spermatogenesis with different cell stages and a good number of spermatozoa; however, most of them (> 90%) are immotile.

Table 2.2: Descriptions of materials used in this study

S. No.	Horse ID	Date of castration	Age at Castration Time	Castration Procedure	Fertility Status	Testes Weight	
						Right Testis	Left testis
1	H6	15-04-07	3.5	Local Anaesthesia	Fertile	190	195
2	H11	18-11-07	3	General Anaesthesia	Fertile	200	210
3	H12	20-11-07	6	Local Anaesthesia	Fertile	185	195
4	H13	26-11-07	3	General Anaesthesia	Fertile	205	190
5	H14	15-02-08	5	Local Anaesthesia	Fertile	210	220
6	H15	30-10-08	3.5	Local Anaesthesia	Fertile	200	190
7	H16	17-03-09	4	Local Anaesthesia	Fertile	215	230
8	H17	25-05-09	3	Local Anaesthesia	Fertile	210	244
9	H18	28-05-09	3	Local Anaesthesia	Fertile	362	310
10	H19	09-06-09	6	Local Anaesthesia	Fertile	283	291
11	H20	24-04-09	4.5	General Anaesthesia	Fertile	290	295
12	H22	01-12-09	4	General Anaesthesia	Fertile	122	140
13	H23	14-12-09	4	General Anaesthesia	Fertile	175	180
14	H24	14-12-09	3.5	General Anaesthesia	Fertile	200	190

2.3.2.2. Air dry technique (MI)

2.3.2.2.3. Spermatogenesis cell stages

Different stages with a good-quality preparation of meiosis were observed such as: (1) Primary spermatocyte metaphase (MI), which has 31 autosomal bivalents and XY bivalent with different configurations such as rod, cross and ring shape that can be accurately counted in most of the preparation. However, sometimes the bivalents are twisted and overlapped and the centromer regions appear darker than the rest of the bivalents (Figure 2.4 and 2.5); (2) Primary spermatocyte diakinesis (Figure 2.6); (3) Meiotic metaphase II (MII), in which the chromatin of individual chromosomes are loosely coiled, fuzzy, twisted and slightly separated that make it difficult to count or identify them with the present technique (Figure 2.7); (4) Pre-meiotic mitotic metaphases (spermatogonial metaphases), which were relatively rare in air-dry preparations and have 64 chromosomes. The chromosomes appear shorter than normal mitotic chromosomes and it is difficult to identify individual chromosomes. The chromosomes showed different degree of contraction in different cells. For instance, some cells have clear long chromosomes with centromeres and separated chromatids (Figure 2.8 a and b); however, others have curved and short chromosomes with unclear centromeres (Figure 2.8 c and d). (5) Prophase I (PI), which is the predominant cell type in meiotic preparations and they were numerous in every stallion examined. The chromosomes and bivalents cannot be identified in the cells (Figure 2.9). Different substages of PI were observed such as zygotene and pachytene. (6) Many Sertoli cells were observed that are large in size and usually have 2 or 3 nuclei (Figure 2.10).

The slides were made in different ways such as dropping from a proximal distance (approximately 10 cm) or far distance (approximately 70 cm) and by treating in cold methanol or by blowing. No differences were observed between dropping the cell suspension on the slides from close or far distance; however, blowing on the slides produced a better spreading of metaphase chromosomes than treatment with cold methanol.

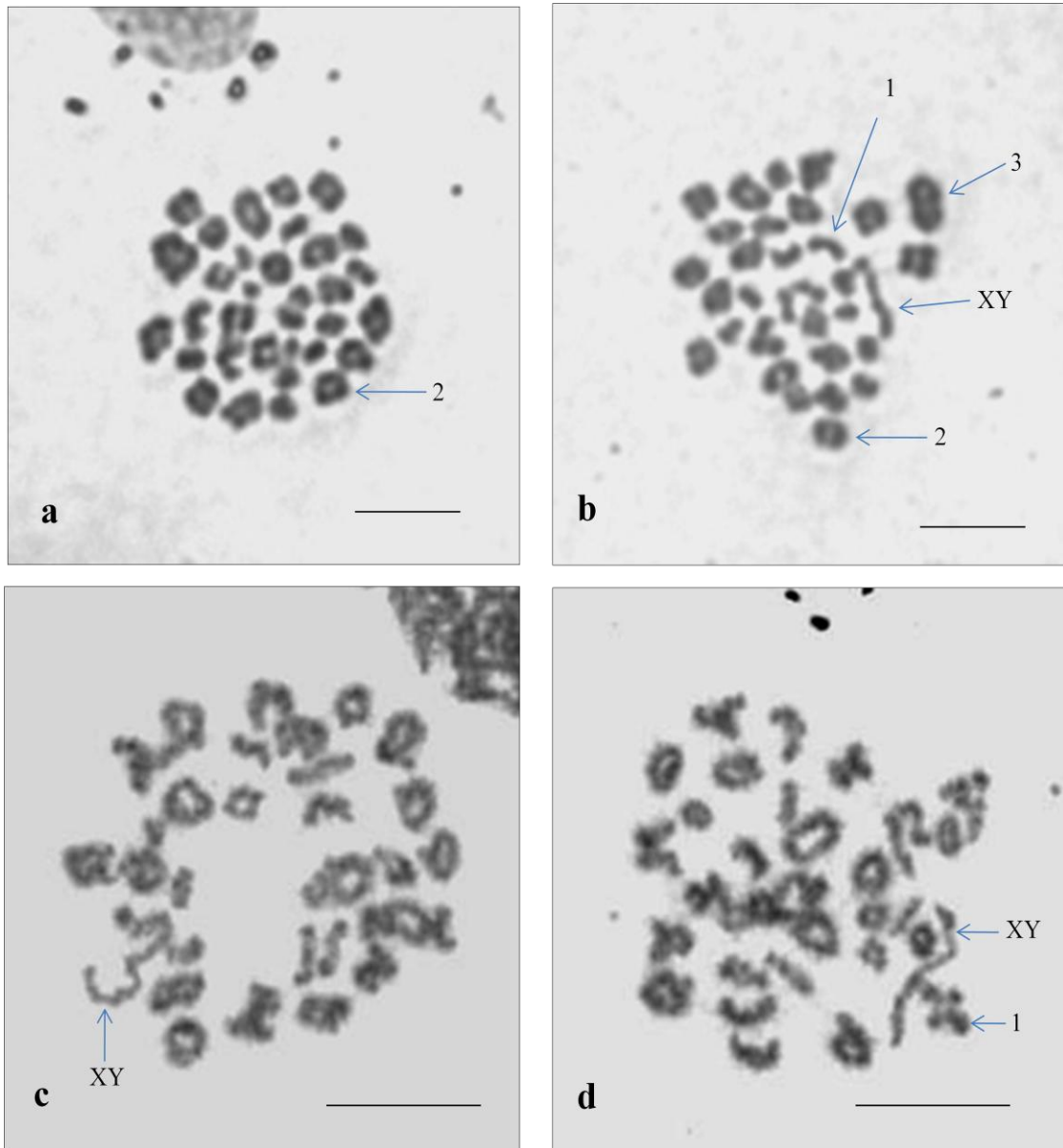


Figure 2.4. Different primary spermatocyte metaphase I (MI) preparations from different normal stallions (a-d). Thirty-one autosomal bivalents and XY bivalent with different configurations such as: (1) Rod or cross shape bivalent with 1 chiasma; (2) Ring shape bivalent with 2 chiasmata; (3) Bivalent with 3 chiasmata. XY bivalent is clear with 1 chiasma and rod shape. Giemsa stain. Scale bar—10 μ m.

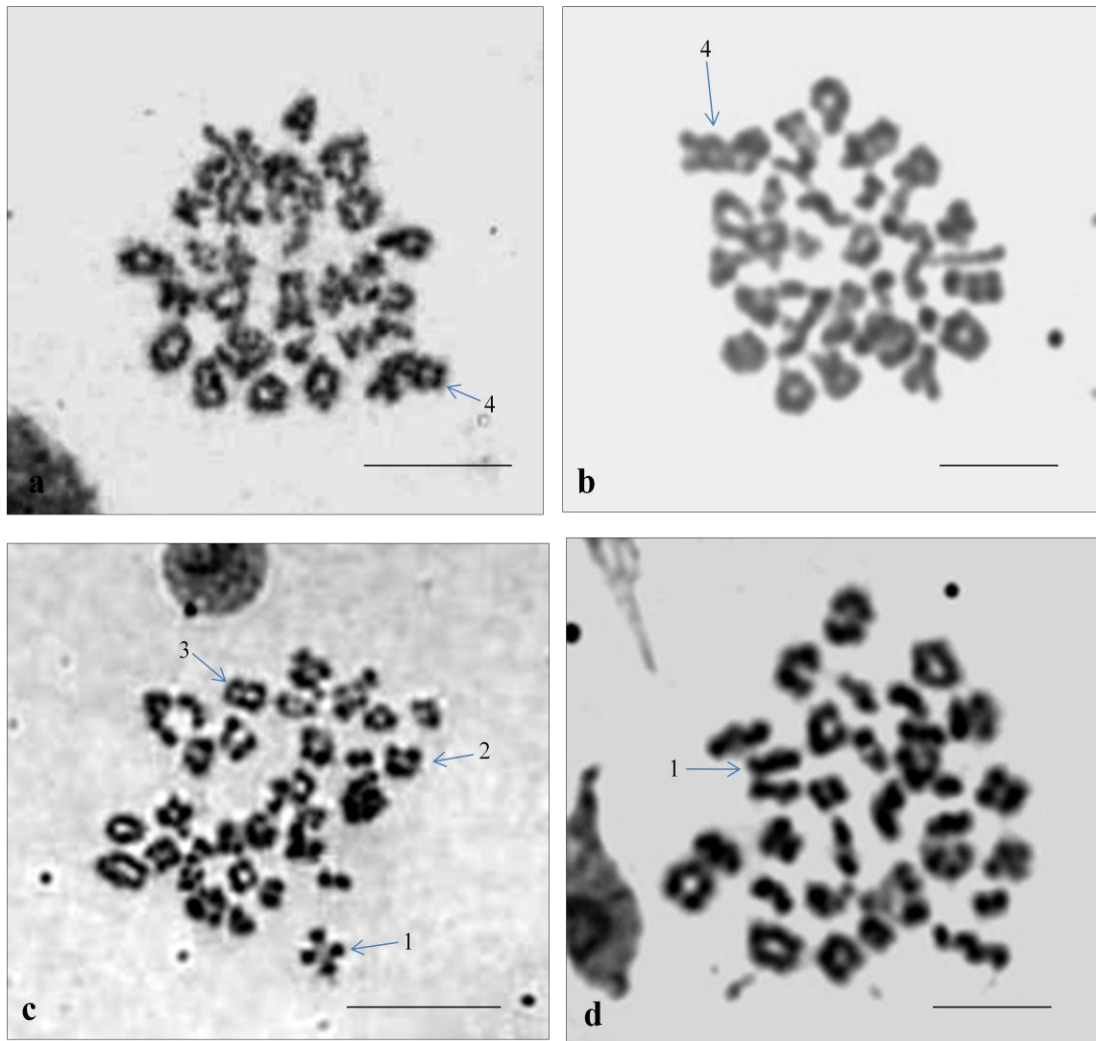


Figure 2.5. Different primary spermatocyte metaphase preparations from normal stallions (a-d). Different configurations can be seen such as: (1) Rod or cross shape bivalent with 1 chiasma; (2) Ring shape bivalent with 2 chiasmata; (3) Bivalent with 3 chiasmata and; (4) bivalent with 4 chiasmata (a and b). (c) MI cell with high chiasmata frequency. (d) MI cell with low chiasmata frequency. Giemsa stain. Scale bar—10 μ m.

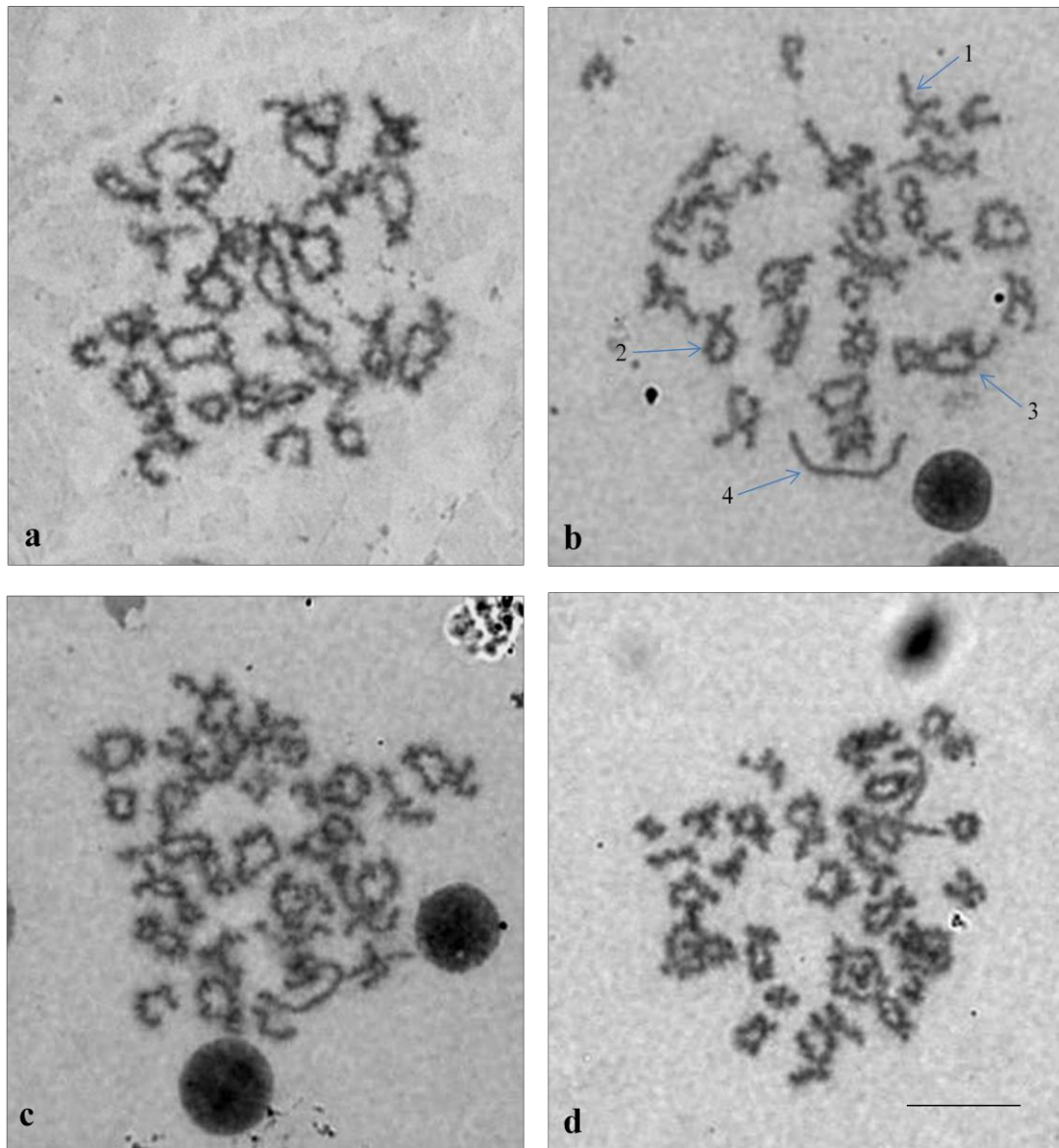


Figure 2.6: Different primary spermatocyte diakinesis preparations from 4 different normal stallions (a-d). This Figures show 32 different bivalents with different configurations. The homologous chromosomes repel each other with different configurations such as: (1) Rod shape bivalent with 1 chiasma; (2) Bivalent with 2 chiasmata; (3) Bivalent with 3 chiasmata and; (4) XY bivalent with 1 chiasma and rod shape. Giemsa stain. Scale bar—10 μ m.

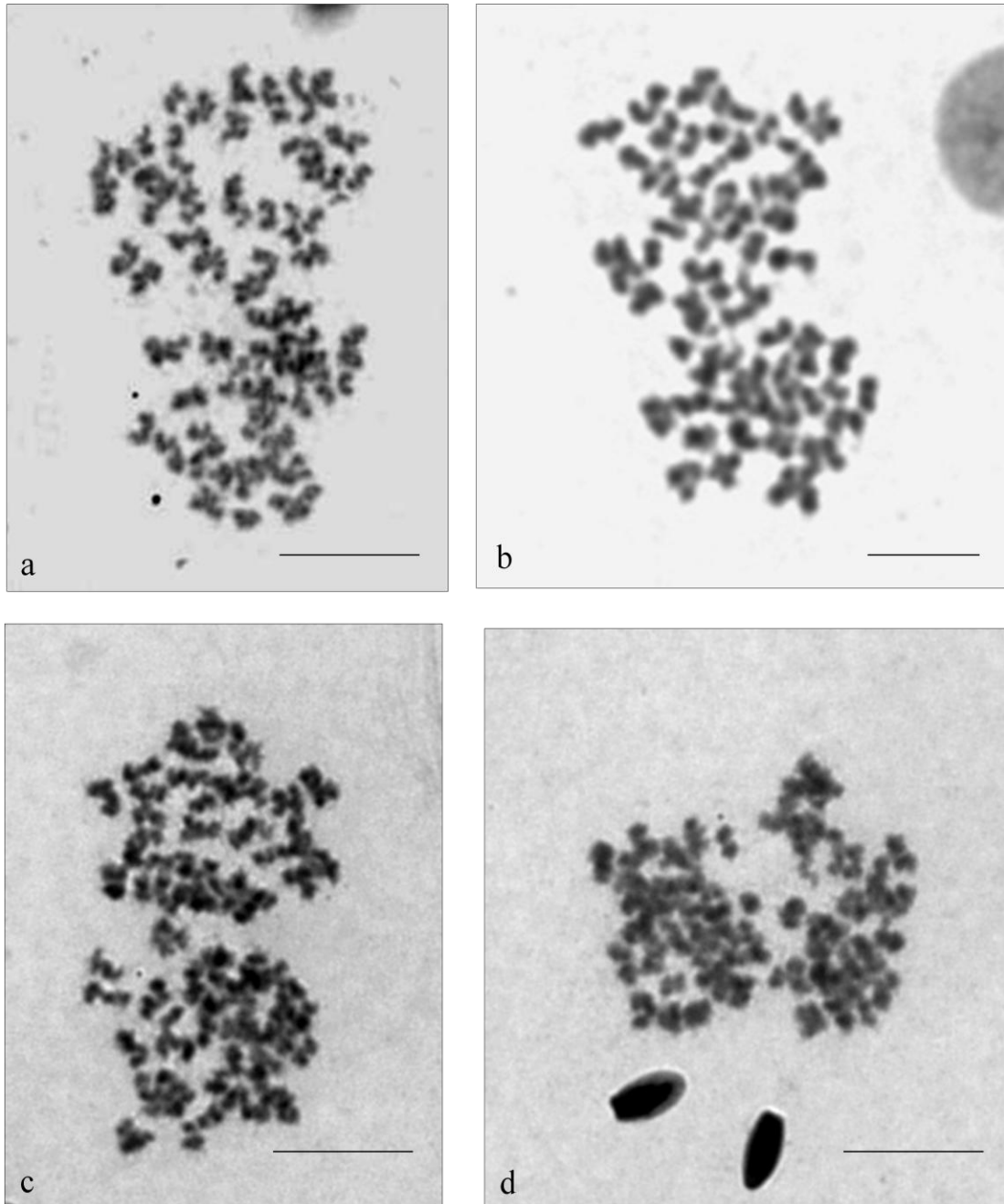


Figure 2.7: Second meiotic metaphase (MII) preparations from 4 different normal stallions (a-d). Chromosomes are coiled, fuzzy and twisted. Giemsa stain. Scale bar—10 μ m.

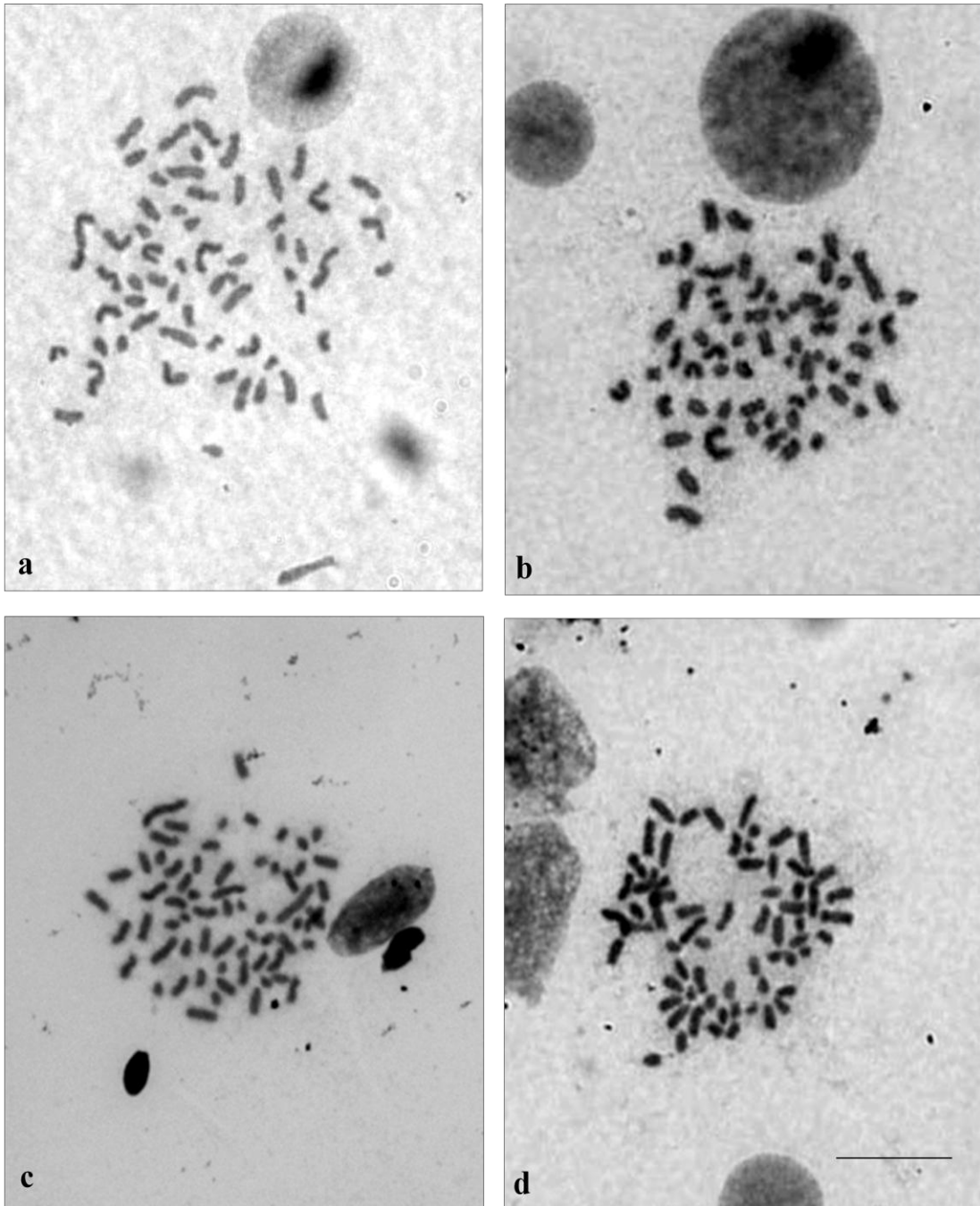


Figure 2.8: Pre-meiotic mitotic metaphase (spermatogonial metaphase) preparations from 4 different normal stallions (a-d). Sixty-four individual chromosomes smaller than mitotic one. Giemsa stain. Scale bar—10 μ m.

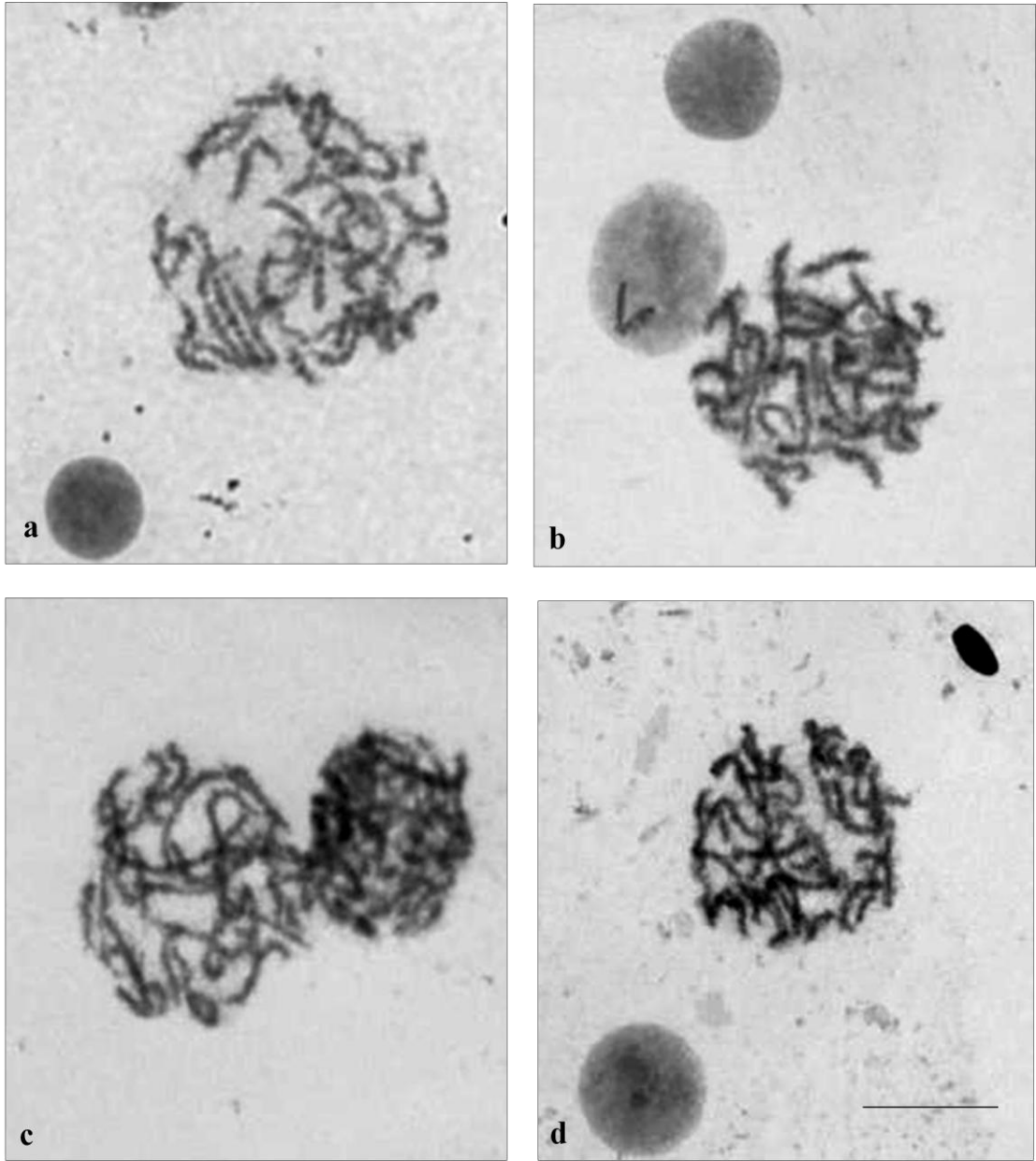


Figure 2.9: Prophase I (PI) preparations from 4 different normal stallions (a-d). Giemsa stain. Scale bar—10 μ m.

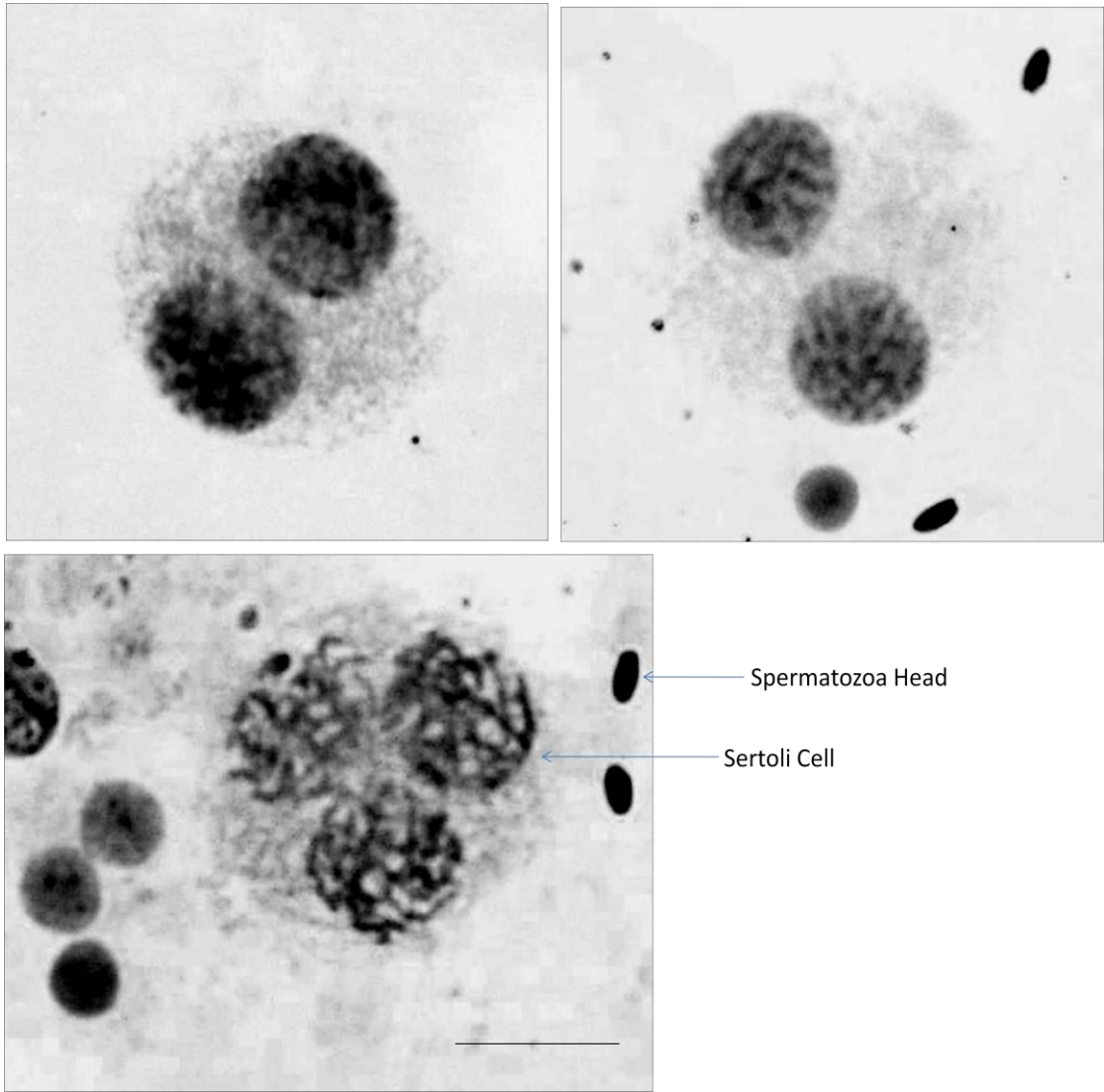


Figure 2.10 Sertoli cells with from 3 different stallions (a-c). This Figures show Sertoli cells that are large and usually have 2-3 nuclei. Giemsa stain. Scale bar—30 μm .

2.3.2.2.2. Chiasmata frequency and distribution

A total of 1107 Giemsa stained cells from 14 stallions at MI stage were photographed and karyotyped. The number of bivalents per cell was 32 with different configurations – there were no univalent or multivalent observed. All the autosomal bivalents had at least one chiasma whereas, all the XY bivalents had just one chiasma, most of which were distally localized. Bivalents appeared as rod, cross and ring shaped bearing one or more chiasma (Figure 2.4 and 2.5).

The number of chiasmata per bivalent ranged from one to four. The number of autosomal bivalents with one chiasma ranged from 9 to 20 (mean \pm SD, 14.7 ± 1.81 ; Table 2.3a and Appendix 1). The bivalents with one chiasma were significantly different across the 14 stallions ($p = 0.000$; Table 2.3b). For the bivalents with 2 chiasmata, the average ranged from 7 to 22 (mean \pm SD, 14.21 ± 1.93 ; Table 2.4a and Appendix 2). The bivalents with 2 chiasmata were significantly different across the 14 stallions ($p = 0.000$; Table 2.4b). For the bivalents with 3 chiasmata, the average ranged from 0 to 5 (mean \pm SD, 2.04 ± 0.84 ; Table 2.5a and Appendix 3). The bivalents with 3 chiasmata were significantly different ($p = 0.000$; Table 2.5b). For the bivalent with 4 chiasmata, the average ranged from 0 to 1 (mean = 0.05; Table 2.6a and Appendix 4). The bivalents with 4 chiasmata were significantly different across the 14 stallions ($p = 0.047$; Table 2.6b).

The total number of the autosomal chiasmata per cell for the 14 stallions ranged from 43 to 56 (mean \pm SD, 49.45 ± 2.07 ; Table 2.7a and Appendix 5). The total number of chiasmata across the 14 stallions were significantly different across the 14 stallions ($p = 0.000$; Table 2.7b). Thus, total number of chiasmata per cell, including XY bivalent, ranged from 44 to 57 (mean \pm SD, 50.45 ± 2.07). The mean number of chiasmata per autosomal bivalent was 1.63. The summary for the frequency of autosomal bivalents with 1-4 chiasmata among 14 stallions are presented in Figure 2.11.

Table 2.3a: Autosomal bivalent frequency with **one chiasma** among 14 stallions (n=1107)

Horse ID	Number of Scored Cells	Mean	SD	Range
H6	60	13.93	1.65	10-18
H11	72	13.36	1.49	11-16
H12	73	15.34	1.48	11-18
H13	77	14.90	1.89	10-19
H14	63	14.67	1.75	11-19
H15	63	14.79	1.55	11-18
H16	114	15.91	1.39	12-20
H17	80	14.65	1.91	9-18
H18	106	15.30	1.80	10-18
H19	94	14.15	1.87	10-17
H20	83	15.11	1.61	11-18
H22	79	14.16	1.62	11-17
H23	69	14.28	1.97	10-18
H24	74	14.27	1.67	10-18
Total	1107	14.70	1.81	9-20

Table 2.3b: ANOVA Table for autosomal bivalent frequency with **one chiasma** among 14 stallions

Source	Sum of Squares	df	Mean Square	F	Sig.
Between Groups	495.336	13	38.103	13.259	0.000
Within Groups	3141.094	1093	2.874		
Total	3636.430	1106			

Table 2.4a: Autosomal bivalent frequency with **two chiasmata** among 14 stallions (n=1107)

Horse ID	Number of Scored Cells	Mean	SD	Range
H6	60	15.12	1.85	10-20
H11	72	15.61	1.60	12-18
H12	73	13.66	1.46	11-18
H13	77	14.05	1.90	10-19
H14	63	14.03	2.04	9-19
H15	63	13.62	1.64	10-18
H16	114	12.82	1.42	7-16
H17	80	14.60	2.16	11-22
H18	106	13.69	2.02	10-20
H19	94	14.55	1.71	11-18
H20	83	13.57	1.71	10-18
H22	79	15.06	1.68	11-19
H23	69	14.70	2.00	11-18
H24	74	14.85	1.75	11-19
Total	1107	14.21	1.93	7-22

Table 2.4b: ANOVA Table for autosomal bivalent frequency with **two chiasmata** among 14 stallions

Source	Sum of Squares	df	Mean Square	F	Sig.
Between Groups	648.366	13	49.874	15.624	0.000
Within Groups	3489.013	1093	3.192		
Total	4137.379	1106			

Table 2.5a: Autosomal bivalent frequency with **three chiasmata** among 14 stallions (n=1107)

Horse ID	Number of Scored Cells	Mean	SD	Range
H6	60	1.88	0.69	1-3
H11	72	2.03	0.73	1-4
H12	73	1.99	0.63	1-3
H13	77	2.01	0.87	0-4
H14	63	2.24	0.96	0-4
H15	63	2.46	0.96	1-5
H16	114	2.17	0.75	1-4
H17	80	1.74	0.72	0-3
H18	106	1.95	0.77	1-4
H19	94	2.27	1.01	0-4
H20	83	2.29	0.88	1-4
H22	79	1.70	0.69	1-4
H23	69	1.99	0.83	0-4
H24	74	1.85	0.81	1-4
Total	1107	2.04	0.84	0-5

Table 2.5b: ANOVA Table for autosomal bivalent frequency with **three chiasmata** among 14 stallions

Source	Sum of Squares	df	Mean Square	F	Sig.
Between Groups	47.435	13	3.649	5.511	0.000
Within Groups	723.736	1093	0.662		
Total	771.171	1106			

Table 2.6a: Autosomal bivalent frequency with **four chiasmata** among 14 stallions (n=1107)

Horse ID	Number of Scored Cells	Mean	Range
H6	60	0.07	0-1
H11	72	0.00	0
H12	73	0.04	0-1
H13	77	0.04	0-1
H14	63	0.06	0-1
H15	63	0.13	0-1
H16	114	0.10	0-1
H17	80	0.01	0-1
H18	106	0.06	0-1
H19	94	0.03	0-1
H20	83	0.04	0-1
H22	79	0.08	0-1
H23	69	0.04	0-1
H24	74	0.03	0-1
Total	1107	0.05	0-1

Table 2.6b: ANOVA Table for autosomal bivalent frequency with **four chiasmata** among 14 stallions

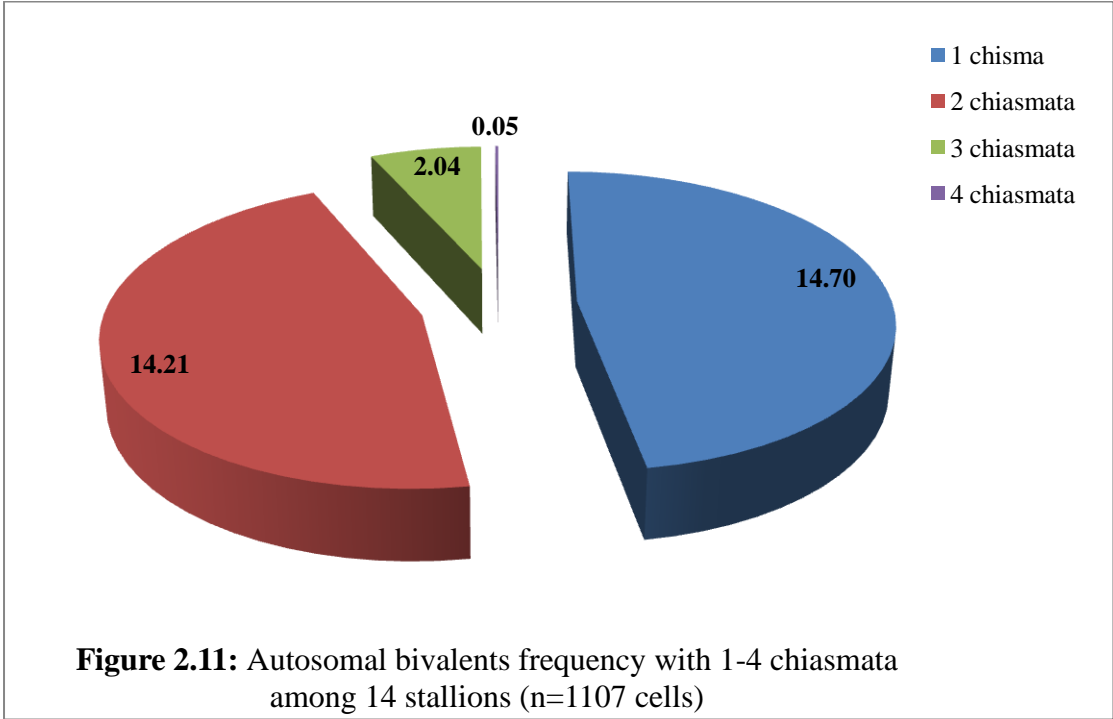
Source	Sum of Squares	df	Mean Square	F	Sig.
Between Groups	1.10	13	0.085	1.75	0.047
Within Groups	52.97	1093	0.048		
Total	54.07	1106			

Table 2.7a: Chiasmata frequency in autosomal bivalents per cell among 14 stallions (n=1107)

Horse ID	Number of Scored Cells	Mean	SD	Range
H6	60	50.08	1.72	47-53
H11	72	50.67	1.71	47-54
H12	73	48.78	1.99	45-56
H13	77	49.19	2.23	43-54
H14	63	49.70	2.00	45-53
H15	63	49.92	1.99	47-55
H16	114	48.45	1.76	45-54
H17	80	49.11	1.91	45-54
H18	106	48.76	1.92	46-55
H19	94	50.18	2.44	46-56
H20	83	49.25	1.94	46-54
H22	79	49.68	1.86	46-54
H23	69	49.80	2.31	45-55
H24	74	49.64	1.93	45-54
Total	1107	49.45	2.07	43-56

Table 2.7b: ANOVA Table for chiasmata frequency in autosomal bivalents per cell among 14 stallions

Source	Sum of Squares	df	Mean Square	F	Sig.
Between Groups	428.347	13	32.950	8.319	0.000
Within Groups	4329.312	1093	3.961		
Total	4757.659	1106			



2.3.2.3. Chiasmata Distribution on 8 Different Horse Chromosomes

After chiasmata were scored, 8 individual autosomes (Chromosome number 2, 6, 10, 13, 15, 24, 26 and 31) were easily and reliably identified by FISH technique. Thus, the number of chiasmata was established for these individual chromosomes. The subsequent FISH analysis for different cell types, such as: primary spermatocyte metaphase (MI), second meiotic metaphase (MII), prophase I (PI) and premeiotic mitotic (spermatogonial) metaphase using labeled probe against these 8 chromosomes are clearly presented in Figures 2.12- 2.15.

The number of chiasmata for chromosomes 2, 13, and 24 were different among scored cells; however, chromosomes 6, 10, 15, 26 and 31 were found to have a fixed number of chiasmata among cells. The number of chiasmata for chromosome 2 ranged from 2 to 3 (mean \pm SD, 2.67 ± 0.47 ; Table 2.8a and appendix 6). The number of chiasmata for chromosome 2 were not significantly different across the 5 stallions ($p = 0.945$; Table 2.8b). For chromosomes 13, the number of chiasmata ranged from 1 to 2 (mean \pm SD, 1.35 ± 0.48 ; Table 2.9a and appendix 7). The number of chiasmata for chromosome 13 were not significantly different across the 5 stallions ($p = 0.541$; Table 2.9b). For chromosome 24, the chiasmata ranged from 1 to 2 (mean = 1.08; Table 2.10a and appendix 8). The chiasmata number of chromosome 24 were not significantly different across the 5 stallions ($p = 0.989$; Table 2.10b). On the other hand, chromosome 6, 10 and 15 have 2 chiasmata in all scored cells, while chromosomes 26 and 31 were found to have 1 chiasma in all scored cells. Summary for chiasmata frequency in the 8 chromosomes among 5 stallions is presented in Table 2.11 and Figure 2.16.

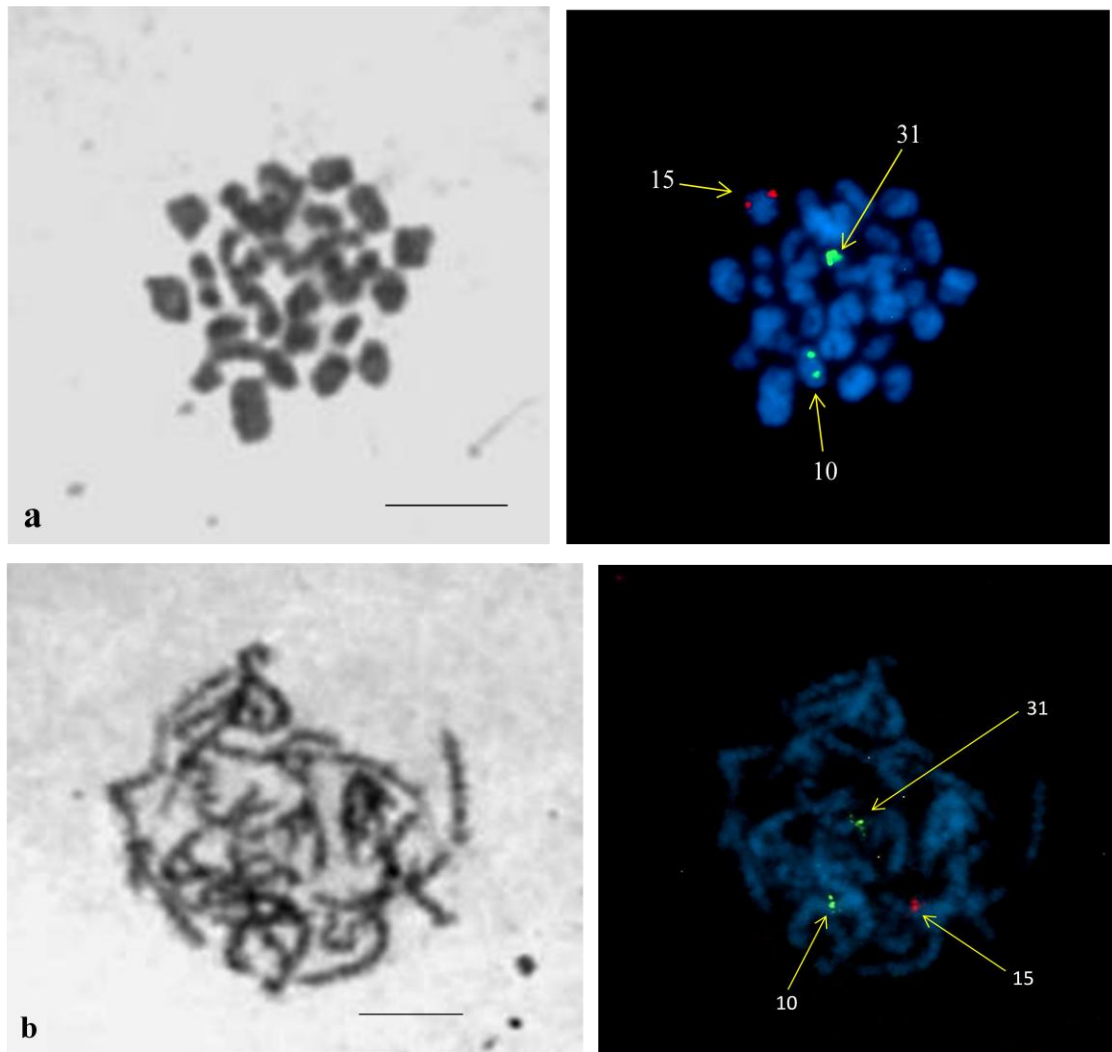


Figure 2.12: Subsequent FISH analysis for chromosome 10 and 31 shown in green (FITC) and chromosome 15 shown in red (TRITC). (a) Primary spermatocyte metaphase. (B) Prophase I. Scale bar—10 μm .

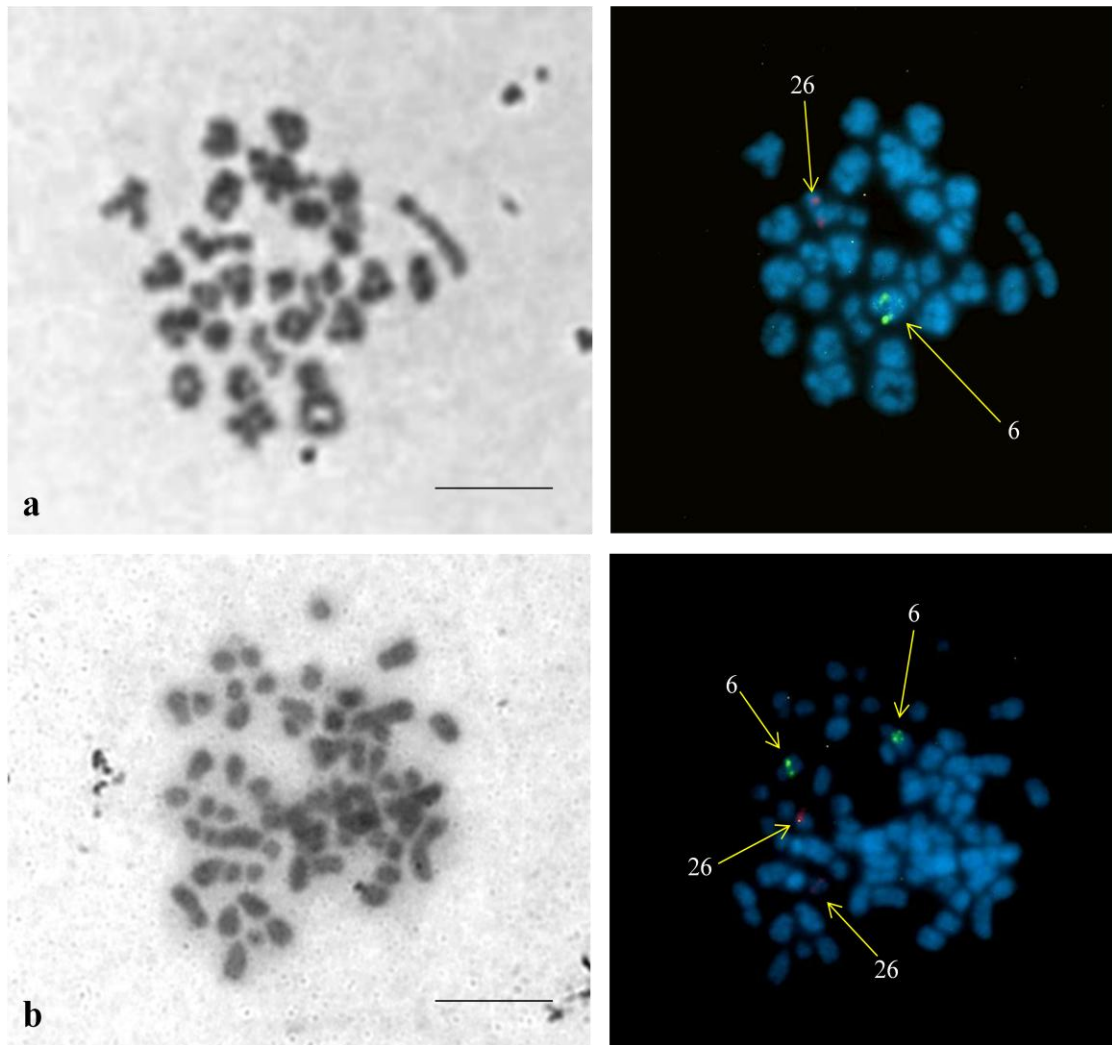


Figure 2.13: Subsequent FISH analysis for chromosome 6 shown in green (FITC) and chromosome 26 shown in red (TRITC). (a) Primary spermatocyte metaphase. (B) Premeiotic mitotic metaphase (spermatogonial metaphase). Scale bar—10 μm .

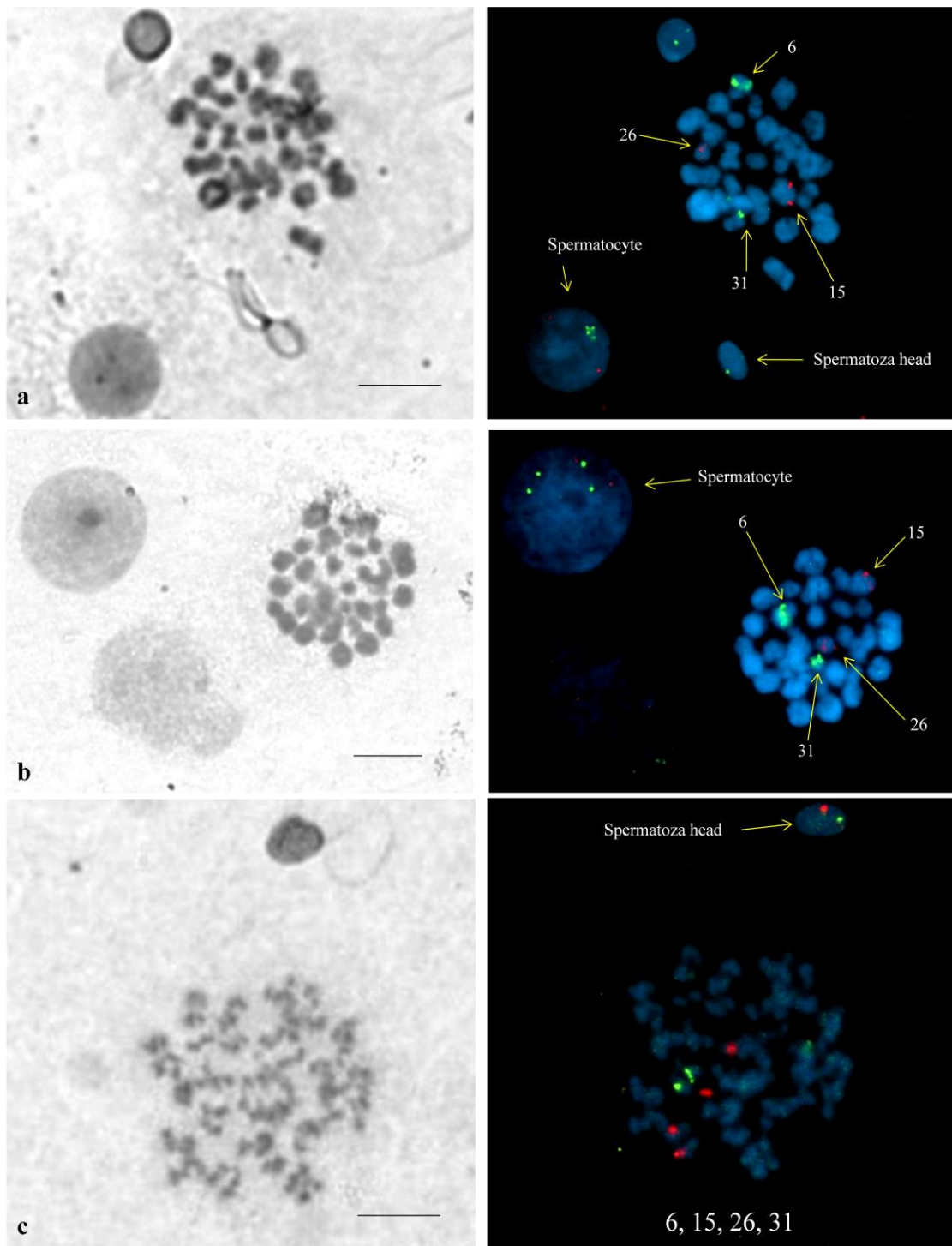


Figure 2.14: Subsequent FISH analysis for chromosome 6 and 31 shown in green (FITC) and chromosome 15 and 26 shown in red (TRITC). (a and b) Primary spermatocyte metaphase. (c) Second meiotic metaphase. The signals of probes are clear in the interphase stage of spermatozoa head as well as primary and secondary spermatocyte cells. Scale bar—10 μ m.

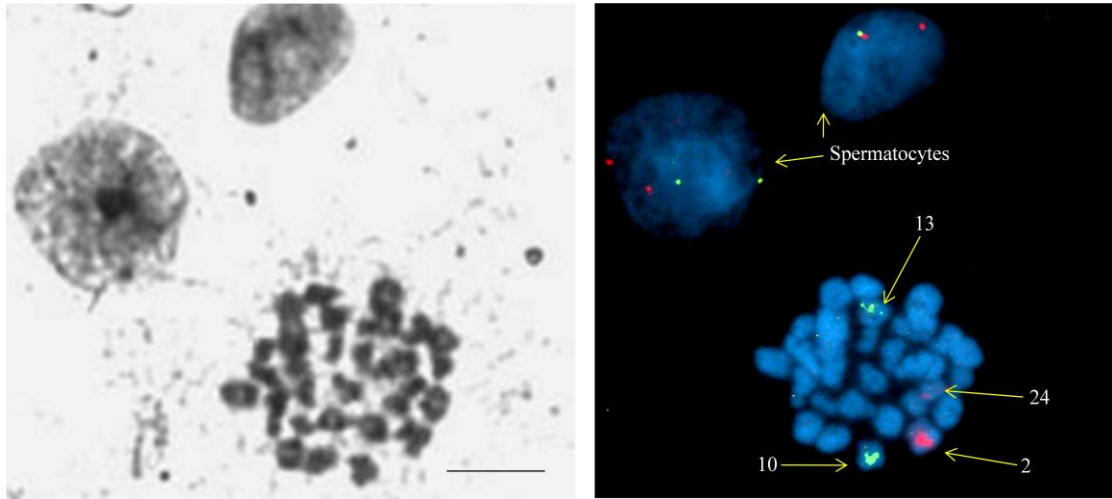


Figure 2.15: Subsequent FISH analysis for chromosome 10 and 13 shown in green (FITC) and chromosome 2 and 14 shown in red (TRITC) for horse primary spermatocyte metaphase. The signals of probes are clear in the interphase stage of spermatocyte cells Scale bar—10 μ m.

Table 2.8a: Chiasmata frequency in **chromosome 2** among 5 stallions (n=73)

Horse ID	Number of Scored Cells	Mean	SD	Range
H16	20	2.65	0.49	2-3
H17	9	2.67	0.50	2-3
H18	18	2.61	0.50	2-3
H19	12	2.75	0.45	2-3
H20	14	2.71	0.47	2-3
Total	73	2.67	0.47	2-3

Table 2.8b: ANOVA Table for chiasmata frequency in **chromosome 2** among 5 stallions

Source	Sum of Squares	df	Mean Square	F	Sig.
Between Groups	0.175	4.000	0.044	0.186	0.945
Within Groups	15.935	68.000	0.234		
Total	16.110	72.000			

Table 2.9a: Chiasmata frequency in **chromosome 13** among 5 stallions (n=63)

Horse ID	Number of Scored Cells	Mean	SD	Range
H16	20	1.30	0.47	1-2
H17	7	1.29	0.49	1-2
H18	15	1.53	0.52	1-2
H19	12	1.33	0.49	1-2
H20	9	1.22	0.44	1-2
Total	63	1.35	0.48	1-2

Table 2.9b: ANOVA Table for chiasmata frequency in **chromosome 13** among 5 stallions

Source	Sum of Squares	df	Mean Square	F	Sig.
Between Groups	0.733	4.000	0.183	0.783	0.541
Within Groups	13.584	58.000	0.234		
Total	14.317	62.000			

Table 2.10a: Chiasmata frequency in **chromosome 24** among 5 stallions (n=72)

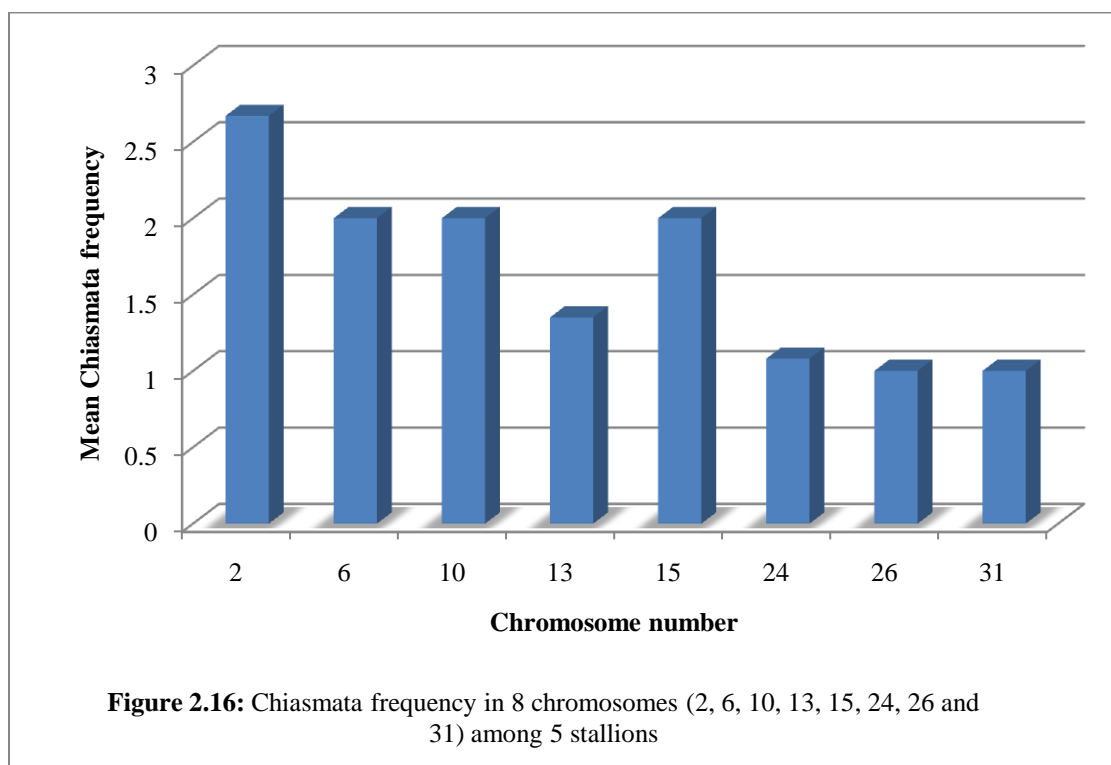
Horse ID	Number of Scored Cells	Mean	SD	Range
H16	20	1.10	0.31	1-2
H17	9	1.11	0.33	1-2
H18	17	1.06	0.24	1-2
H19	12	1.08	0.29	1-2
H20	14	1.07	0.27	1-2
Total	72	1.08	0.28	1-2

Table 2.10b: ANOVA Table for chiasmata frequency in **chromosome 24** among 5 stallions

Source	Sum of Squares	df	Mean Square	F	Sig.
Between Groups	0.025	4.000	0.006	0.076	0.989
Within Groups	5.475	67.000	0.082		
Total	5.500	71.000			

Table 2.11: Chiasmata frequency in 8 individual chromosomes (2, 6, 10, 13, 15, 24, 26 and 31) among 5 stallions

Chromosome number	Total scored cells	Bivalent		
		Mean	SD	Range
2	73	2.67	0.47	2-3
6	87	2	0	2
10	96	2	0	2
13	63	1.35	0.48	1-2
15	73	2	0	2
24	72	1.08	0.28	1-2
26	80	1	0	1
31	74	1	0	1



2.4. Discussion

Different cell stages, such as primary spermatocytes, secondary spermatocytes, spermatids, mature spermatozoa and other supporting cells like Sertoli cells, were detected in air dry preparations from all stallions. Moreover, different meiotic cells, such as premeiotic mitotic metaphase, primary spermatocyte metaphase I and secondary spermatocyte metaphase II, are visualised in all preparations. These findings indicate that stallions have normal spermatogenesis. The number of premeiotic mitotic metaphase was relatively rare in preparation from all stallions. This could be due to the natural presence of these cells close to basal epithelium compartment, thus most of these cells remain in the tubules during preparation of cell suspension. The number of secondary spermatocyte metaphase II (MII), which indicates that crossover has occurred and chromosomes segregated efficiently at AI, was low in the present study. This could be due to the short life span of MII stage. Prophase I (PI) predominated in the preparation and this is due to the time length of pairing, synapsis and crossing over that take place during PI.

The domestic horse has 31 autosomes, 13 metacentric or submetacentric and 18 acrocentric, in addition to sex chromosomes X, which is metacentric, and Y, which is acrocentric (Evans, 1992; Bowling *et al.*, 1997). The number of chiasma was different between chromosomes, which mostly correlated with the chromosome length. Small chromosomes showed typically 1 chiasma while long chromosomes showed 2 or more chiasmata. Although the number of chiasma was different from chromosome to chromosome, at least one obligate chiasma is formed per chromosome pair irrespective of its length. This chiasma is important to ensure regular orientation of the maternal and paternal chromosome at MI and proper segregation at AI. The numbers of additional chiasmata over the obligate one are dependent on the length of the chromosome. The maximum number of chiasmata per chromosome was 4, which is mainly observed for chromosome 1. The chiasmata distribution showed interference since they are non-randomly distributed within a chromosome but separated by large chromosome segments. The occurrence of one chiasma would reduce the likelihood of another chiasma to form in close proximity (Hultèn, 1974).

Most of metacentric or submetacentric autosomes showed two or more chiasmata. Some of these autosomes have three and rarely four chiasmata, which are mainly long chromosomes since there is a correlation between the length of the chromosome and

the number of exchanges (Sun *et al.*, 2004). The X-Y bivalent at metaphase I, which has one chiasma, demonstrated that the Y chromosome paired with the X chromosome.

Failure of chiasma formation between maternal and paternal chromosomes can lead to formation of univalents and random segregation. Thus daughter cells could receive both maternal and paternal, one of them or none of these. Results from this study did not show any univalent.

The present study has provided detailed information on chiasma formation in stallion. The average number of autosomal chiasmata per nucleus was 49.45 ± 2.07 among 14 stallions with a total number of 1,107 primary spermatocyte metaphases. Significant heterogeneity for the individual mean of chiasmata frequency for autosomal chromosomes was observed among stallions ($P = 0.000$), inter-individual difference of 4.5% with a range of $48.45 \pm 1.76 - 50.67 \pm 1.71$. Horse number H11 showed the highest average of chiasmata number (50.67), while the minimum average of chiasmata number was detected in horse number H16 (48.45).

Around half of the chromosomes (47.4%) showed 1 chiasma, while 45.8% of the chromosomes showed 2 chiasmata. Chromosomes with 3 and 4 chiasmata were 6.6% and 0.2% respectively (Figure 2.11). The average number of chromosomes with 1, 2, 3 and 4 chiasmata were significantly different among the 14 stallions ($P = 0.000$).

The importance of studying the number of chiasmata, which holds the homologous chromosomes together during MI, is to construct genetic maps and to estimate the total length of the genome since it can be detected cytogenetically as a site of crossover. Chiasmata are the mature crossovers, thus their occurrences indicate that pairing, synapsis and crossover have been successful during PI. The genetic map distance is calculated as a half of the average number of chiasmata in the interval concerned, since each chiasma may give rise to half of the gametes (2 gametes) as recombinant and other half (2 gametes) as non-recombinant gametes. It means that genetic map distance can be obtained by multiply the average number of chiasmata by 50. Thus an average of 49.45 horse male autosomal chiasmata corresponds to genetic map length of 2,472.5 centimorgans (cM). Taking into account that one chiasma always take place between XY bivalent, which equal to 50 cM, the total genome length of the horse male is 2,522.5 cM, which compares to 2772 cM from linkage data (Swinburne *et al.*, 2006). This show a remarkable degree of correspondence, especially when one considers that in many organisms genetic mapping frequently

results in maps with lengths exceeding those based on chiasma frequency (Sybenga, 1996). Moreover, genetic map length, presented here, is very similar to the human males 2,490 cM that based on chiasma count, which compares to 2729.7 cM from linkage data. (Dib *et al.*, 1996; Sun *et al.*, 2004).

A comparison of the mean chiasma frequency in the horse and other species is presented in Table 2.12.

The horse male mean frequency of chiasmata per nucleus reported in this study, 50.45 ± 2.07 , is different from that obtained by Scott and Long (1980), 54.4 ± 1.8 per cell. These discordant data could be related to different factors, such as stallion, and methodology. Similar discordant results for chiasmata frequency in human males were obtained from different studies (Table 2.13).

The average size of the horse genome is very similar to that of mammals (~3 billion base pairs) especially humans (Chowdhary & Raudsepp, 2008). The total numbers of chiasmata in horse male are very close to the human male one, 50.61 ± 3.87 per cell. Although horse have more chromosomes (31 autosomes) than humans (22 autosomes), the horse has more acrocentric (18 acrocentric chromosomes) and short chromosomes compared with humans (5 acrocentric chromosomes; Kaback *et al.*, 1992).

Horse male shows very close autosomal chiasmata frequency to other domestic species such as sheep (51.2 ± 4.7) that have 26 autosomes, goats (49.7 ± 4.0) that have 29 autosomes and cows (49.5 ± 4.1) that have 29 autosomes. This coordinate is due to the close genome size and similar chromosome number of these animals.

After chiasmata were karyotyped in different air dry preparations, different autosomes were identified by FISH. Correct identification of autosome and facilitating the FISH signals depends on the quality of cells in the preparations as well as the condensation of the chromatin after fixation. In this work, 8 different autosomes were identified by FISH as well as the numbers and distributions of chiasmata were established for these individual autosomes. Therefore, abnormal processes in any of the 8 autosomes can be characterized. These 8 autosomes are not randomly selected but represent different group size and centromere position of horse autosomes. Autosomes 2, 6, 10 and 13 are metacentric, while autosomes number 15, 24, 26 and 31 are acrocentric with different sizes. The mean number of chiasmata ranged from low of 1.00 ± 0 , for the smallest chromosome (31) and chromosome 26, to 2.67 ± 0.47 , for chromosome 2.

Chromosome 1, which mostly had 3 or 4 chiasmata, was not studied in this part of investigation. Fixed numbers of chiasmata were identified in 5 autosomes, autosomes 6, 10 and 15 that showed 2 chiasmata, while autosomes 26 and 31 received 1 chiasma in all scored cells, which is generally near the telomere. For autosomes 6 and 10, one chiasma was identified in each arm (p and q arm) and giving a ring shape chromosomal configuration. However, the distribution of the 2 chiasmata in autosome 15, were commonly in medial and distal loci of q arm, showing ring with open end shape chromosomal configuration.

Around 67% of the scored cells for autosome 2, 73 cells, showed 3 chiasmata. Autosome 2 is large submetacentric, in which p arm is smaller than q arm. The distribution of chiasma showed 1 chiasma in p arm and mostly (67%) 2 chiasmata in q arm. Autosome 13 showed 1 chiasma in around 65% of the scored cells, 63 cells. It is the smallest metacentric autosome. The distribution of chiasma showed 1 chiasma in q arm, which is larger than p arm that rarely showed 1 chiasma (35% of cases). For autosome 24, 1 chiasma was detected in most of cells, 91.7% of scored cells. The distribution of a single chiasma, and rarely 2 chiasmata, were showed on q arm, since autosome 24 is small and acrocentric. Since chromosome 1 is the largest horse chromosome and chromosome 2, which is close in size to chromosome 1, was identified by FISH technique, thus chromosome 1 can be easily identified. The chiasmata frequency for chromosome 1 was also estimated to range between 2 to 4 (mean \pm SD, 3.05 ± 0.24).

The genetic length for the eight autosomes, from present study, is close to that obtained from linkage map (Table 2.14). Autosome 31, the smallest horse chromosome, and autosome 26 received a single chiasma that representing 50 cM. The genetic length of autosome 26, from linkage map (24.4 cM), is less than the one which reported here (50 cM). This is due to the fact that at least 1 chiasma is obligate per bivalent, for proper segregation, which equal to 50 cM.

Table 2.12: Average chiasmata frequency per cell for different species

Species	Average number of Chiasma (mean \pm SD)	Number of scored cells	Reference
Horse Male	50.45 \pm 2.07	1,107	present report
Horse Male	54.4 \pm 1.8	221	Scott and Long (1980)
Human Male	50.61 \pm 3.87	41	Hultèn (1974)
Sheep Male	51.2 \pm 4.7	50	Logue (1977)
Goat Male	49.7 \pm 4.0	325	Logue (1977)
Cow Male	49.5 \pm 4.1	20	Logue (1977)

Table 2.13: Mean chiasmata number in human males reported from different studies

No. of individuals	No. of cells	Mean chiasmata No.	Range	Genetic length (cM)	Reference
21	516	53.7	43 - 62	2685	McDermott (1973)
1	41	50.6	43 - 60	2530	Hultèn (1974)
7	408	52.3	49.6 - 53.7	2566.5	Laurie and Hultèn (1985)
6	91	45.3	32 - 58	2566.5	Fang and Jagiello (1988)

Table 2.14: Chiasmata frequency and the genetic length of 8 individual chromosomes (2, 6, 10, 13, 15, 24, 26 and 31) among 5 stallions

Chromosome No.	Total scored cells	Mean chiasmata No.	Genetic length (cM)	Linkage map (cM) ^a
2	73	2.67	133.5	128.8
6	87	2	100	126.8
10	96	2	100	105.8
13	63	1.35	67.5	58
15	73	2	100	96.7
24	72	1.08	54	47.2
26	80	1	50	24.4
31	74	1	50	41.1

^aReference: Swinburne *et al.*, (2006)

2.5. Conclusion

This is the first report of chiasma frequency maps for all autosomes in normal horse males as well as complete characterization of chiasmata distribution in 8 horse autosomes using FISH assay. Results prove that FISH is a feasible and reliable method for identification of horse meiotic chromosomes. Chiasmata maps demonstrate a preference for distal exchanges with repression of chiasma near the centromeres and chiasmata interference inferred for all bivalents. The autosomal length and the location of centromere predict the number and the distribution of chiasmata and, therefore, the genetic map length. There is a relationship between autosome length and average number of chiasmata per autosome.

Chapter 3

Prophase I: Homologous Pairing and Recombination Frequency

3.1. Introduction

Prophase I is the longest stage in meiosis. During prophase I, for proper segregation of homologous chromosomes and formation of normal haploid gametes, homologous chromosomes pair, synapse and recombine. When homologous chromosomes pair and synapse, the synaptonemal complex (SC), a proteinaceous structure that hold the homologs in close proximity, forms along the axis of the chromosomes (Codina-Pascual *et al.*, 2004). SC consists of two lateral elements, to which the two sister chromatids of each chromosome are attached, and one central element (Judis *et al.*, 2004). Prophase I can be divided into four substages: leptotene, in which the chromosomes search their homologue; zygotene, in which the homologous chromosomes start to pair and synapse and SC start to form; pachetene, in which homologous chromosomes are fully synapsed and; diplotene, in which the homologous chromosomes start to desynapse and repel from each other and SC breaks down (Judis *et al.*, 2004).

Recombination encompasses a series of steps, mediated by a large number of proteins (Smith & Nicolas, 1998; Cohen & Pollard, 2001; Critchlow *et al.*, 2004). Molecular components of some of these proteins have been identified in lower organisms as well as mammals. These discoveries have opened a new approach for research using immunofluorescence (IF) techniques, which are used by many researchers these days to visualise the SCs and recombination nodules (RNs), providing an alternative approach to silver nitrate staining (Hultèn *et al.*, 1974; Codina-Pascual *et al.*, 2004), and MI cytogenetic or diakinesis preparations that are laborious and slow to analyze (Sun *et al.*, 2004). The major advantage of IF technique is that numerous cells at pachytene stage can be recovered, which is not the case in MI nuclei. It is particularly

of interest for females gametes where one can simultaneously analyse the homologous synapsis and meiotic recombination sites (Sun *et al.*, 2004, Barlow and Hultèn, 1998; Sun *et al.*, 2004). Antibodies against SC components, such as SCP2 and SCP3 for lateral element and SCP1 for the central element, are used to visualize the structure of SC as well as directly monitor the germ cell's progression through prophase I substages to metaphase I (Anderson *et al.*, 1998 & Judis *et al.*, 2004). SC proteins show low conservation and sequence homology (Schwazacher, 2003). Calcinosis, Raynaud's phenomenon, Esophageal dysfunction, Sclerodactyly, Telangiectasia (CREST) antisera also have been used to localize the centromere of all chromosomes (Sun *et al.*, 2004). Moreover, MLH1 protein, a DNA mismatch repair protein, also involved in recombination since the localization of it on SCs at pachytene stage shows good correspondence with sites of chiasmata at MI, and mutation in MLH1 protein results in formation of many univalents at metaphase I, even when chromosomes are normally synapsed, suggesting that the defect is in crossover not in synapsis (Baker, 1996; Anderson *et al.*, 1998).

Recombination mapping along the chromosomes is an important step for understanding the recombination regulation (Anderson *et al.*, 1998). For this purpose, some physical maps based on chiasmata localization at diplotene have been produced (Henderson, 1963). Electron microscopy has also been used to map late RNs on SCs (Carpenter, 1975). In the last decade, combined techniques of immunofluorescence in spermatocytes followed by FISH, which is used by many researchers, can provide a recombination map for individual chromosomes. The first identification of all SCs was achieved in mouse, in which two rounds of multicolor FISH chromosome specific were used (Froenicke *et al.*, 2002; Codina-Pascual *et al.*, 2004). Recently, multicolor FISH using specific centromeric probes (cenM-FISH) (Sun *et al.*, 2004) or subtelomeric-specific probe (stM-FISH) (Codina-Pascual *et al.*, 2004) were applied to characterized human male SCs recombination maps.

Surprisingly, no study has so far described equine homologous pairing and recombination frequency using IF technology. Thus, this is the first study to used IF technique to characterize the meiotic recombination patterns in normal equine spermatogenesis by using antibodies against SCP3, to visualize SCs and to investigate the homologous pairing, and against MLH1, to identify meiotic recombination loci (Judis *et al.*, 2004). The distribution of MLH1 in stallion spermatocytes was examined

as markers for identification of meiotic recombination loci frequency and distribution (Barlow and Hultèn, 1998).

3.2. Materials and Methods

3.2.1. Surface Spreading Technique (Prophase I)

Slides used for this technique were cleaned with methanol and glow-discharged by exposing them to ultra-violet light in vacuum for two min at -1 Torr using EMITECH K100X (EMITCK, Kent, England) to make them hydrophilic. Two different protocols were used for spreading of equine meiotic chromosomes (see below).

3.2.1.1. Lipsol spreading for equine meiotic chromosomes

The specimens were processed for analysis using Barlow and Hultèn (1998) protocol with minor modification. A drop of phosphate free detergent (0.03% lipsol) was mixed with a drop of cell suspension (in Ham F10 media; Invitrogene, UK), on a clean microscopic slide that was pre-warmed on a hot plate in a fume hood. Optimization was carried out by incubating at different temperatures (from 22 °C to 32 °C) and timings (from 4 min to 10 min). Ten drops of 2% formaldehyde fixative (Sigma, Germany), containing 0.02% sodium dodecyl sulfate (SDS) buffered to pH 8.0 with sodium tetra borate, were added to the cell suspension on the slide and incubated for 10 min. The slide was then dapped on tissue paper and washed gently in distilled water before being left to air dry at room temperature. Subsequently some of the slides were stained with silver stain as describe below and the rest were either process for immunofluorescence immediately or stored at -80 °C for future needs.

3.2.1.2. Sucrose spreading for equine meiotic chromosomes

The tissue was gently cut into small and loose pieces of seminiferous tubules and transferred to freshly prepared hypotonic extraction buffer (30 mM Tris, pH 8.2; 50 mM sucrose; 17 mM citric acid; 5 mM EDTA; 0.5 mM DTT; 0.1 mM PMSF, pH 8.2-8.4) and incubated in ice for 45 min to 60 min (depending on the size of the tissue).

The tissue pieces were taken out of the buffer and macerated in 100 mM sucrose solution pH 8.2. The cell suspension was diluted to appropriate amount with 100 mM sucrose solution. One drop was deposited on a slide that had been overlaid with 1% formaldehyde solution (Sigma, Germany) pH 9.2 containing 0.15% Triton X-100, incubated in a humidified sealed chamber for 2 h at room temperature and removed from the humidified chamber and air dried. Slides were immersed two times in Phosphate Buffer Saline (PBS) (Oxoid, UK) for 5 min each and one time in distilled water for 5 min. Finally each slide was air dried and either process for immunofluorescence immediately or store at -80 °C for future needs.

3.2.1.3. Electron Microscopy Spreading for Meiotic Chromosomes

Slides used for this technique were cleaned with acid-alcohol and coated with Optilux (0.75% of plastic pieces from Petri dish dissolved in chloroform). Slides were glow-discharged by exposing them to ultra-violet light in vacuum for two min at -1 Torr using EMITECH K100X (EMITCK, Kent, England) to make them hydrophilic. Meiotic cells were spreaded on the coated slides using both lipsol and sucrose spreading protocols (see above). After the slides were air-dried at room temperature, subsequently some slides were stained with silver nitrate as described below and examined under the light microscope to localize the PI cells. The interested area was cut out and the plastic film floated off on distilled water and picked up on a mesh grid. The grids were air dried at room temperature and examined under the electron microscope (CM10, Philips) for the appearance of SCs and recombination nodules.

3.2.2. Silver Staining

Two drops of 50% silver stain (50% silver nitrate solution in de-ionised distilled water) were placed on either end of each slide. Slides were covered with silver stain wet mesh and incubated at 60 °C for 1 h. Slides were washed under running tap water for 30 min after floating the mesh of in water. Air dried slides were examine under a light microscope and an electron microscope.

3.2.3. Immunostaining of Meiotic Spreads

Air-dried slides were blocked by soaking them 3 times at room temperature in PBT (1XPBS, 0.15% bovine serum albumin (BSA) and 0.1% Tween 20) for 10 min each. The slides were overlaid with around 100 µl primary antibodies cocktail [(Rabbit SCP3 (1:200) (SantaCruzBiotechnonogy, CA, USA), Mouse anti-Human MLH1 (1:50) (BD Pharmingen, USA) and Human CREST antisera (from 1:50 to 1:500) (SantaCruzBioechnonogy, CA, USA) in 1X Antibody Dilution Buffer (ADB) (1XPBS, 0.13% sodium azide, 0.1%BSA, 0.1% Tween 20) and incubated in a humidified chamber overnight at room temperature. After 3 washes at room temperature with PBT, 10 min each, slides were incubated with 100 µl of secondary antibodies cocktail [(TRITC Donkey Anti-Rabbit (1:400), FITC Donkey Anti-Mouse (1:200) and AMCA Donkey Anti-Goat (from 1:200 to 1:1000) in 1X ABD] (Jackson ImmunoResearch, USA) in humidified chamber at 37 °C for 1 h. Slides were washed 3 times at room temperature with PBT, for 10 min each, and air-dried in the dark at room temperature. Antifade without DAPI was applied on the slides and the covered immunostained slides were studied with Olympus BX61 microscope (Olympus, Japan), images were captured using Applied Imaging Cytovision 3.1 software (Applied Immaging, UK).

3.2.4. Localization of MLH1 foci to synaptonemal complex

Micromasure 3.3, which is an image analysis application that allows collection of data for a wide variety of chromosome parameters from digitally captured images (available from the Micromasure Website,

<http://colostate.edu/Depts/Biology/Micromasure>), was used to measure the SC length of total and individual chromosome as well as determine the positions of MLH1 foci. Twenty-four pachytene nuclei from 6 different horses (H18, H19, H20, H22, H23 and H24), average of four nuclei from each horse, were analysed. The average as well as minimum absolute and relative distance between foci was calculated.

Since individual SC could not be identified, autosomal SCs from each nucleus were ranked in sequence of their relative length. The absolute as well as relative positions of each MLH1 focus on each SC were recorded using distance from telomere. Moreover, the chromosomes were categories into 4 different groups depending on

their number of MLH1 foci. The absolute and relative interference distance between two MLH1 foci in each group was determined.

3.2.5. Statistical Analysis:

The descriptive and inferential statistics were applied through SPSS (version 16) and using the statistical software in the Excel package (Version 2007, Microsoft Corporation, Redmond, WA, USA). The statistics used were F statistics (ANOVA) to test the viability and variability across horses. In all cases, significance level was set at $P < 0.05$.

3.3. Results:

3.3.1. Mouse prophase I sub-stages

Mouse samples were used to practise the techniques and good-quality surface spreading preparations were obtained. Nineteen autosomal bivalents and XY bivalent were visualised.

Different prophase I sub-stages were easily recognized by using anti-SCP3 antibody, such as: early zygotene, in which the lateral elements are partially paired (Figure 3.1a), late zygotene, in which the lateral elements are not fully paired (Figure 3.1b), pachytene, which have clear 20 lateral elements that are fully paired (Figure 3.2).

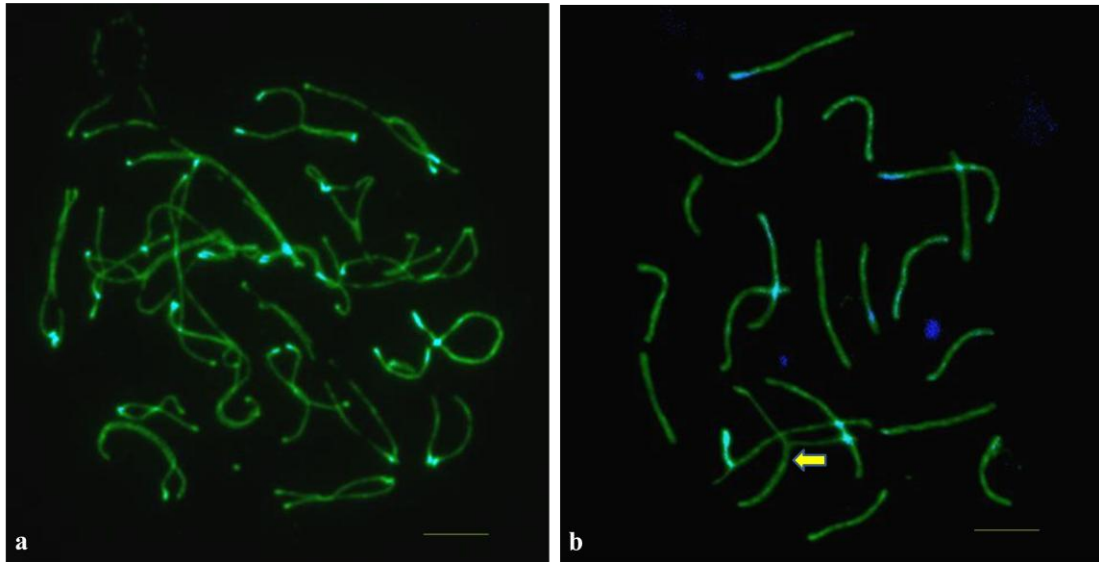


Figure 3.1: Surface spread mice spermatocytes labeled with anti-SCP3 (green) and anti-CREST (blue). (a) Early zygotene nucleus with partially synapsed lateral elements. (b) Late zygotene nucleus from 2 different mice with incomplete synapse lateral elements (arrow). Scale bar—5 μm .

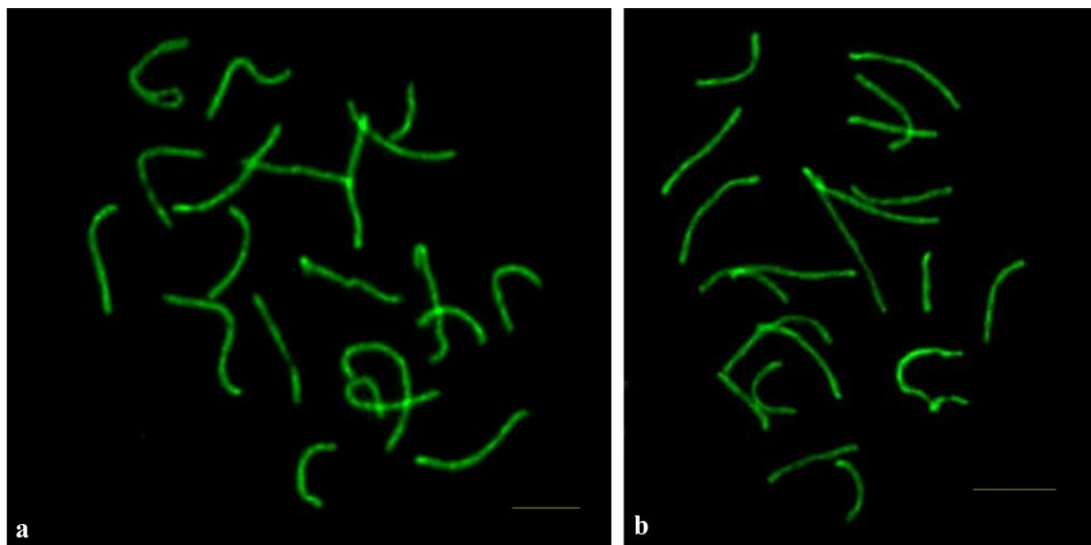


Figure 3.2: Surface spread mouse spermatocytes labeled with anti-SCP3 (green). (a and b) Pachytene nucleus from 2 mice with complete synapsed lateral elements. Scale bar—5 μm .

3.3.2. Horse prophase I sub-stages

By applying anti-SCP3 antibody (to monitor the formation of the axial/lateral elements of the synaptonemal complex) to surface spread preparations from horse testicular samples, it became possible to determine the stage of spermatocytes and to monitor the progression of meiosis division through different sub-stages of prophase I. Different sub-stages with excellent-quality preparation of prophase I were observed such as: (1) Leptotene stage, in which multiple small SCP3 positive fragments, axial elements (Figure 3.3); (2) Zygotene stage, in which full-length SCP3 (axial element) were observed with either partially limited association or pairing especially in telomeric regions, early zygotene, or not fully association or unsynapsed segments of homologous chromosomes, late zygotene (Figure 3.4). (3) Pachtene stage, if the 64 axial elements are fully paired to form 32 lateral elements that can divided into: early pachytene, in which the large region of XY bivalent are synapsed (Figure 3.5a), and late pachytene, in which the nuclei containing a shredded and anastomised XY bivalent (Figure 3.5b). In general, pachytene stage predominated in the preparations, since it is the longest stage of prophase I.

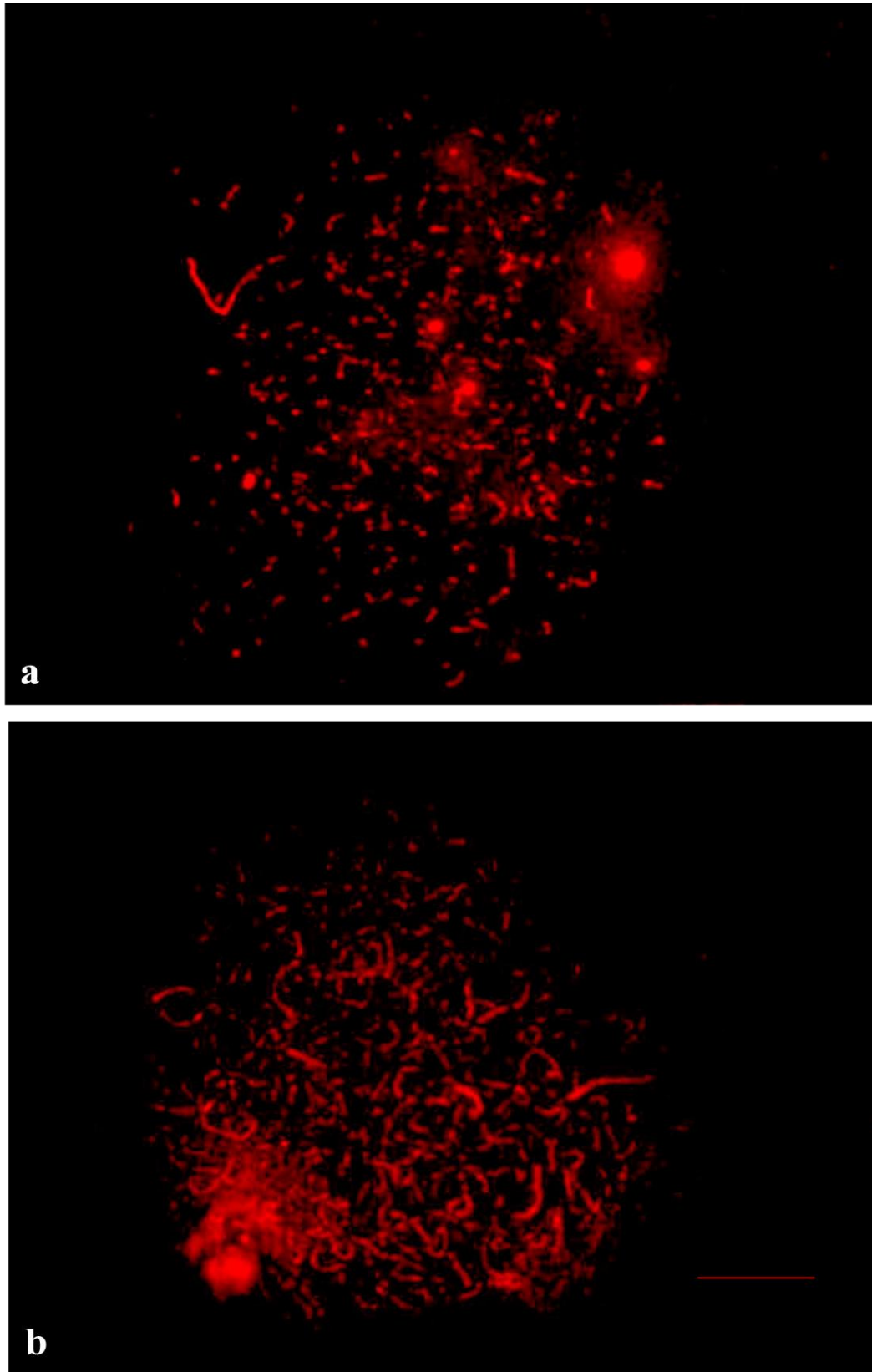


Figure 3.3: Surface spread of horse spermatocytes labelled with anti-SCP3 (red). (a and b) Leptotene nuclei, with short segments of axial elements are first visualised, from 2 stallions. Scale bar—10 μ m.

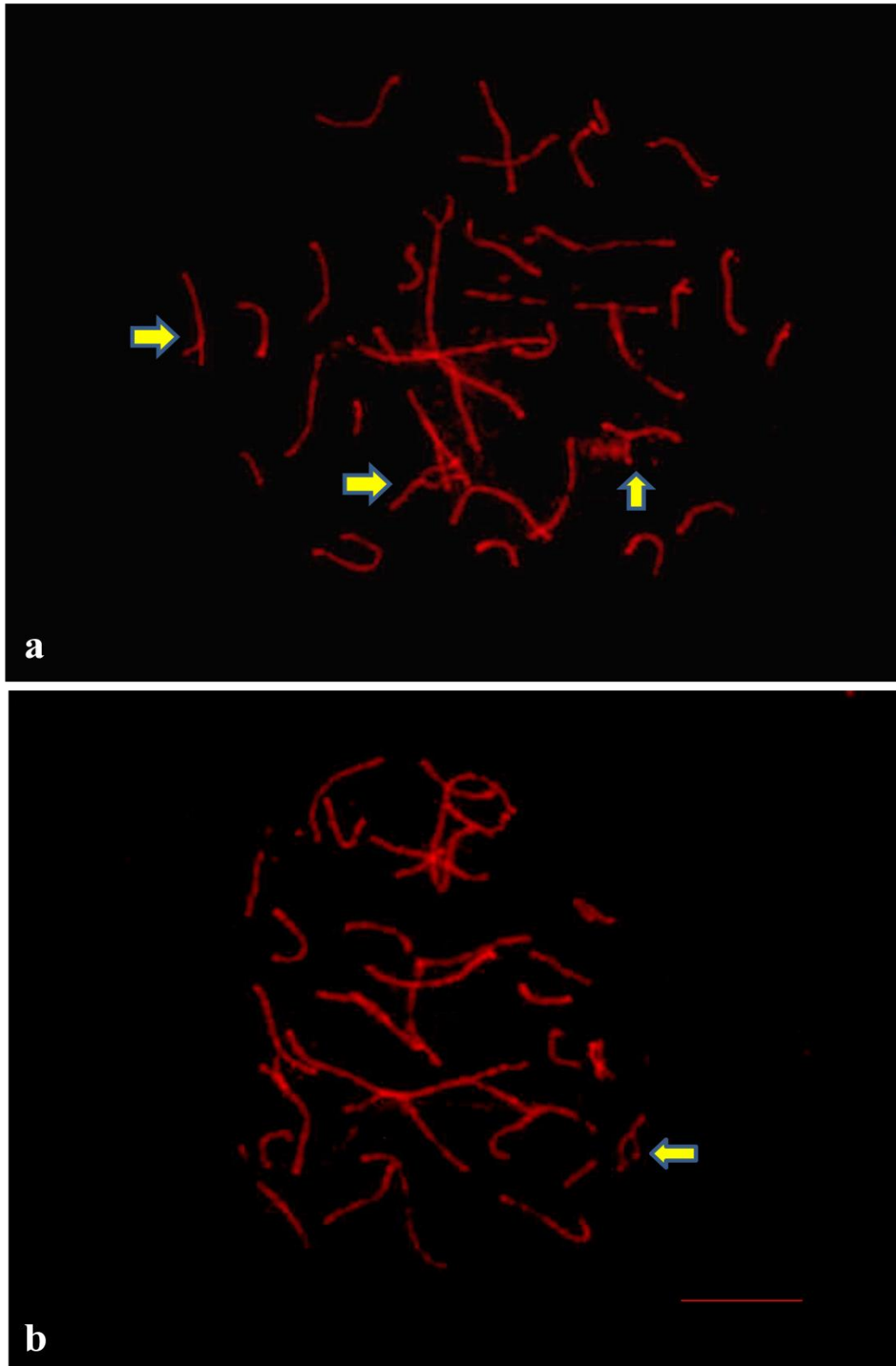


Figure 3.4: Surface spread of horse spermatocytes labeled with anti-SCP3 (red). Zygotene stage nuclei in which the lateral elements are partially synapsed. (a) Early zygotene nucleus (arrow) with partially synapsed lateral elements. (b-d) Late zygotene nuclei with incomplete synapse of lateral elements. Arrows indicate unsynapsis segments in different homologous chromosomes. Scale bar—10 μ m.

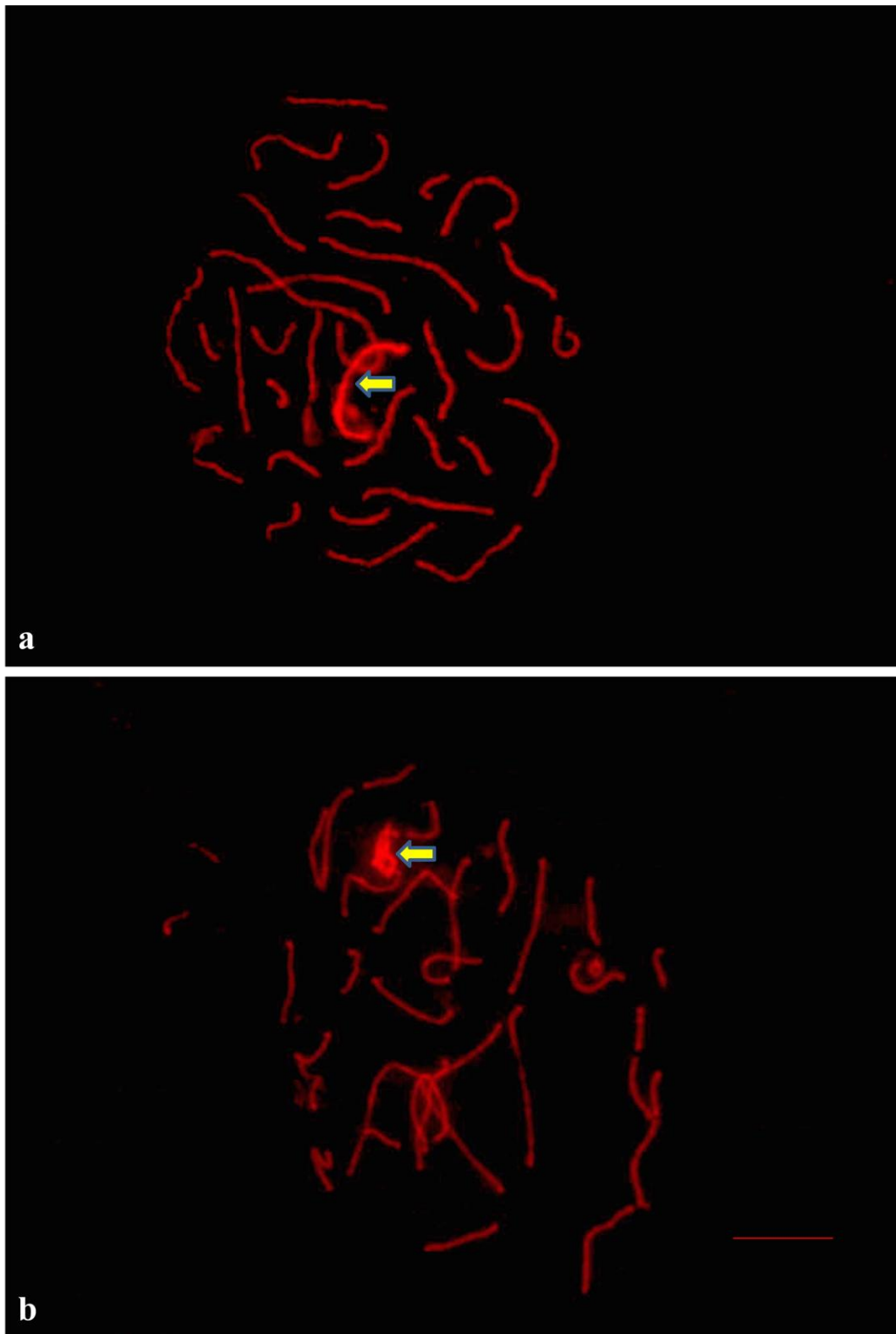


Figure 3.5: Surface spread of horse spermatocytes labelled with anti-SCP3 (red). Pachytene stage in which the two lateral are fully synapse. (a and b) Early pachytene nuclei. Arrow showing large region of XY bivalent are synapsed. (c and d) Late pachytene nuclei. Arrows indicate shredded and anastomised XY bivalent. Scale bar—10 μ m.

3.3.3. Light and electron microscopy spreading for prophase I

Different cells were analysed from some stallions silver stained surface spread preparations. Light microscopy revealed good preparations, mainly for pachytene stage which have 32 paired axial elements, with little background (Figure 3.6).

Electron microscopic examinations for pachytene stages revealed clearly that synaptonemal complex is consist of two lateral elements with a constant distant between them. No central elements or recombination nodules were visualised in the preparations that could be due to preparation method. Different stages of PI were detected such as (1) Pachytene stage, in which the 64 elements are fully synapsed and forming 31 autosomal bivalents and one XY bivalent, sex vesicle (Figure 3.7 and 3.8). (2) Zygotene stage, in which the axial or lateral elements are partially synapse, early zygotene (Figure 3.9 a) or incomplete synapsed, late zygotene (Figure 3.9b and c).

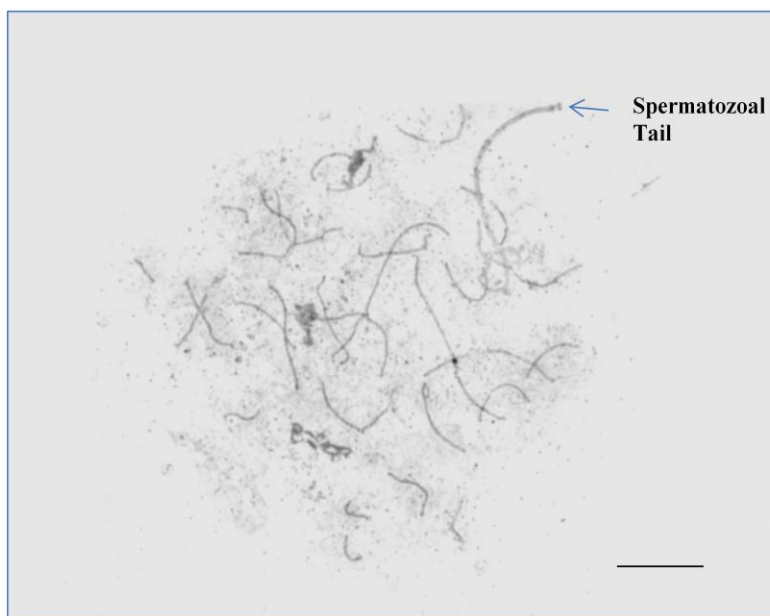
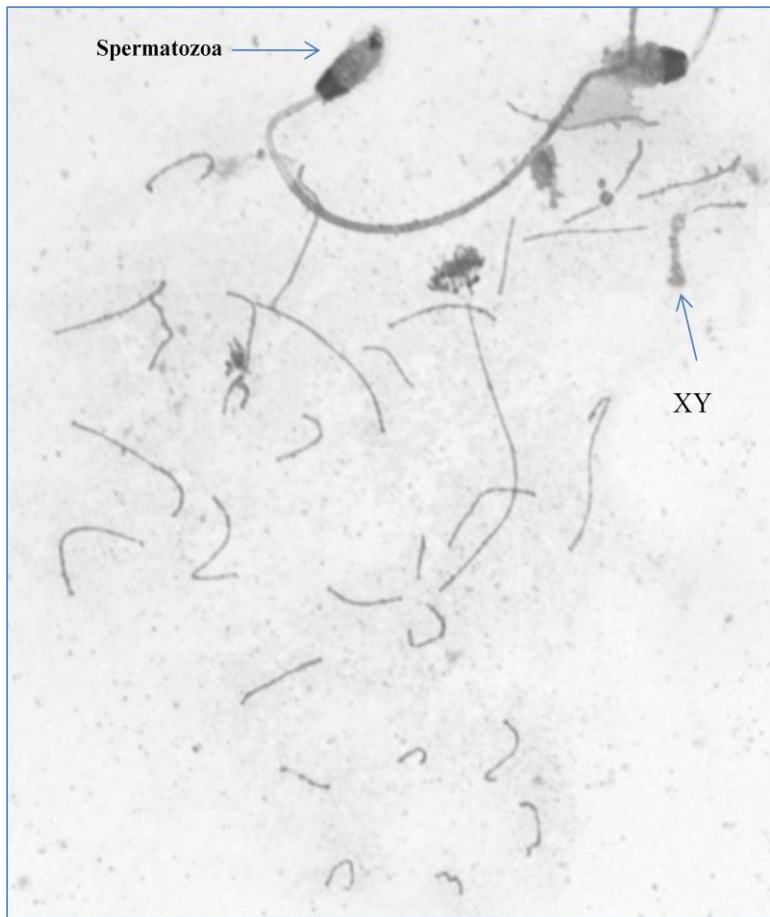


Figure 3.6: Light microscopy for meiotic prophase I of silver-stained preparations of stallion spermatocytes. (a and b) Pachytene stage with 31 paired lateral elements and clear XY bivalent. Scale bar—10 μm .

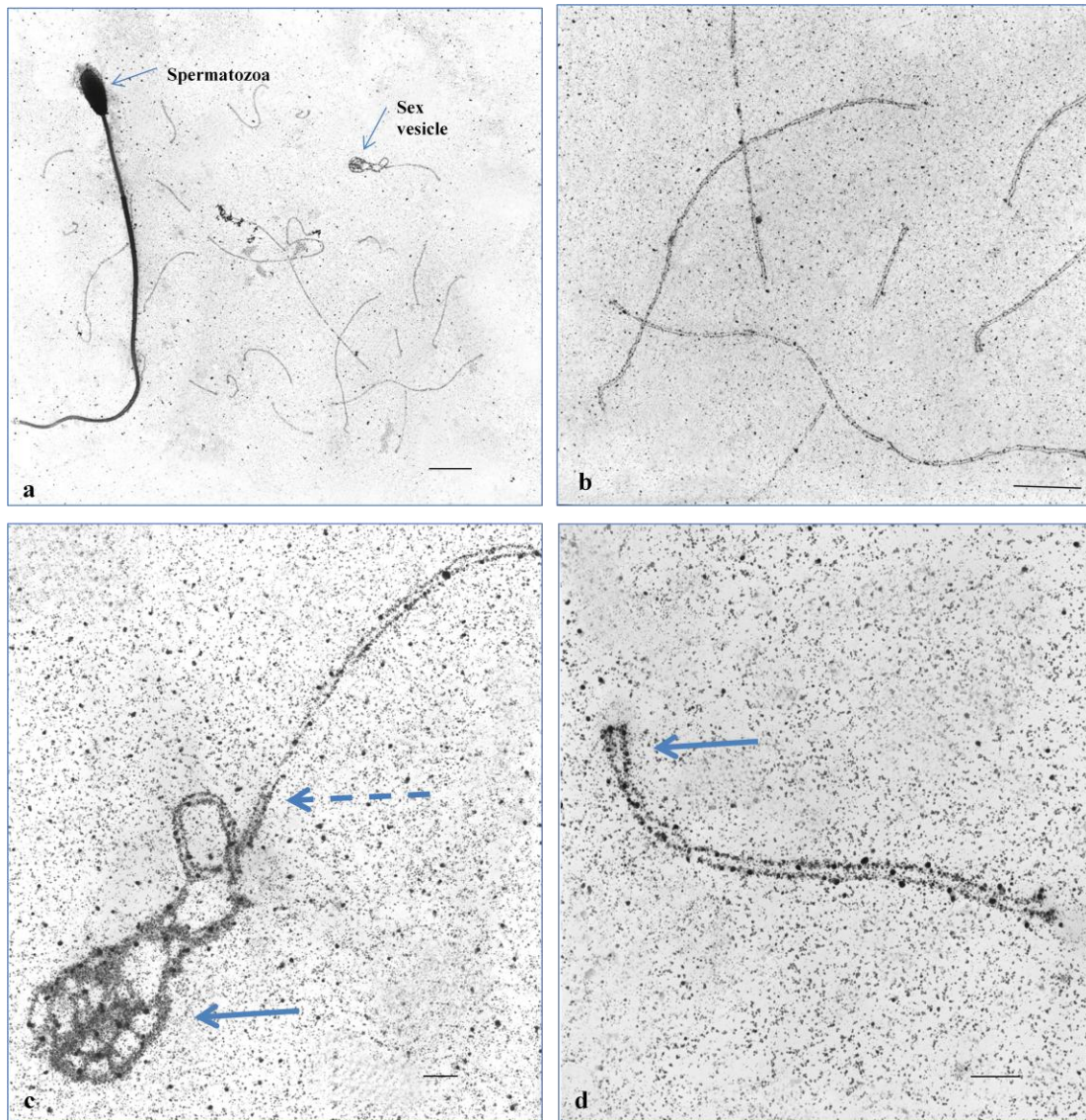


Figure 3.7: An EM surface spread preparation of fully paired horse male pachytene nucleus showing normal 32 bivalents with two lateral elements and without central element. a) Full nucleus with spermatozoa and sex vesicle. Scale bar—10 μm . (b-d) Enlarged parts of nucleus in a. (b) Different autosomes at low magnification showing enlarged part of nucleus. Scale bar—5 μm . (c) Sex vesicle showing folding of XY-bivalents (arrow) and one autosome with looped terminal (dash arrow). Scale bar—1 μm . (d) Small acrocentric autosomes (arrow points to the centromer end) showing clear lateral elements but without central element. Scale bar—1 μm .

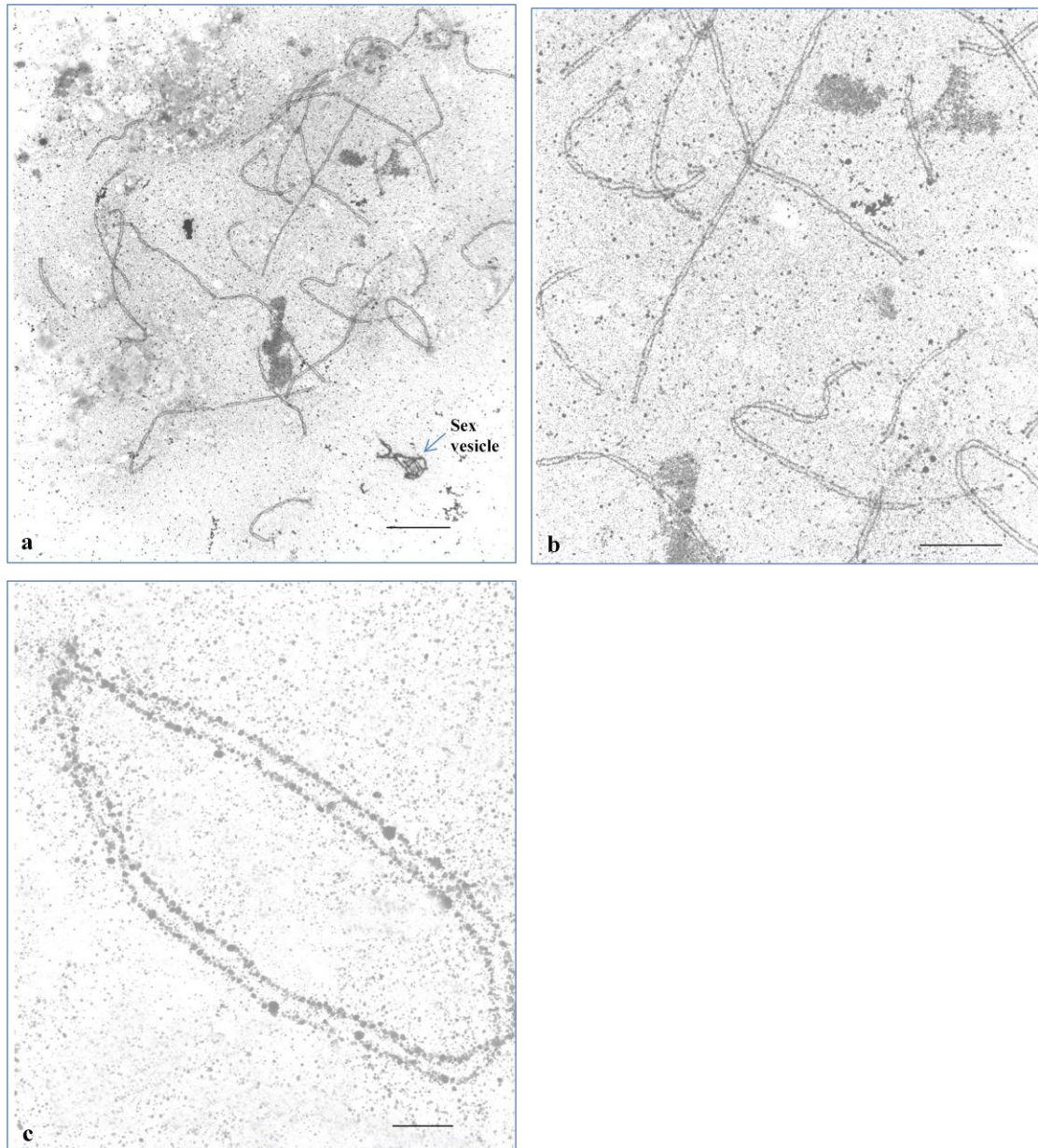


Figure 3.8: Another example of EM surface spread preparation of fully paired horse male pachytene nucleus showing normal bivalents with two lateral elements and without central element. (a) Full nucleus with 31 autosomal bivalents and sex vesicle. Scale bar—10 μm . (b-c) Enlarged parts of nucleus in a. (b) Different fully paired autosomes. Scale bar—5 μm . (c) Small autosome with clear two lateral elements and without central element or recombination nodules. Scale bar—1 μm .

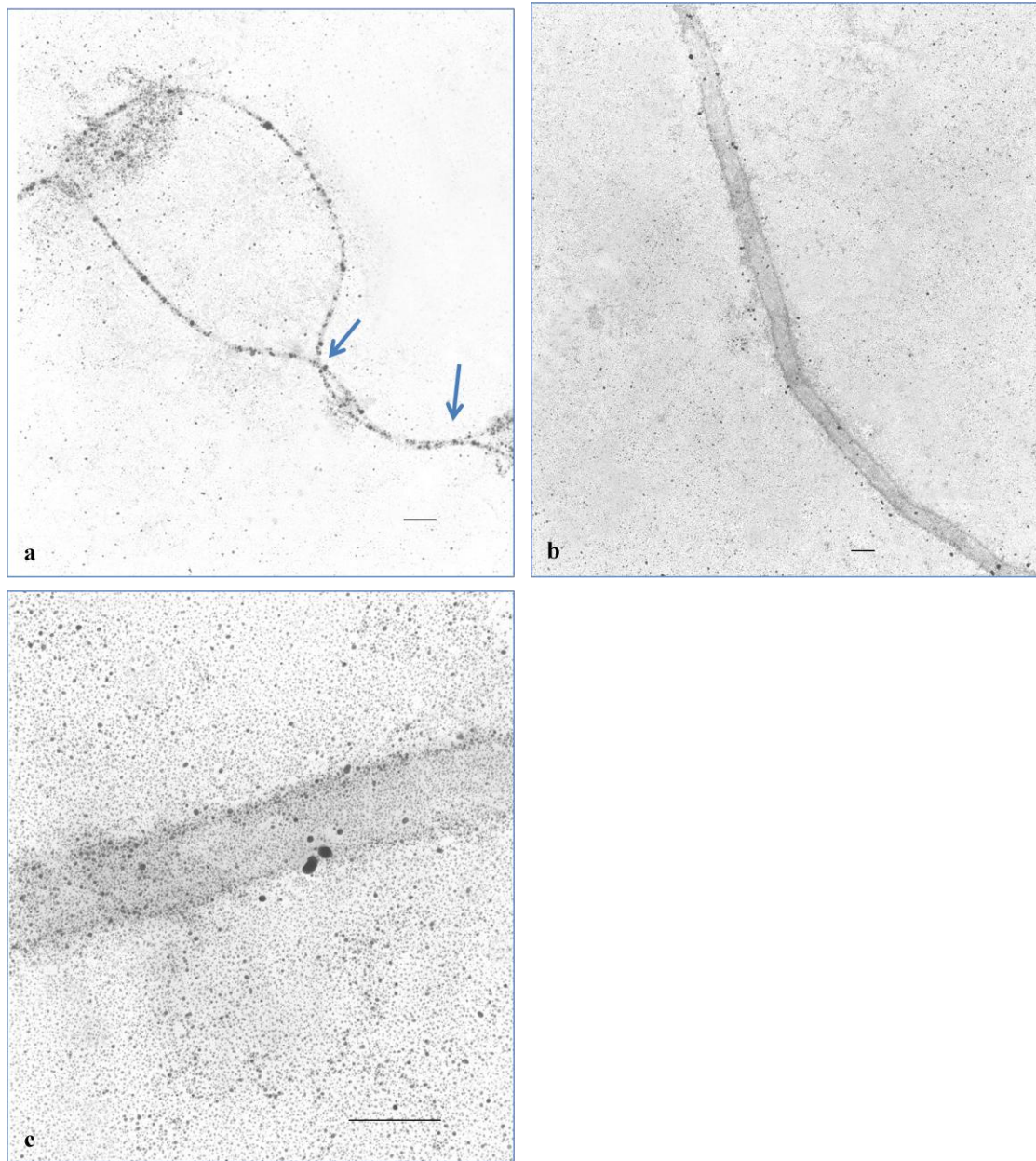


Figure 3.9: An EM surface spread preparation of different stages of PI male horse. (a) Autosome at early zygotene stage with unsynapsed segments at both ends (arrow showing the pairing segment). Scale bar—1 μm . (b) Autosome at late zygotene stage where there are almost complete paired lateral elements. Scale bar—1 μm . (c) Enlarged segment with high magnification of autosome in b clearly showing two lateral elements but without central element or recombination nodules. Scale bar—1 μm . Scale bar—1 μm .

3.3.4. MLH1 Foci frequency and distribution

A total of 523 fluorescently labelled pachytene nuclei were photographed and the frequency of MLH1 foci was calculated for each nucleus. However, 180 nuclei out of them were spread well in a way to be able to identify individual SC. The number of SCs per nucleus was 31 autosomal SCs, in addition to one XY SC. MLH1 foci were found regularly on pachytene SCs, but not on zygotene or diplotene SCs. All the autosomal SCs had at least one MLH1 focus. Most of the XY SC had just one focus which was distally localized. No XY SC had more than one focus (Figure 3.10). The number of MLH1 foci per SC ranged from one to four, with an average of 1.62 foci per autosomal SC. Short SCs average at least one MLH1 focus. In rare cases, MLH1 foci were very close (Figure 3.11).

For the 180 nuclei, the number of autosomal SCs with one MLH1 focus ranged from 10 to 18 (mean \pm SD, 15.22 ± 1.81 ; Table 3.1a and Appendix 9). The number of SCs with one MLH focus was not significantly different across the 6 stallions ($p = 0.060$; Table 3.1b). For SCs with 2 MLH1 foci, the average number ranged from 10 to 19 (mean \pm SD, 13.59 ± 1.68 ; Table 3.2a and Appendix 10). The number SCs with 2 MLH1 foci was significantly different across the 6 stallions ($p = 0.000$; Table 3.2b). For SCs with 3 MLH1 foci, the average number ranged from 1 to 4 (mean \pm SD, 2.08 ± 0.89 ; Table 3.3a and Appendix 11). The number of SCs with 3 MLH1 foci was significantly different across the 6 stallions ($p = 0.002$; Table 3.3b). For SCs with 4 MLH1 foci, the average number ranged from 0 to 1 (mean = 0.12; Table 3.4a and Appendix 12). The number of SCs with 4 MLH1 foci was not significantly different ($p = 0.683$; Table 3.4b). The total number of MLH1 foci per autosomal chromosomes ranged from 46 to 57 (mean \pm SD, 50.11 ± 2.35 ; Table 3.5 and Appendix 13). The total number of MLH1 foci per autosomal chromosomes was not significantly different across the 6 stallions ($p = 0.482$; Table 3.5b). Thus, total number of MLH1 foci per cell, including XY bivalent, ranged from 47 to 58 (mean \pm SD, 51.11 ± 2.35). The mean number of MLH1 foci per autosomal SC was 1.62.

For all scored nuclei (523), which include the 180 well spreaded nuclei, the total number of the autosomal MLH1 foci per nucleus among the 6 stallions ranged from 46 to 58 (mean \pm SD, 49.62 ± 2.26 ; Table 3.6a and Appendix 14). The total number of autosomal MLH1 foci, for the 523 nuclei, was not significantly different across the 6

stallions ($p = 0.071$; Table 3.6b). The mean number of MLH1 foci per autosomal SC was 1.60.

The summary for the frequency of autosomal bivalents with 1-4 MLH1 foci among 6 stallions are presented in Figure 3.12.

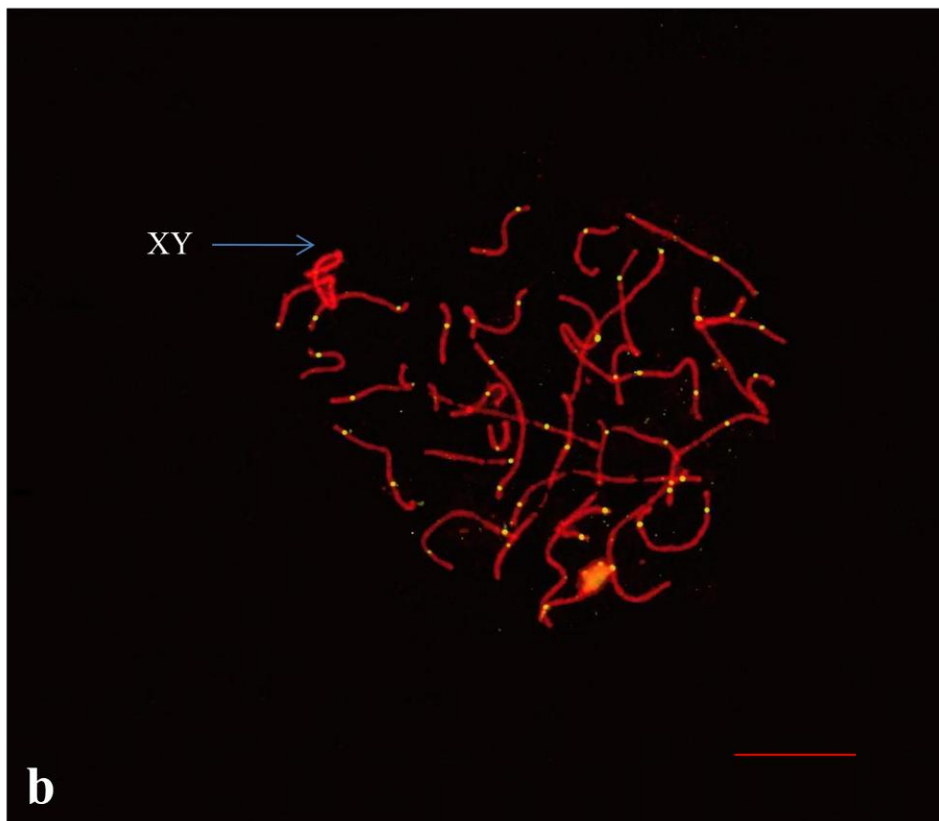


Figure 3.10: SC spreading of horse spermatocytes at pachytene stage labelled with anti-SCP3 antibody (red) and anti-MLH1 antibody (green). XY indicates sex bivalent (a and b). There are 31 autosomal SC and one Sex SC. The longest SC is for chromosome 1 with three MLH1 foci. Scale bar—10 μ m.

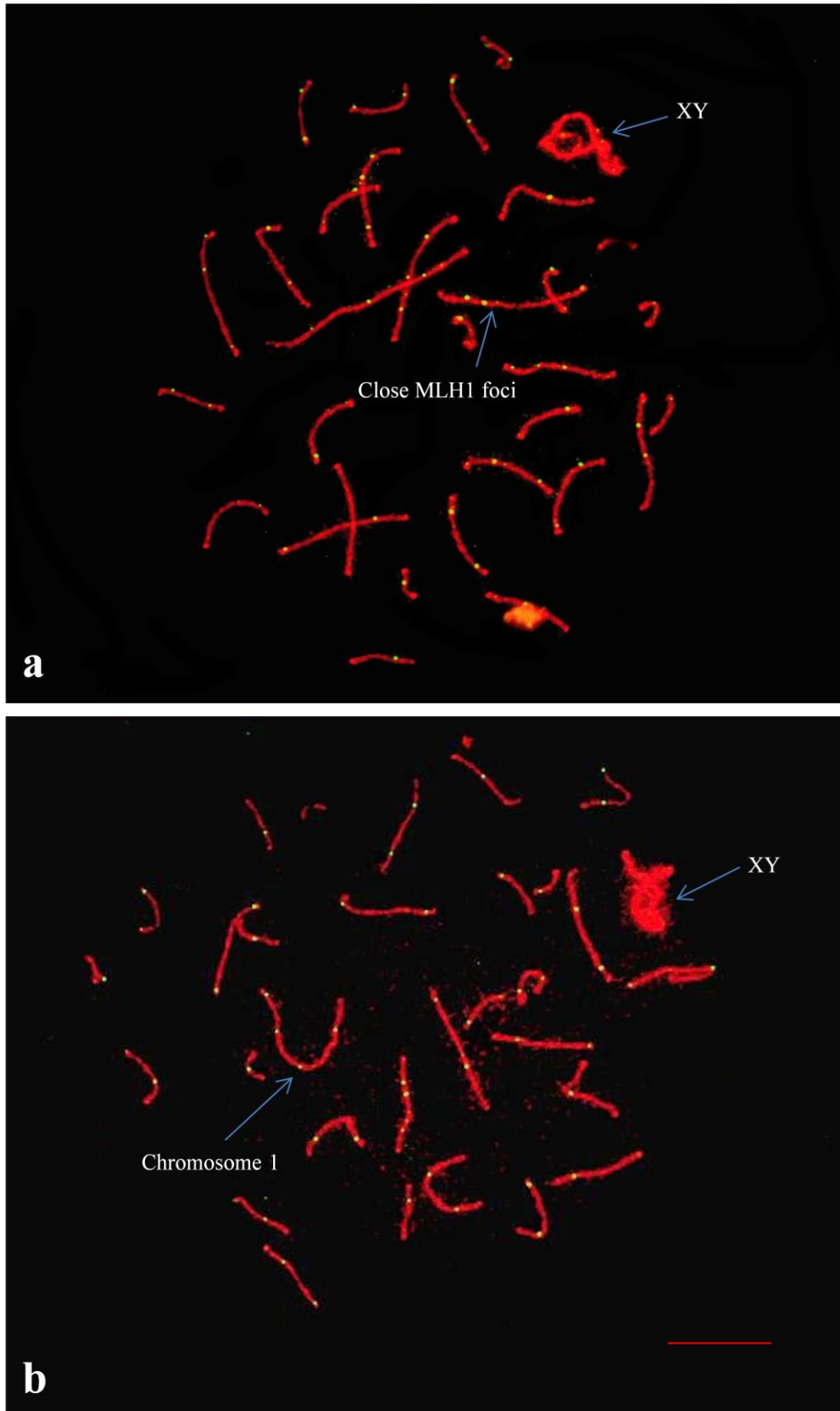


Figure 3.11: SC spreading from horse spermatocytes at pachytene stage labelled with anti-SCP3 antibody (red) and anti-MLH1 antibody (green). XY indicates sex bivalent. There are 31 autosomal SC and one Sex SC. (a) Showing one long chromosome with close MLH1 foci. (b) Showing The chromosome 1 with four MLH1 foci. Scale bar—10 μ m.

Table 3.1a: Autosomal SCs frequency with **one MLH1 focus** among 6 stallions (n=180)

Horse ID	Number of Scored Cells	Mean	SD	Range
H18	19	14.95	1.68	12-19
H19	34	15.24	1.79	13-19
H20	20	15.60	1.64	14-18
H22	28	15.36	1.97	12-19
H23	32	15.88	1.83	12-19
H24	47	14.64	1.72	11-19
Total	180	14.22	1.81	11-19

Table 3.1b: ANOVA Table for autosomal Scs frequency with **one MLH1 focus** among 6 stallions

Source	Sum of Squares	Df	Mean Square	F	Sig.
Between Groups	34.466	5	6.893	2.170	0.060
Within Groups	552.645	174	3.176		
Total	587.111	179			

Table 3.2a: Autosomal SCs frequency with **two MLH1 foci** among 6 stallions (n=180)

Horse ID	Number of Scored Cells	Mean	SD	Range
H18	19	13.74	1.37	12-18
H19	34	13.44	1.64	11-16
H20	20	12.95	1.61	10-16
H22	28	13.04	1.48	11-16
H23	32	13.06	1.72	11-19
H24	47	14.60	1.53	11-18
Total	180	13.59	1.68	10-19

Table 3.2b: ANOVA Table for autosomal Scs frequency with **two MLH1 foci** among 6 stallions

Source	Sum of Squares	Df	Mean Square	F	Sig.
Between Groups	74.40	5	14.88	6.03	0.000
Within Groups	429.17	174	2.47		
Total	503.58	179			

Table 3.3a: Autosomal SCs frequency with **three MLH1 foci** among 6 stallions (n=180)

Horse ID	Number of Scored Cells	Mean	SD	Range
H18	19	2.21	0.98	1-4
H19	34	2.26	0.99	1-4
H20	20	2.25	0.72	1-3
H22	28	2.50	0.88	1-4
H23	32	1.91	0.82	1-4
H24	47	1.70	0.75	1-4
Total	180	2.08	0.89	1-4

Table 3.3b: ANOVA Table for autosomal Scs frequency with **three MLH1 foci** among 6 stallions

Source	Sum of Squares	Df	Mean Square	F	Sig.
Between Groups	14.68	5	2.94	4.02	0.002
Within Groups	127.07	174	0.73		
Total	141.75	179			

Table 3.4a: Autosomal SCs frequency with **four MLH1 foci** among 6 stallions (n=180)

Horse ID	Number of Scored Cells	Mean	Minimum
H18	19	0.11	0-1
H19	34	0.12	0-1
H20	20	0.20	0-1
H22	28	0.11	0-1
H23	32	0.16	0-1
H24	47	0.06	0-1
Total	180	0.12	0-1

Table 3.4b: ANOVA Table for autosomal Scs frequency with **four MLH1 foci** among 6 stallions

Source	Sum of Squares	Df	Mean Square	F	Sig.
Between Groups	0.33	5	0.07	0.62	0.683
Within Groups	18.22	174	0.10		
Total	18.55	179			

Table 3.5a: MLH1 focus frequency in autosomal SCs per cell among 6 stallions (n=180)

Horse ID	Number of Scored Cells	Mean	SD	Range
H18	19	50.47	2.44	46-55
H19	34	50.32	2.43	46-55
H20	20	50.05	2.01	47-53
H22	28	50.36	2.64	46-56
H23	32	49.34	2.36	46-55
H24	47	50.19	2.20	46-57
Total	180	50.11	2.35	46-57

Table 3.5b: ANOVA Table for MLH1 focus frequency in autosomal SCs per cell among 6 stallions

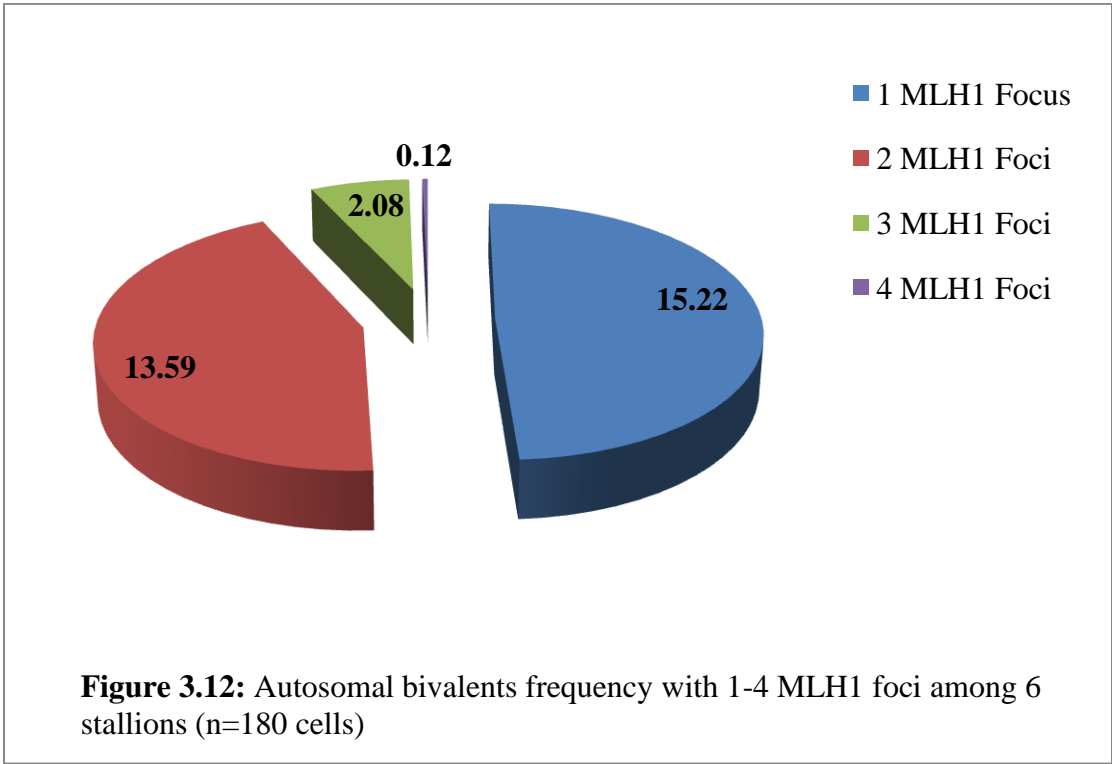
Source	Sum of Squares	Df	Mean Square	F	Sig.
Between Groups	24.94	5	4.99	0.90	0.482
Within Groups	964.05	174	5.54		
Total	988.99	179			

Table 3.6a: MLH1 focus frequency in autosomal SCs per cell among 6 stallions (n=523)

Horse ID	Number of Scored Cells	Mean	SD	Range
H18	81	49.41	2.45	46-58
H19	85	50.08	2.19	46-55
H20	82	49.23	2.06	46-55
H22	95	49.72	2.50	46-56
H23	78	49.28	2.12	46-55
H24	102	49.89	2.09	46-57
Total	523	49.62	2.26	46-58

Table 3.6b: ANOVA Table for MLH1 focus frequency in autosomal SCs per cell among 6 stallions

Source	Sum of Squares	Df	Mean Square	F	Sig.
Between Groups	51.53	5	10.31	2.05	0.071
Within Groups	2603.51	517	5.04		
Total	2655.04	522			



3.3.5. Localization of MLH1 foci to synaptonemal complex

The total lengths of SCs as well as the absolute and relative length of individual SC were measured for 24 different nuclei from sex stallions. Since centromeric regions could not be identified for SCs, telomeric regions were used to measure the SCs length as well as the position of MLH1 foci. Individual SC was difficult to identify with confidence. Thus, as alternative autosomal SCs were ranked in sequence according to their relative length (Table 3.7). The total length of all autosomal SCs ranged from around 230 μm to 282 μm (mean \pm SD, 254.55 \pm 3.68).

The distributions of a single MLH1 focus are different among the SC with the same length. SCs with one MLH1 focus showed different position of the focus among nuclei. Most of them were skewed toward the telomeres, very distally localized on SC, while others were interstitially. Two foci were rarely found on short SCs. Occasionally, one tended to lie nearer to the distal telomere and the other in the interstitial. In general, MLH1 foci were distally localised in most of SC.

The positions of MLH1 foci in each SC were measured and the distance between foci was calculated. The average of absolute distance varied among SC; however, the relative distance was not significantly different. The minimum absolute and relative distance between any MLH1 foci in the same SC was calculated among SCs with 4, 3 and 2 foci (Table 3.8). The average SCs relative length and the average number of MLH1 foci are highly correlated and the correlation is positive ($P = 0.000$; $R = 0.961$; Figure 3.13).

Table 3.7: Average absolute and relative lengths of stallion autosomal SCs (n=24 SC sets)

SC rank	Absolute lengths of SCs		Relative lengths of SCs	
	Average SC length \pm SD (μm)	Range of SC length (μm)	Average SC length \pm SD (%)	Range of SC length (%)
1	18.99 \pm 2.73	10.93 - 24.63	7.5 \pm 1.12	5.58 - 10
2	14.48 \pm 2.2	9.05 - 18.8	5.69 \pm 0.7	4.62 - 7.88
3	13.27 \pm 2.17	8.77 - 17.29	5.21 \pm 0.6	4.48 - 7.49
4	12.27 \pm 1.62	8.62 - 15.59	4.81 \pm 0.25	4.4 - 5.47
5	11.76 \pm 1.64	8.43 - 15.55	4.61 \pm 0.23	4.23 - 5.1
6	11.12 \pm 1.54	8.05 - 13.57	4.36 \pm 0.21	3.89 - 4.76
7	10.73 \pm 1.35	7.97 - 13.36	4.21 \pm 0.14	3.87 - 4.45
8	10.42 \pm 1.31	7.96 - 12.79	4.09 \pm 0.16	3.84 - 4.42
9	10.13 \pm 1.26	7.88 - 12.65	3.98 \pm 0.15	3.68 - 4.31
10	9.77 \pm 1.16	7.72 - 12	3.84 \pm 0.13	3.52 - 4.06
11	9.48 \pm 1.14	7.13 - 11.56	3.72 \pm 0.14	3.37 - 4.03
12	9.19 \pm 1.13	6.99 - 11.36	3.61 \pm 0.17	3.23 - 3.98
13	8.77 \pm 1.11	6.7 - 11.22	3.44 \pm 0.14	3.11 - 3.73
14	8.5 \pm 1.08	6.47 - 11.19	3.34 \pm 0.15	2.99 - 3.72
15	8.15 \pm 1.11	5.74 - 10.99	3.2 \pm 0.16	2.76 - 3.65
16	7.8 \pm 1.07	5.7 - 10.33	3.06 \pm 0.15	2.74 - 3.43
17	7.46 \pm 0.97	5.65 - 9.25	2.93 \pm 0.15	2.47 - 3.23
18	7.14 \pm 0.87	5.53 - 8.36	2.8 \pm 0.16	2.45 - 3.14
19	6.86 \pm 0.89	5.23 - 8.19	2.69 \pm 0.18	2.38 - 3.05
20	6.57 \pm 0.83	5.21 - 7.92	2.58 \pm 0.16	2.37 - 3.02
21	6.23 \pm 0.66	5.18 - 7.4	2.45 \pm 0.15	2.21 - 2.97
22	6.02 \pm 0.67	5.02 - 7.38	2.37 \pm 0.12	2.11 - 2.62
23	5.77 \pm 0.66	4.82 - 7.02	2.27 \pm 0.12	2.09 - 2.62
24	5.52 \pm 0.64	4.2 - 6.55	2.17 \pm 0.1	1.98 - 2.4
25	5.17 \pm 0.76	3.67 - 6.2	2.03 \pm 0.18	1.54 - 2.3
26	4.84 \pm 0.72	3.47 - 5.89	1.9 \pm 0.2	1.46 - 2.27
27	4.17 \pm 0.49	3.39 - 4.99	1.64 \pm 0.15	1.45 - 2.2
28	3.89 \pm 0.44	3.1 - 4.83	1.53 \pm 0.12	1.3 - 1.8
29	3.65 \pm 0.35	3.06 - 4.45	1.44 \pm 0.11	1.26 - 1.71
30	3.45 \pm 0.39	2.51 - 4.17	1.36 \pm 0.12	1.05 - 1.6
31	2.99 \pm 0.55	1.64 - 3.9	1.18 \pm 0.22	0.64 - 1.56

Table 3.8: The minimum absolute and relative distances between any two MLH1 foci among SCs with 4, 3 and 2 foci.

SC and No. of foci	Minimum absolute interfocal distance (μm)	Minimum relative interfocal distance (%)
SC with 4 MLH1 foci	3.6	16.09
SC with 3 MLH1 foci	1.23	9.89
SC with 2 MLH1 foci	1.14	12.66

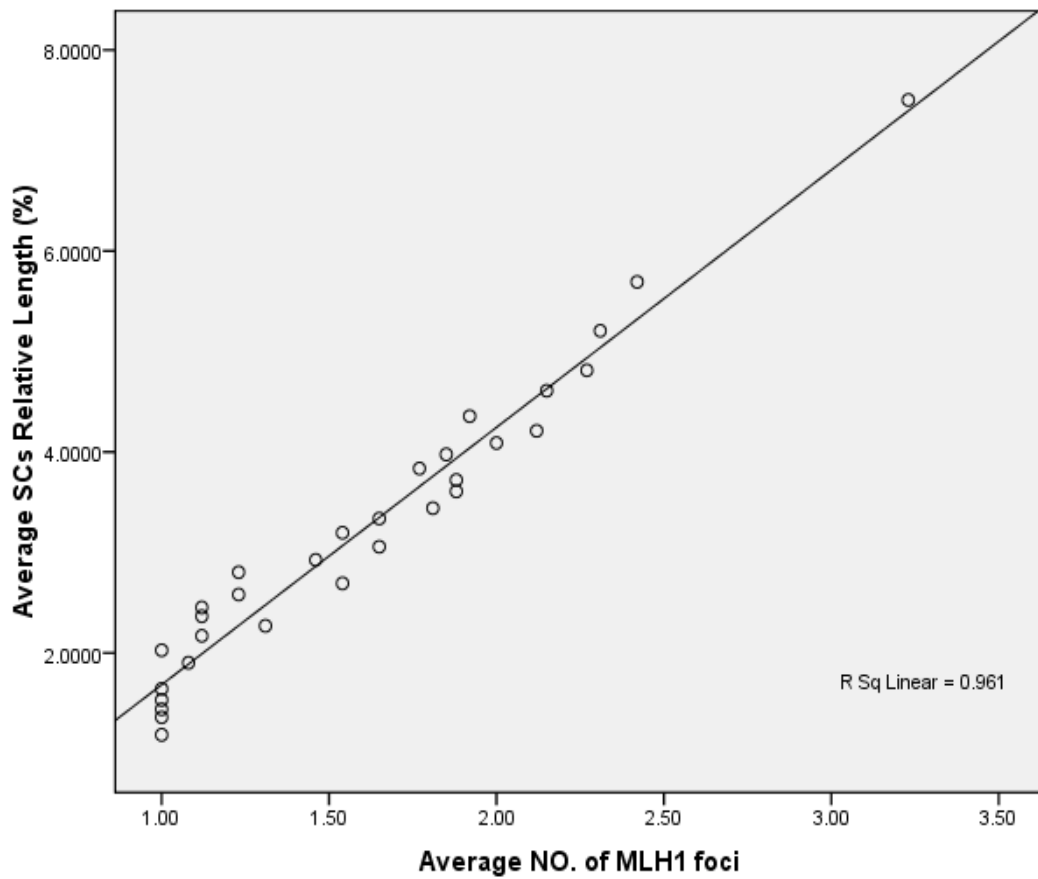


Figure 3.13: Correlation between the average SCs relative length and the average number of MLH1 foci.

3.4. Discussion

Fertility is a trait of main interest in domestic animals especially horse due to economic breeding value. Spermatogenesis abnormalities are major problem facing horse breeders due to a significant economic loss especially for valuable stallions. Meiosis I, which is a genetically controlled process, is the most important division in spermatogenesis. It is believed that most idiopathic non-obstructive azoospermia have genetic basis that could have complete or partial block at meiosis (Hargreave, 2000). Many of these cases are due to abnormalities in pairing, synapsis and/or recombination at prophase I of the first meiotic division (Bascom-Slack *et al.*, 1997). Surprisingly, little is known about spermatogenesis and meiotic processes in the horse. Thus, the purpose of this chapter was to study pairing, synapses and recombination process during PI in normal fertile stallions. This can help in future assessing the spermatogenesis in infertile and subfertile stallions. Moreover, implementing these findings in clinical practice will help equine clinicians in finding out the origins of any alterations in spermatozoa production as well as in taking a decision in subsequent therapeutic approaches.

In PI, homologous chromosomes undergo coordinated processes of recognition and pairing that followed by recombination. Any chromosome segment should undergo pairing with its homologous counterpart during synaptic phase. Lack or insufficient pairing between homologous chromosomal segments could result in abnormal chromosome pairing behavior. This could lead to a meiotic arrest of the cell since it has been believed that crossing over, which is essential for normal chromosome segregation, depends on efficient pairing of homologous chromosomes (Chandley, 1986). Clear association has been found between failure of chromosome pairing and reduced fertility in humans (Speed, 1988). Moreover, unpaired chromosome or partially paired chromosome segments can undergo anomalous synapsis and pair with non-homologous chromosomes that can interpreted as chromosomal translocation. This is often associated with sex chromosomes. For instance, X-autosome translocations, which well known in human and different domestic animals, can lead to cell arrest at meiosis (Villagómez and Pinton, 2008).

The homologous chromosomes recognition and pairing facilitate their synapsis, which results in the formation of SC. The SC, the protein structure which holds the

homologous chromosomes together, consists of two lateral elements and one central element that join the lateral elements together. This will follow by crossing over, which are crucial for stabilization of homologues and proper segregation at anaphase I (Barlow and Hultèn, 1998). Chiasmata counts were used previously as a direct indicators of crossing over. However, this method is a time consuming and restricted approach due to the low number of MI cells recovered and inaccurate to some degree in determining the chiasma location. Electron microscopy was another method to visualise the crossing over through using silver nitrate staining to recognise the recombination nodules. This method is also tedious and time consuming. On the other hand, through recognition of different recombination proteins and the development of antibodies against these proteins, an immunofluorescent approach has been developed, which improved the meiotic process analysis (Barlow and Hultèn, 1998).

The synaptonemal complex protein 3 (SCP3), is a main component of the axial/lateral elements of the SC. Using antibody against SCP3 protein permits visualisation of different PI substages from early leptotene till pachytene stages (Villagómez and Pinton, 2008). Results here indicate that using anti-SCP3 enabled the efficient identification and characterization of leptotene, zygotene and pachytene of the first meiotic prophase stages in horse males of proven fertility. This would allow assessment if there is any disturbance in the recombination pathway which is associated with chromosome pairing and synapsis during PI that could affect the chromosome segregation at AI. These are associated mainly with meiotic arrest as well as with chromosomal segregation abnormalities and non-disjunction (Judis *et al.* 2004). Meiotic arrest can be defined by the inability of the germ line to cross a distinct stage of development (de Boer *et al.*, 2004). Lange *et al.* (1997) found that 17.5% of human male infertile patients showed abnormalities in SC.

DNA mismatch repair protein, MLH1, is component of late recombination nodules (Roeder, 1997). Using a combination of antibodies against SCP3 and MLH1 proteins allowed examining the important parts of meiosis, which include, initiation and processing of meiotic recombination, establishment of SC and maintenance of sister chromatide cohesion as well as chiasmata formation and production of gametes (Judis *et al.*, 2004). Two criteria were applied during analysis to select pachytene nuclei for analysis: 1) SC should be complete and not broken; 2) The number of MLH1 per nucleus should be 31 or more per autosomal SCs, which is the lowest threshold of

MLH1 on autosomal SCs. Anti-MLH1 antibody has produced labeling of discrete foci on the SCs, which mark the sites of crossing over at PI that would be resolved as chiasmata by MI. Different size of MLH1 foci were detected in the same nucleus, which could be due to differential access of MLH1 antibodies as a result of the spreading procedure or the pachetene sub-stages of the nucleus that may affect the gain or loss of MLH1 proteins (Anderson *et al.*, 1999). MLH1 results demonstrate positive interference. However, MLH1 foci were very close, in rare instance (< 5% of cells; Figure 3.11a), showing that it is physically possible to get close neighboring exchange. Sun and colleagues (2004) reported similar results (~3%-4% of cells) in human male.

Around 80% of the SC of XY was found to have MLH1 foci. Failure of XY from receiving MLH1 focus could be due to sub-stage of particular pachytene nucleus, since MLH1 on XY SC may not appear or disappear in the same time as autosomal ones, or an indication of presence of numbers of spermatocytes destined for spermatogenic arrest (Barlow and Hultèn, 1998). This observation is higher than human male (58.8%), in which the MLH1 focus can persist long after desynapsing the majority of synaptic region (Barlow and Hultèn, 1998). However, in mouse spermatocyte, MLH1 focus was consistently observed on the SC of XY in early stages but not in later stages (Baker *et al.*, 1996). Thus, this indicates that MLH1 is transient and appears on XY at a different time than autosomes.

The present study has provided a detail about the average number of autosomal MLH1 per pachytene nucleus. The average, which ranged from 49.34 to 50.47 autosomal foci for horses number H23 and H18 respectively, was calculated (Mean \pm SD; 50.11 ± 2.35) among 6 stallions with a total number of 180 nuclei. No significant difference was detected among individuals ($P = 0.482$). Around half of the SCs (49.1%) showed 1 MLH1 focus with no significant differences among stallions ($P = 0.060$). However, SCs with 4 foci, which usually visualised in chromosome 1, were rarely detected, 0.4% of the SCs. This mainly correlated to the size of the chromosomes and the location of the centromere as well as the position of the first foci. Most of the horse chromosomes are small and acrocentric (18 chromosomes). This agreed with the results obtained from measuring the SCs length that showed a high correlation between the average SC relative length and the average number of MLH1 foci. For instance, the average relative length of the longest SC (7.5%),

chromosome 1, is six times more than the smallest SC (1.18%). However, the longest SC showed a maximum of 4 foci compared to the smallest SC, which showed 1 focus all the time. This could be due to the presence of the centromere, which is metacentric for chromosome 1 while acrocentric for the smallest chromosomes, that exert crossover interferences. Moreover, at least 1 crossover is required for each homologous chromosome regardless of its length.

The number of MLH1 foci was varied from cell to cell, which could be due to stage of the cell at which the MLH1 was estimated or MLH1 interferences since again the position of the first crossover usually determine the number of extra foci on the same chromosome. Fluctuation in the MLH1 foci was reported with an initial increase by mid pachytene followed by a gradual decrease and the disappearance of anti-MLH1 antibody in mouse and human spermatocytes by late pachytene (Baker *et al.*, 1996; Barlow and Hultèn, 1998).

The present study showed an average of 50.11 MLH1 foci for horse autosomes, reciprocal recombination events, that corresponds to a genetic map length in horse male autosomes of 2,505.5 cM, considering that each focus corresponding to one crossing over and each crossing over is equal to 50 cM. However, one crossing over, which always takes place in the pseudoautosomal region of the XY bivalent (50 cM), should be added and the total genome length of the horse male is 2,555.5 cM, which compares to 2772 cM from linkage data (Swinburne *et al.*, 2006). Similar differences were observed in different mammalian, such as human, in which the genetic map from linkage analysis more than those from chiasma or MLH1 counts. For instance, Barlow and Hultèn (1998) reported 50.9 MLH1 foci in fertile human male that makes the genetic length 2545 cM, which compare to 2729 cM obtained from linkage analysis.

Although mammals have different numbers of chromosomes, the average of their genome size are close. As for other mammals, the average size of horse genome (~ 3 billion base pair) is very similar to human genome size (Chowdhary & Raudsepp, 2008). Thus, frequency of autosomal MLH1 in horse males reported here, 50.11 ± 2.35 , is very close to the human male autosomal MLH1, 49.8 ± 4.3 . Comparing to the human, which have 22 autosomes (17 metacentric and 5 acrocentric), horse have 31 autosomes but most of them are short and acrocentric, 13 metacentric and submetacentric as well as 18 acrocentric (Kaback *et al.*, 1992). Horse male showed different autosomal MLH1 foci frequency from other domestic species such as bull

(42.0±4.0) that have 29 autosomes, dog male (40.0±1.4) that have 38 autosomes and cat male (42.5±0.8) that have 18 autosomes. These discordant data could be related to different research groups and animals (Table 3.9).

Although this study did not identify individual chromosome or centromere, results obtained from measuring the SCs absolute and relative length enable us to rank the SCs in sequence depending on their relative length. This ranking, which depend on SCs relative length, does not necessary to correspond to the mitotic chromosomes ranking, which usually identified by their GF-banding. Different reports showed discorrelate of both ranking in other species. For example, the average relative length of human chromosome 22 (2.01%) is longer than that of chromosome 21 (1.44%; Sun *et al.*, 2004). The average physical length of horse male autosomal SCs (254.55 µm) is smaller than human one (297.85 µm; Sun *et al.*, 2004). The minimum absolute interfocal distance between any two MLH1 foci varied among SCs with 4, 3, and 2 foci; however, their relative interfocal distance are close except the short SC that rarely shows two foci. This could be related mainly to the length of SC and the position of the centromere, which exerts crossover interferences. Thus, in case of meta- or submetacentric chromosomes, the distance between any two foci located in both sides of centromere expected to be longer than the ones without centromere interferences. Moreover, the absolute distance between any two foci on the same SC is different from nucleus to nucleus which could be due to the position of the first obligatory focus on the SC.

Table 3.9: Average MLH1 frequency per spermatocyte for different species

Species	Average number of MLH1 foci (mean \pm SD)	Number of scored cells	Reference
Horse Male	50.11 \pm 2.35	180	present report ^a
Human Male	49.8 \pm 4.3	100	Sun <i>et al.</i> (2004) ^a
Bull	42.0 \pm 4.0	5,285	Hart <i>et al.</i> (2008)
Dog Male	40.0 \pm 1.4	124	Basheva <i>et al.</i> (2008)
Cat Male	42.5 \pm 0.8	61	Borodin <i>et al.</i> (2007)

^a Data for autosomes only (MLH1 focus from XY bivalent not included).

3.5. Conclusion

This is the first report presented immunocytological recombination maps for all horse male chromosomes. Based on the results obtained it is concluded that the analysis of prophase of the first meiotic division in horse using immunofluorescence approach, is efficient and reliable for identifying and characterization of different stages of PI as well as for localization of crossing over events. This will help in assessment the recombination pathway and the gametes formation. Crossover interference seems to affect the placement of pairs of MLH1 foci and the SC length predicts the number of crossovers and, therefore, the genetic length.

Chapter 4

Viability of Stallion Spermatozoa

4.1. Introduction

The previous chapters dealt with meiotic process while this chapter investigated the final stage of spermatozoa development and formation. Spermatozoon is a vehicle that delivers the paternal haploid genome into the oocyte during fertilization. Equine Spermatozoon, like other mammalian spermatozoa, consists of a head (which comprises the nucleus and the acrosome), mid-piece (which include the mitochondria) and tail (Ramalho-Santos *et al.*, 2007; Samper, 2009).

Spermatogenesis is the process of spermatozoa production by the seminiferous epithelium of the testis. In this process, spermatogonial stem cells generate primary spermatocytes, through mitotic division, which later undergo the two meiotic divisions to generate spermatids. The resulting spermatids undergo morphological differentiation to generate mature spermatozoa. This differentiation includes: elongation of cellular shape, super condensation of chromatin, formation of the digestive enzymes (including hyaluronidase and acrosin) that fill the acrosome, and assembly of the axoneme for motility that include mitochondria and tail formation (Samper, 2009). Spermatozoa detach from the surface of seminiferous epithelium and travel through the lumen of the seminiferous tubule to the epididymal ducts that can be ejaculated later on (de Jonge & Barratt, 2006). Different spermatozoa maturation processes, such as surface and membrane differentiation, take place after they have been released (Holstein *et al.*, 2003).

Different laboratory assays have been developed to evaluate the fertilizing potential of the semen sample (Ramalho-Santos *et al.*, 2007). Conventional evaluations are either quantitative, such as volume and count, or qualitative, such as percentage of motile spermatozoa and spermatozoa morphology (Samper, 2009). This information provides the first evaluation about the success of spermatogenesis and remains the most

common evaluation. In addition to this, several functional tests have been developed to improve the prediction of stallion fertility (Samper, 2009). Different classical stains such as eosin, trypan blue (TB) and chicao sky blue (CSB) as well as different fluorescent stains, such as diamidino-phenylindole (DAPI) and SYBR-14, have been used to evaluate spermatozoa viability. Viable spermatozoa do not permit the penetration of the stains into the cell whereas non-viable spermatozoa stain (Kútvölgyi *et al.*, 2006; Ramalho-Santos *et al.*, 2007).

The formation and development of spermatozoa are affected by meiotic irregularity and chromatin imbalance as well as other malformations that occur in a large number of spermatids, mainly: 1) nucleus, in which chromatin condensation may be disturbed; 2) acrosomes, malformation or absence of which severely affects the fertility; 3) flagellum, malformation or absence of which will hinder the mobility of the spermatozoa ; 4) and finally a combination of the above malformations (Holstein *et al.*, 2003). Spermatozoa may be considered infertile if they are immotile, have a damaged acrosome or any nuclear aberrations; however, for fertilization, only a minority of cells are required to be functional. Fertile stallions can have abnormal semen profiles with a very heterogeneous spermatozoa population, while subfertile or infertile stallions can present normal ones (Gamboa & Ramalho-Santos, 2005).

The main function of the acrosome is to help in spermatozoa penetration of the *zona pellucida* and fusion with the oolemma (Casey *et al.*, 1993). Spermatozoa receptor on *zona pellucida*, which is species-specific, stimulates fusion between the oocyte plasma membrane and outer acrosomal membrane. This fusion leads to the acrosome leaking the acrosomal enzymes, which allow the spermatozoa to pass through the *zona pellucida* to deliver the paternal genome. Stallion spermatozoa that lose their acrosome can not bind to the *zona pellucida* and are therefore not capable of fertilization (Samper, 2009). Transmission electron microscopy is the most accurate method to evaluate the acrosomal status, but it is tedious and expensive. Light microscopic unstained acrosomal evaluation was used for species with large acrosomes, such as cattle and hamsters; however, it is not possible with other species, such as human, mouse and horse, since the acrosome is too small to be visualized (Casey *et al.*, 1993). Most methods available to assess the spermatozoa acrosomal integrity are based on using dyes or fluorescent markers. Fluorescein-conjugated lectins, such as *Pisum sativum* Agglutinin (FITC-PSA), can determine the acrosome

integrity, presence or absence of the acrosome, in different mammalian spermatozoa by binding the glycoconjugates in the spermatozoa acrosomal matrix (Ramalho-Santos *et al.*, 2007). Farlin *et al.* (1992) used the FITC-PSA lectin to evaluate the spermatozoa acrosomal integrity of fresh and cryodamaged horse semen.

Horse fertility has also been associated with spermatozoa motility. Spermatozoa mitochondria provide the energy for motility. Thus evaluation of spermatozoa mitochondrial function is important since any changes in it may reflect in spermatozoa motility (Gravance *et al.*, 1999). Different fluorescent vital dyes, such as MitoTracer Green, have been used to assess the spermatozoa mitochondrial function in many species (Ramalho-Santos *et al.*, 2007). The mitochondria labeling is combined with supravital stain, Hoechst 33342, to stain the chromatin.

The fertility of an individual stallion is evaluated by clarifying if quantitative and qualitative spermatological parameters are in compliance with the minimum requirements for stallion semen (Samper, 2009). Light microscopic evaluation of the ejaculate helps in the assessment of cellular components such as volume (50-150 ml), count (250-500 million per ml), shape (> 65% normal), pH (around 7.5), colour (milky) and motility patterns of spermatozoa (\geq 60% progressive motile). The spermatozoa count depends mainly on the seasonal influences and ejaculation frequency. There are always some abnormal sized and shaped (immature spermatozoa, abnormal cells with curved tails and deformed heads etc) but if defective spermatozoa numbers exceed 30-40%, the stallion may have fertility problems (Thomas, 2001). Differentiation between viable and nonviable spermatozoa is important not only to assess the fertility, but also for applied studies since it will help in selecting the optimal incubation and storage techniques (Casey *et al.*, 1993). However, if all this information is not enough, biopsies of the testes may be necessary to obtain valid information about the quality of spermatogenesis (Holstein *et al.*, 2003).

Herein, different methods and microscopic techniques were used to assess different spermatozoa structure such as viability of head and tail, acrosome integrity and spermatozoa mitochondrial function.

4.2. Materials and Methods

Seminal fluid was collected from the epididymal ducts of 13 stallions to check for normal spermatozoa morphology and appearance, in addition to studying the spermatozoa viability as well as acrosome integrity and mitochondrial function.

4.2.1. Spermatozoa Viability Test

Semen samples were diluted 1:40 in phosphate buffer saline (PBS), containing 0.06% K_2HPO_4 and 0.825% NaCl. A drop (~20 μ l) of 0.16% Chicago sky blue (CSB; Sigma-Aldrich, Germany) was mixed with a drop (~20 μ l) of diluted semen on clean microscopic slides. Smears were made using a second slide. Air-dried slides were fixed at room temperature in fixative (86 ml of 1 N HCl plus 14 ml of 37% formaldehyde solution and 0.2 g neutral red, stable for 1 year) for 4 min. After washing with tap water the slides were rinsed with distilled water. Slides were stained in 7.5% Geimsa stain at room temperature for 2 h after which the excess stain was washed with tap water before being rinsed in distilled water. Air-dried slides were examined under the light microscope for the percentage of live and dead (head and tail) of spermatozoa.

4.2.2. Assessment of Spermatozoa: Acrosome Integrity

Semen samples from eight stallions were diluted 1:40 in phosphate buffer saline (PBS), containing 0.06% K_2HPO_4 and 0.825% NaCl. Diluted semen (100 μ l) was incubated at 35 °C for 10 min with 2% paraformaldehyde. After spinning for 3 min at 600xg and discarding the supernatant, 200 μ l of 95% ethanol (190 μ l absolute ethanol with 10 μ l Hanks Hepes (HH) containing 1% BSA) was added and incubated at 4 °C for 30 min to permeabilize the spermatozoa plasma membrane. The spermatozoa were washed with 100 μ l HH after spinning for 3 min at 600xg and discarding the supernatant. The spermatozoa sample was incubated at 4 °C for 15 min with 50 μ l of 1 mg/ml FITC-PSA (Sigma, Germany). Finally, a drop (5 μ l) of the sample was placed

on microscopic slide and 500 spermatozoa were examined to evaluate the acrosome integrity using Olympus BX61 fluorescence microscope (Olympus, Japan).

4.2.3. Assessment of Spermatozoa: Mitochondrial Function

Semen samples from eight stallions were diluted 1:40 in phosphate buffer saline (PBS) containing 0.06% K_2HPO_4 and 0.825% NaCl. Diluted semen (20 μ l) was incubated with 50 μ l of 200 nM MitoTracer Green (Molecular Probes, USA) at 37 °C for 30 min. To stain spermatozoa DNA, 7 μ l of diluted Hoeschst 33342 (1:100) was added and incubated at 37 °C for another 10 min. Finally, a drop (5 μ l) of the sample was placed on microscopic slide and 500 spermatozoa were examined to evaluate the spermatozoa mitochondrial function using Olympus BX61 fluorescence microscope (Olympus, Japan).

4.2.4. Statistical Analysis

The descriptive and inferential statistics were applied through SPSS (version 16) and using the statistical software in the Excel package (Version 2007, Microsoft Corporation, Redmond, WA, USA). The statistics used were F statistics (ANOVA) to test the viability and variability across horses. In all cases, significance level was set at $P < 0.05$.

4.3. Results

4.3.1. Sperm viability

Chicago sky blue stained slides revealed good sperm staining with acceptable background that resulted in good differentiation between live and dead spermatozoa, heads and tails and sufficient acrosome staining. Sperm with live heads were white, and those with the dead heads were dark grayish-blue. Whereas tails of live sperm were light pink and dead tails were black. The intact acrosome was purple and the damaged one was lavender while sperm with no acrosome were pale gray (Figure 4.1). Different spermatozoa morphological abnormalities were visualised for the heads and tails, particularly for the head (such as spermatozoa with double heads, microheads, pointed heads etc) (Figure 4.2).

The average numbers of spermatozoa with live heads and tails were calculated for 13 stallions by scoring 6500 spermatozoa, 500 spermatozoa for each stallion. The average spermatozoa with live heads and tails ranged from 77% to 93% (mean \pm SD, 81.26 ± 5.06 ; Table 4.1a and Appendix 15). The spermatozoa with live heads and tails were significantly different across the 13 stallions ($p = 0.000$; Table 4.1b). The average spermatozoa with dead heads and tails ranged from 2% to 15% (mean \pm SD, 10.46 ± 2.84 ; Table 4.2a and Appendix 16). The spermatozoa with dead heads and tails were significantly different across the 13 horses ($p = 0.000$; Table 4.2b). The average spermatozoa with dead heads but live tails ranged from 1% to 8% (mean \pm SD, 3.92 ± 1.81 ; Table 4.3a and Appendix 17). The spermatozoa with dead heads but live tails were significantly different across the 13 stallions ($p = 0.000$; Table 4.3b). The average of spermatozoa with dead tails but live heads ranged from 1% to 9% (mean \pm SD, 4.38 ± 2.42 ; Table 4.4a and Appendix 18). The spermatozoa with dead tails but live heads were significantly different across the 13 stallions ($p = 0.000$; Table 4.4b).

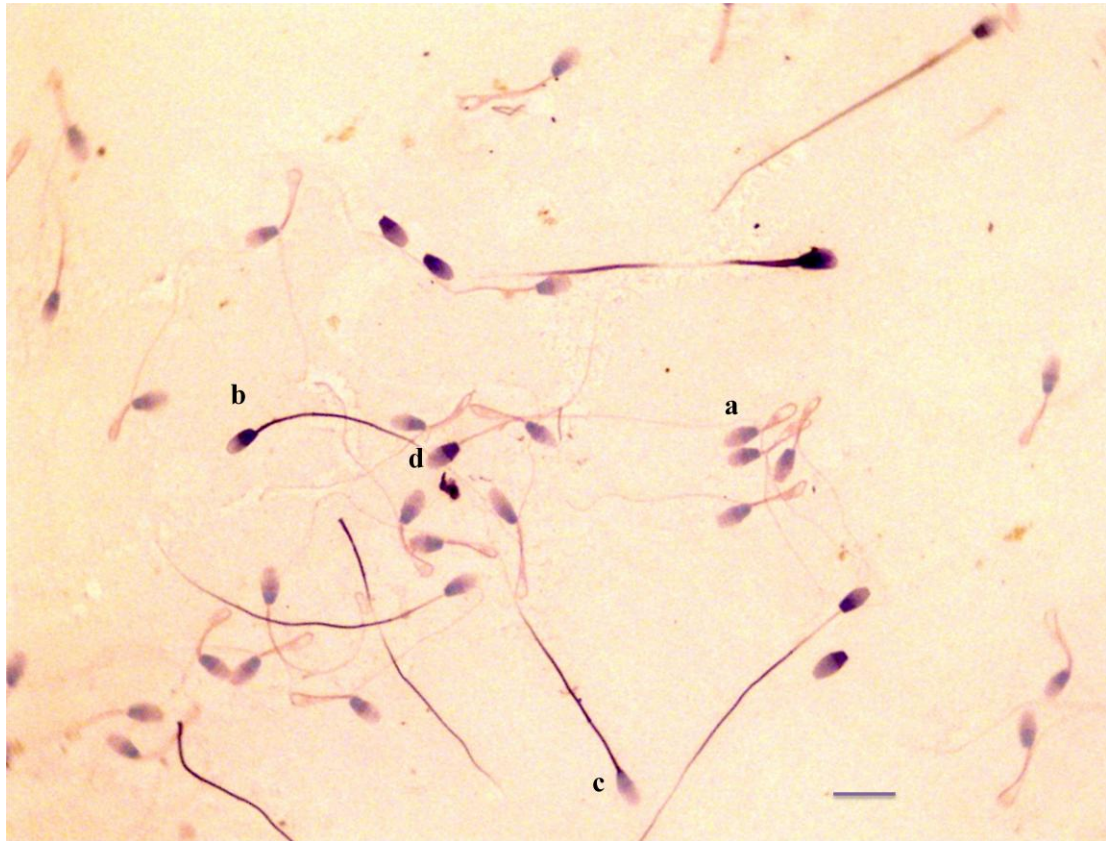


Figure 4.1: Stallion spermatozoa stained with Chicago sky blue staining. a) Spermatozoon with intact head, tail and acrosome membrane. b) Spermatozoon with damaged head, tail and acrosome membrane. c) Spermatozoon with intact head and damaged tail membrane. d) spermatozoon with damaged head and intact tail membrane. Scale bar—10 μ m.

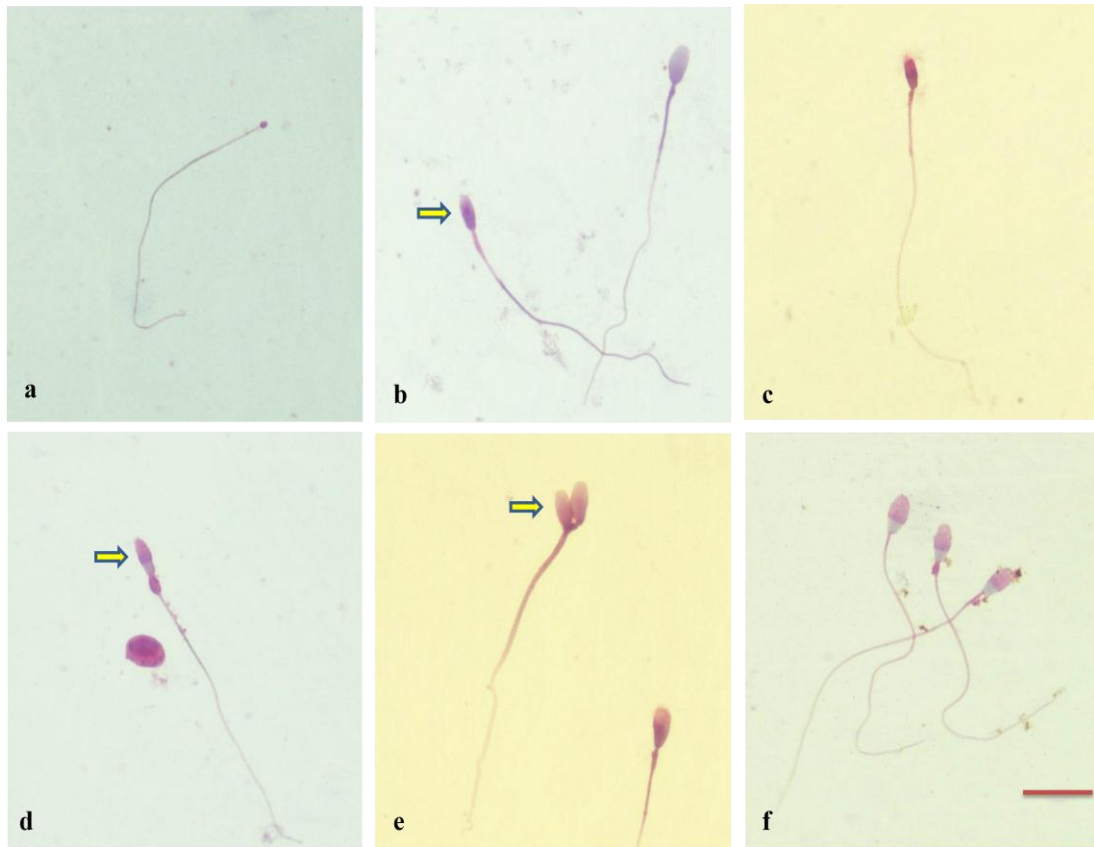


Figure 4.2: Stallion spermatozoa stained with Chicago sky blue staining to visualise morphological abnormalities; (a) microhead; (b) small head (arrow); (c) small head; (d) small head with proximal cytoplasmic droplet (arrow); (e) double head (arrow) and (f) normal spermatozoa. Scale bar—10 μ m.

Table 4.1a: Viability test of spermatozoa with **live heads and tails** among 13 stallions (n=6500)

Horse ID	Number of Scored Spermatozoa	Mean	SD	Range
H11	500	78.8	1.10	77-80
H12	500	79.6	2.97	75-83
H13	500	78.6	3.36	75-83
H14	500	80.2	2.59	77-83
H15	500	75.8	3.42	72-81
H16	500	76.8	1.92	74-79
H17	500	84.6	1.14	83-86
H18	500	86.8	1.79	85-89
H19	500	91.8	0.84	91-93
H20	500	87.4	1.34	86-89
H22	500	78	1.58	76-80
H23	500	78.2	1.79	76-80
H24	500	79.8	1.92	77-82
Total	6500	81.26	5.06	72-93

Table 4.1b: ANOVA Table for viability test of spermatozoa with **live heads and tails** among 13 stallions

Source	Sum of Squares	df	Mean Square	F	Sig.
Between Groups	1397.354	12.000	116.446	25.314	0.000
Within Groups	239.200	52.000	4.600		
Total	1636.554	64.000			

Table 4.2a: Viability test of spermatozoa with **dead heads and tails** among 13 stallions (n=6500)

Horse ID	Number of Scored Spermatozoa	Mean	SD	Range
H11	500	10.8	1.30	9-12
H12	500	11.2	2.28	9-15
H13	500	11.6	2.41	9-15
H14	500	10.6	1.52	9-13
H15	500	12.8	2.59	10-15
H16	500	14	1.73	11-15
H17	500	9	1.22	8-11
H18	500	9.6	1.82	8-12
H19	500	4	1.22	2-5
H20	500	9.2	1.30	8-11
H22	500	12.8	1.30	11-14
H23	500	10.8	1.64	9-13
H24	500	9.6	1.14	8-11
Total	6500	10.46	2.84	2-15

Table 4.2b: ANOVA table for viability test of spermatozoa with **dead heads and tails** among 13 stallions

Source	Sum of Squares	df	Mean Square	F	Sig.
Between Groups	362.554	12.000	30.213	10.228	0.000
Within Groups	153.600	52.000	2.954		
Total	516.154	64.000			

Table 4.3a: Viability test of spermatozoa with **dead heads and live tails** among 13 stallions (n=6500)

Horse ID	Number of Scored Spermatozoa	Mean	SD	Range
H11	500	2.8	0.45	2-3
H12	500	4	1.22	3-6
H13	500	4.4	1.14	3-6
H14	500	3.6	0.55	3-4
H15	500	5	1.00	4-6
H16	500	2.4	0.55	2-3
H17	500	4.2	1.64	2-6
H18	500	2.4	0.55	2-3
H19	500	2.8	1.30	1-4
H20	500	2.2	0.45	2-3
H22	500	3	0.71	2-4
H23	500	7.6	0.55	7-8
H24	500	6.6	0.55	6-7
Total	6500	3.92	1.81	1-8

Table 4.3b: ANOVA Table for viability test of spermatozoa with **dead heads and live tails** among 13 stallions

Source	Sum of Squares	df	Mean Square	F	Sig.
Between Groups	166.215	12.000	13.851	16.987	0.000
Within Groups	42.400	52.000	0.815		
Total	208.615	64.000			

Table 4.4a: Viability test of spermatozoa with **dead tails and live heads** among 13 stallions (n=6500)

Horse ID	Number of Scored Spermatozoa	Mean	SD	Range
H11	500	7.6	1.14	6-9
H12	500	5.2	1.10	4-7
H13	500	5.4	1.14	4-7
H14	500	5.6	2.19	3-9
H15	500	6.4	1.67	5-9
H16	500	6.8	2.17	4-9
H17	500	2.2	0.45	2-3
H18	500	1.6	0.55	1-2
H19	500	1.4	0.55	1-2
H20	500	1.2	0.45	1-2
H22	500	6.2	0.45	6-7
H23	500	3.4	0.89	2-4
H24	500	4	1.22	3-6
Total	6500	4.38	2.42	1-9

Table 4.4b: ANOVA Table for viability test of spermatozoa with **dead tails and live heads** among 13 stallions

Source	Sum of Squares	df	Mean Square	F	Sig.
Between Groups	296.985	12.000	24.749	16.415	0.000
Within Groups	78.400	52.000	1.508		
Total	375.385	64.000			

4.3.2. Spermatozoa Acrosome Integrity

Excellent results were obtained for staining sperm acrosome from different stallion semen samples using FITC-PSA. Two patterns of spermatozoa can be clearly differentiated: spermatozoa with intact acrosome (intense completely green fluorescent), and spermatozoa with reacted acrosome (only fluorescent band at the spermatozoa equational segment) (Figure 4.3).

Stallion spermatozoa with different morphological abnormalities were visualized, such as abnormal head (small head, round head, pointed head and double head) or mid-piece or tail, such as short or coiled tail (figure 4.4).

The percentage of spermatozoa with intact acrosome was calculated for eight stallions: by scoring 4000 spermatozoa, 500 spermatozoa for each stallion. The overall average spermatozoa with intact acrosome ranged from 89% to 97% (mean \pm SD, 93.85 ± 1.9 ; Table 4.5a and Appendix 19). The spermatozoa with intact acrosomes were significantly different across the eight stallions ($p = 0.000$; Table 4.5b).

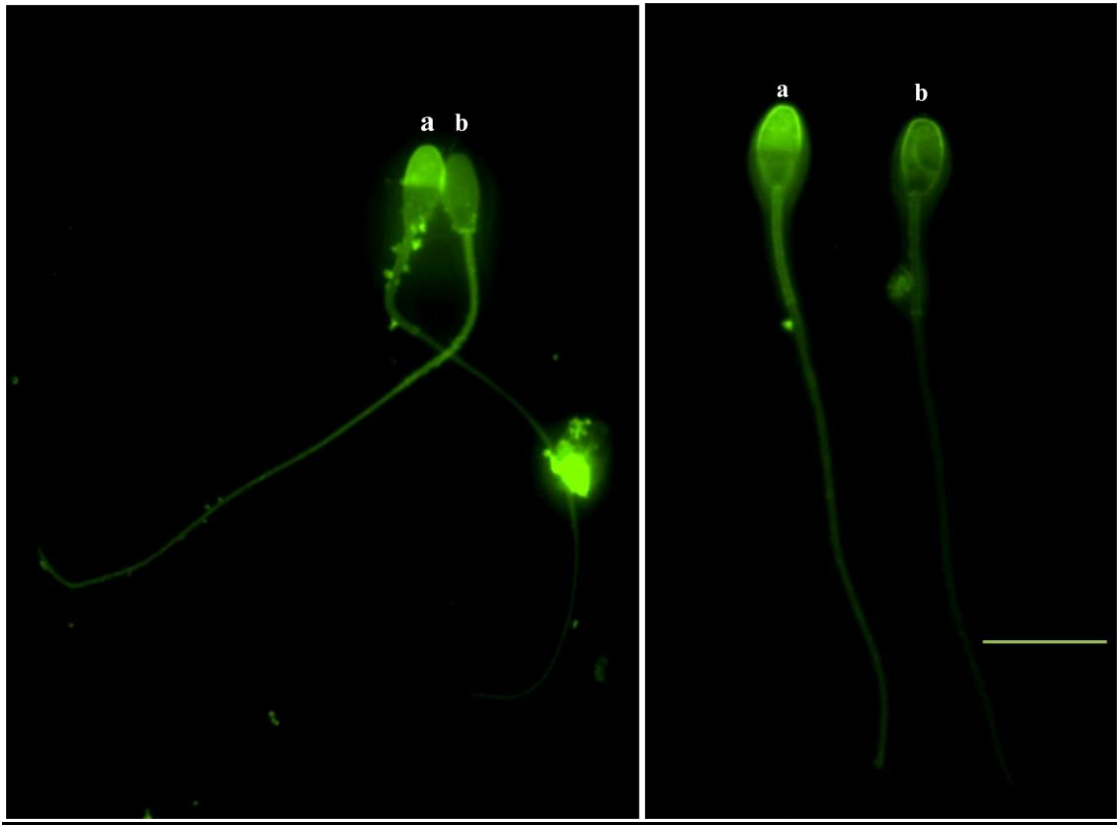


Figure 4.3: Fluorescence microscopy method. Stallion spermatozoa labelled with acrosomal stain (FITC-PSA). (a) Spermatozoon with intact acrosome (intense green fluorescence). (b) Spermatozoon with reacted acrosome. Scale bar—10 μ m.

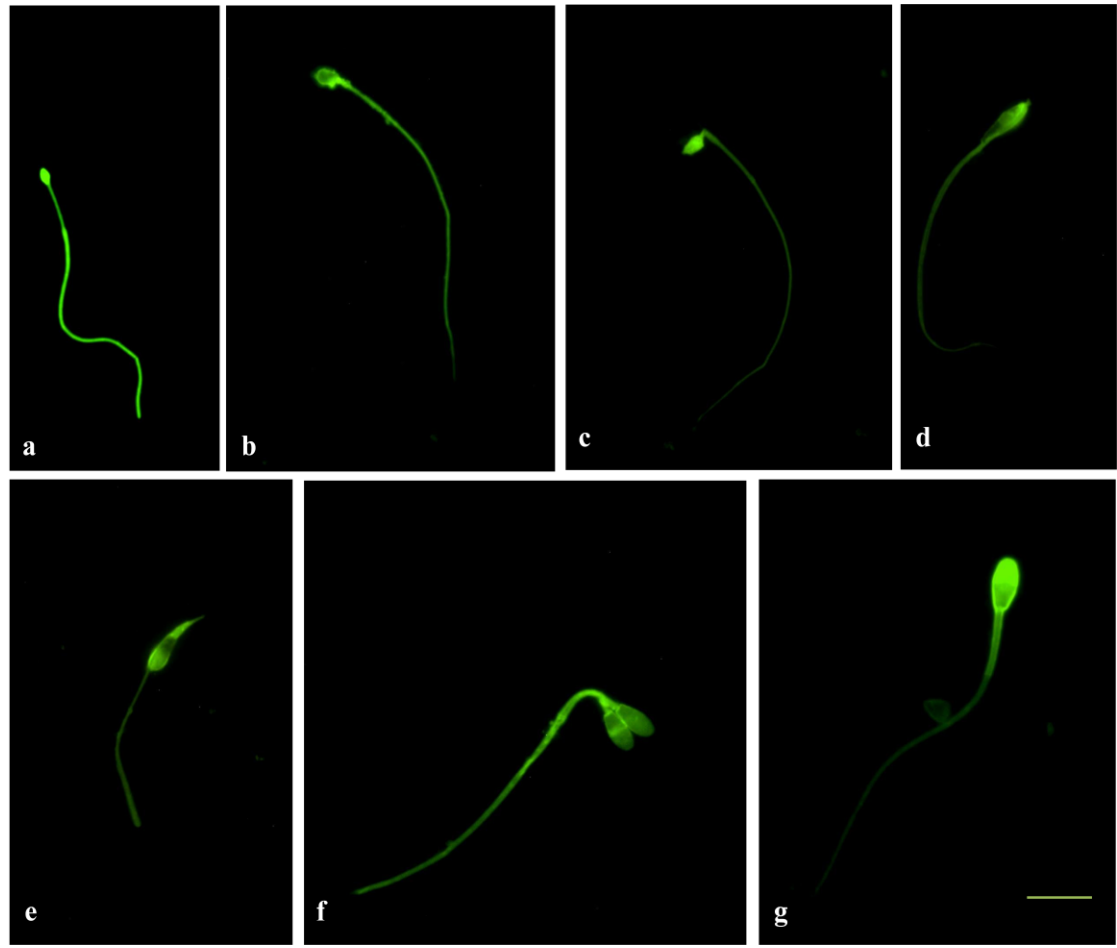


Figure 4.4: Fluorescent microscopy method: Morphological abnormalities; (a) micro head with abnormal tail; (b) small and round head; (c) small head with abnormal mid-piece; (d) abnormal head and tail; (e) abnormal pointed head and tail; (f) double head and (g) normal spermatozoa. Scale bar—10 μm .

Table 4.5a: Acrosome integrity test of spermatozoa with **intact acrosome** among 8 stallions (n=4000)

Horse ID	Number of Scored Spermatozoa	Mean (%)	SD	Range
H16	500	90.4	1.14	89-92
H17	500	94.8	1.30	93-96
H18	500	95.6	0.55	95-96
H19	500	95	1.00	94-96
H20	500	95.4	1.14	94-97
H22	500	92.6	1.14	91-94
H23	500	93.2	0.84	92-94
H24	500	93.8	0.84	93-95
Total	4000	93.85	1.90	89-97

Table 4.5b: ANOVA Table for acrosome integrity test of spermatozoa with **intact acrosome** among 8 stallions

Source	Sum of Squares	df	Mean Square	F	Sig.
Between Groups	107.900	7.000	15.414	14.857	0.000
Within Groups	33.200	32.000	1.038		
Total	141.100	39.000			

4.3.3. Spermatozoa Mitochondrial Function

Stallion mitochondrial spermatozoa were clearly visualized and assessed using MitoTracer green. The mid-piece of spermatozoa with functional mitochondria present as green fluorescence, while the one with non-functional mitochondria remain non-fluorescence (Figure 4.5).

The percentage of spermatozoa with functional mitochondria was calculated for eight stallions by scoring 4000 spermatozoa, 500 spermatozoa for each stallion. The over all spermatozoa with functional mitochondria ranged from 91% to 98% (mean \pm SD, 95.63 ± 1.63 ; Table 4.6a and Appendix 20). The spermatozoa with functional mitochondria were significantly different across the eight stallions ($p = 0.000$; Table 4.6b).

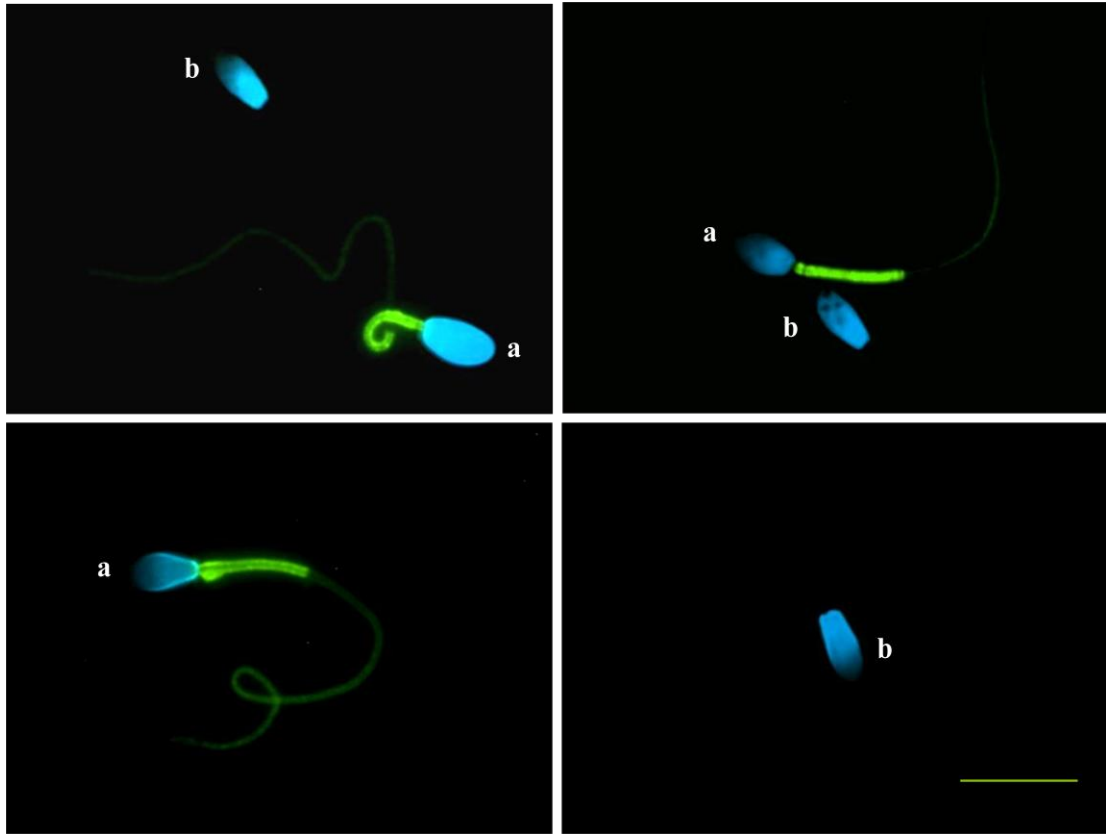


Figure 4.5: Fluorescence microscopy method to analyze stallion spermatozoa labelled with mitochondria stain (MitoTracer Green) and DNA stain (Hoechst 33342). (a) Spermatozoa with functional mitochondria (b) Spermatozoa without functional mitochondria. Scale bar—10 μm .

Table 4.6a: Mitochondrial function test of spermatozoa with **functional mitochondria** among 8 stallions (n=4000)

Horse ID	Number of Scored Spermatozoa	Mean (%)	SD	Range
H16	500	92.8	1.30	91-94
H17	500	94.4	1.14	93-96
H18	500	95.8	1.30	94-97
H19	500	95.6	1.14	94-97
H20	500	97	0.71	96-98
H22	500	96.6	0.89	96-98
H23	500	96.8	0.84	96-98
H24	500	96	0.71	95-97
Total	4000	95.63	1.63	91-98

Table 4.6a: ANOVA Table for mitochondrial function test of spermatozoa with **functional mitochondria** among 8 stallions

Source	Sum of Squares	df	Mean Square	F	Sig.
Between Groups	69.375	7.000	9.911	9.328	0.000
Within Groups	34.000	32.000	1.063		
Total	103.375	39.000			

4.4. Discussion

Fertility is a complex status and many things should be considered and tested before a meaningful understanding of the reproductive abilities of a given stallion is accomplished. Male fertility does not depend only on the absolute assay and traditional semen analysis that does not give much information. In fact, semen samples should be subjected to multi-parametric analysis (Phetudomsinsuk *et al.*, 2008). The purpose of the assay and the available resources can determine the methods of choice (Ramahho-Santos *et al.*, 2007). The assays described in this thesis have been used for the evaluation of epididymally collected stallion semen for the first time.

Viable spermatozoa are the cells that possess intact plasma membrane (Alessandra *et al.*, 2010). Differentiation of intact and damaged spermatozoa plasma membrane of heads and tails are very important for evaluating semen quality. Different viability assays were used to assess the integrity of plasma membrane. Dyes, such as Chicago sky blue (CSB), have the capacity and strong affinity to bind to proteins of the spermatozoa. CSB staining method is simply used to evaluate stallion spermatozoa heads and tails membrane integrity and morphology. This staining method showed a good repeatability and staining uniformity, thereby providing more reliable and satisfactory evaluation for stallion spermatozoa.

The average number of the live heads and tails that were fertile for the 13 stallions was 81.26% while the average of the dead ones was 18.74%. This includes 10.46% with dead heads and tails, 3.92% with dead heads but live tails and 4.38% with dead tails but live heads (immotile). The percentage of each type of spermatozoa viability was significantly varied across the 13 stallion ($P = 0.000$). This result is close to, with little discordance, to the one (mean = 75 ± 6) which was reported by Casey and colleagues (1993) using H258 fluorescent dye and ejaculated semen samples. This slightly discordant data could be related to different factors, such as different stallions, nature of the sample (ejaculated or collected from epididymal ducts), season, and stain methodology. Present results may not give a clear picture of stallion fertility since the samples were collected from the epididymal ducts, where some of the spermatozoa may be immature, rather than fresh ejaculated semen samples. Some of abnormal cells could be destroyed by apoptotic pathway during the final stages of spermatozoa maturation. Also, different factors should be kept in mind that could affect the

spermatozoa viability, such as: the date of sample collection and age of the stallion at the time of collection. It is documented that the highest spermatozoa production occurs between May and June while the minimum production occurs in July and August (Mckinnon & Voss, 1992). The highest viability results were obtained for stallion's number H17, H18, H19 and H20, which are collected during the breeding season, from the end of April till the middle of June. Moreover, stallion number H19 was the oldest one (6 yrs), which achieve the highest viability result.

The acrosome is a large secretory vesicle overlaying the nucleus, which contains hydrolytic enzymes to aid in penetration of spermatozoa through the oocyte *zona pellucida*. Thus, sperm with intact acrosome will be able to fertilize an oocyte and lacking the acrosome in any circumstance signals that the spermatozoa will likely not be fully functional (Casey *et al.*, 1993). Assessment of spermatozoa acrosomal status is important since male infertility may be caused by a lack of spermatozoa with intact acrosome (Cheng *et al.*, 1996). Phase-contrast microscope was used to assess the acrosomal status of spermatozoa for pig, which have large acrosome, but not for stallion, due to limited size acrosomal spermatozoa (Gadella *et al.*, 1991).

In this report, FITC-PSA was successfully used to assess the acrosome status of stallion spermatozoa. The FITC-PSA has been successfully and widely used as spermatozoa acrosome staining to identify the presence or absence of acrosomal contents in mammalian such as in humans, pigs, goats and stallion ejaculated spermatozoa (Cross and Meizel, 1989; Casey *et al.*, 1993) and has now been applied to epididymal collected semen. Using fluorescence microscopy, it appeared that the FITC-PSA binding was mainly limited to the acrosomal cap, which makes it reliably used as probe for evaluation of acrosomal status of stallion spermatozoa. This method is rapid, inexpensive, and easy to perform and scores the acrosomal status of viable and dead spermatozoa. Also, more informative classifications of spermatozoa among the intact cells, such as intact spermatozoa with no morphological abnormalities and those with different morphologic aberrations (proximal or distal cytoplasmic droplets, tail or mid-piece defect etc), can be made.

The average number of spermatozoa with intact acrosome was 93.84% which is significantly different across the eight stallions ($P = 0.000$). The highest percentages of spermatozoa with intact acrosome were obtained from the stallion samples which are collected during the breeding season (stallion number H17, H18, H19 and H20).

This result is higher than the one which reported by Cheng and colleagues (1996; 63.2%) from freshly ejaculated stallion semen samples using FITC-Peanut agglutinin (FITC-PNA) as spermatozoa acrosome staining (Cheng *et al.*, 1996). The result here is also higher than the one obtained for bovine (67.17%) frozen ejaculated semen using double staining with FITC-PSA and Hoechst (Jankovičová J *et al.*, 2008). This difference could be related mainly to different samples since samples used in this study are collected from epididymal ducts that could have some immature spermatozoa rather than fresh or frozen ejaculated semen samples used by other researchers. Some spermatozoa are lost during centrifugation and washing, which may preferentially affect certain spermatozoa subpopulations (Casey *et al.*, 1993). Some spermatozoa can be stressed and lose their intact acrosomes due to repeated centrifugation (Sukardi *et al.*, 1997). The present study benefits from gentle mixing and centrifugation which appear satisfactory and do not stress the cell membrane or distorting the distribution of staining patterns of the stallion's spermatozoa.

Spermatozoa mitochondria are important organelles in spermatozoa through providing energy for the spermatozoa movement through oxidative phosphorylation (Ramahho-Santos *et al.*, 2007). Spermatozoa motility is a very important parameter for semen quality evaluation (Alessandra *et al.*, 2010). The combined application of MitoTracer green and Hoechst 33342 identified the mitochondria of functional stallion spermatozoa, thus permitting a distinction between spermatozoa with functional and non-functional mitochondria.

In the current investigation, this study has found that the mitochondrial function is not related to the motility test in accordance with data reported by Alessandra and colleagues, which could be explained by the involvement of many factors in spermatozoa motility (Alessandra *et al.*, 2010). This indicates that some cells, called viable non-motile spermatozoa, have active mitochondria and are indeed alive and capable of excluding supravital dye. This group of spermatozoa can be used by artificially placing them in contact with the oolemma using subzonal insemination.

The average number of spermatozoa with functional mitochondria was 95.63% which is significantly different across the 8 stallions ($P = 0.000$). The highest percentage of spermatozoa with functional mitochondria were found in stallions number H20, H21 and H22. This result is little higher than results reported by Gravance and colleagues

(2000) (92.5%) for freshly ejaculated stallion semen samples using fluorescent carbocyanine probe, JC-1, and assessed by flow cytometry.

Stallion number H16 scored as the lowest spermatozoa with both acrosomal integrity (90.4%) and mitochondria function (92.8%), which could be due to stallion age (3 yrs) and the season of sample collection (non-breeding season).

4.5. Conclusion

Simultaneous evaluation of the viability, acrosome integrity and mitochondrial function of spermatozoa, which represent the whole sample population, permit an accurate evaluation of semen quality and stallion fertility status. A rapid and reliable assessment of viable heads and tails, acrosomal and mitochondrial status of stallion spermatozoa collected from epididymal ducts were demonstrated in this study. The data presented here may not represent the actual ejaculated spermatozoa, but they provide a good understanding about the spermatogenesis status for particular stallion. This finding will enable spermatozoa biologist to make further progress by critically investigating the spermatozoa physiology in the horse to pinpoint stallion fertility problems in order to improve stallion's fertility.

Chapter 5

General Discussion

The horse has played an important role in human civilizations. The horse is commercially an important animal in UAE. Horse breeding, maintenance and training contribute greatly to UAE economy and way of life. A variety of horse activities takes place in UAE throughout the year. Today the richest race in the world, the Dubai World Cup, is held annually in Dubai, with a purse of six million dollars. UAE also has a multi-million racecourse called Meydan, which reported to be the world's largest race track.

The horse was agreed to be described cytogenetically in 1989 at the Second International Conference for Standardization of Domestic Animal Karyotypes. Horse has 31 autosomal chromosome pairs, 13 are metacentric and submetacentric, and 18 are acrocentric, and one pair of sex chromosomes, X, which is the second largest chromosome, and Y, which is the smallest acrocentric chromosome (Evans, 1992; Bowling *et al.*, 1997). Moreover, the genetic linkage map of horse with 742 markers spans 2772 cM (Swinburne *et al.*, 2006).

Horse fertility is an important aspect facing horse breeder particularly for valuable horses which have high economic impact. Pregnancy and foaling rates are the index of horse fertility, which is influenced by different factors such as stallion's and mare's reproductive capacity as well as breeding management (Alessandra *et al.*, 2010). Stallion reproductive performance depends mainly on 3 factors: stallion fertility, which includes semen quality, libido and mating ability; fertility of inseminated mares; and breeding management (Amann, 2005; Neild *et al.*, 2005). Fertility problems in mares can result in a low conception or foaling rate of any normal stallion (Pycock, 2010). Poor management of the stallion, such as lack or excess of discipline, frequency of ejaculation, times of the day, housing and nutrition, may adversely affect his ability to perform his natural sexual function. Compared with other farm animals, stallion fertility is lower and more variable. This is probably due to selection of stallion for breeding is not based on fertility but mainly on pedigree, performance and looks. Fertility examinations are seldom performed unless fertility is clearly low

(Cheng *et al.*, 1996). During a typical breeding season, the average stallion can breed with 40–50 mares naturally and 120–140 mares using artificial insemination (Varner *et al.*, 1991; Neild *et al.*, 2005). Valuable stallions are restricted for three to four matings a day and can breed around 80–100 mares per breeding season. Fertility problems, which are not uncommon in stallions, are considered as a major problem facing horse breeders (Thomas, 2001; Pycock, 2010). There have been few well documented stallion infertility reports. However, fertility statistics of different stallions are difficult to compare due to the influence of different breeds as well as system of stud management (Pycock, 2010).

Field data is impractical, expensive and time-consuming, and there is a need for laboratory tests that will increase the accuracy of stallion fertility prediction prior to breeding. In addition, most of the stallion's current fertility tests concentrate on the semen quality and hormonal levels. This is in part due to the lack of data available describing the spermatogenesis, particularly meiosis division, in detail. Genetic inadequacies should be considered if infertile or subfertile stallions show no trauma or infectious disease (Pycock, 2010). Therefore, there is a critical need, from diagnostic and therapeutic approaches in horse reproductive medicine, to keep pace with rapidly developing genetic knowledge of horse reproduction and to implement this knowledge in clinical practice to be addressed meaningfully (Seshagiri, 2001). Early detection of horse infertility problems can help in taking appropriate measures before losing the breeding season, which is relatively short (Thomas, 2001).

It is believed that a lot of cases of males with unexplained azoospermia could have a block, completely or partially, at meiosis I, which may be associated with failure of pairing/synapsis or segregation of homologous chromosomes (Judis *et al.*, 2004). This would result in either complete meiotic arrest, as in infertility cases, or meiosis impairment but with some sperm production, as in sub-fertility cases. Thus, the cytologic approach through studying testicular samples used in this study may be useful in explaining a portion of idiopathic stallion infertility cases. This would have clinical significance in subsequent therapeutic approaches in reproductive medicine, such as *in vitro* fertilization (IVF) or intra-cytoplasmic sperm injection (ICSI) or round spermatid nuclear injection (RSNI or ROSNI) approaches.

Spermatogenesis is a complex process of spermatozoa production by the seminiferous epithelium of the testis. It starts with one mitotic division followed by two meiotic divisions and gives rise of four haploid cells, spermatids, which can differentiated to

form mature spermatozoa (Bruce *et al.*, 1994). Meiotic division I is the most important division in spermatogenesis, in which the genetic content is reduced from diploid precursor cells to haploid gametic cells (Barlow and Hultèn, 1998). It is a long and complex process, during which homologous chromosomes pair, synapse and recombine at prophase I (PI) in order to exchange the genetic material. This can be visualised as chiasmata at metaphase I (MI). Little is known about horse spermatogenesis especially meiotic division. Therefore, the present study is the first study that explores more in-depth horse spermatogenesis, in particular meiotic prophase I and metaphase I in fertile horses.

Recombination analysis is the cornerstone of genetic researches (Lynn *et al.*, 2002). Previously, two different methods have been used to map the recombination events: 1) Electron microscopy approach, in which recombination can be visualised through mapping the late recombination nodules on synaptonemal complexes (SCs) using silver nitrate staining (Carpenter, 1975). This method is time-consuming and tedious. 2) Chiasmata counting and localisation used as direct indicators of crossing over at MI. This method is inaccurate to a certain degree in determining the crossover location as well as time consuming due to the low number of MI cells recovered. On the other hand, immunofluorescent techniques for SC analysis coupled with markers of crossover have opened a new avenue for studying the synapsis and crossover events (Barlow and Hultèn, 1998). It has improved meiotic process analysis through allowing the study of causative association between abnormal chromosome synapsis during meiosis and germ cell death (Villagómez and Pinton, 2008).

The present study has a major advantage over previous work as it combines the fluorescent microscopic study of chromosome pairing and recombination, MLH1 foci, at PI with air dry preparation study of chiasmata and chromosome configuration at MI. This gave a more complete view of meiotic chromosome behaviour in horse. Another advantage of this study over previous work is that different spermatozoa functions were investigated.

Three techniques were used with different objectives. Electron microscopy was used to visualise the SC with high magnification. Chiasmata count was used as a reference to investigate the crossovers frequency and distribution at MI, since chiasmata is the mature crossover at MI. While immunofluorescent technique was used to monitor the pairing process, using antibodies against SCP3, as well as counting and localising the crossovers event, using antibodies against MLH1, that is believed to be a component

of late recombination nodules. In addition, the possibility of using MLH1 count as alternative to chiasmata counting in horse was assessed.

Light microscopic investigation using silver staining indicates that the horse has 31 autosomal SCs with different length and one XY SC with different configuration. While electron microscopic images reveal that these SCs, like most of species, consist of two lateral elements but without a central element or recombination nodules, which could be due to technical difficulties. Thus, the present study has confirmed SC formation at PI that connects the homologous chromosomes of horse spermatocyte in order to synapse and recombine.

Air dry preparation is a reliable method for chiasmata counting and localisation. Different cell stages, from the spermatogonial cell stage until mature spermatozoa, were evaluated. Moreover, three different metaphases, premeiotic mitotic metaphase, primary spermatocyte metaphase and secondary spermatocyte metaphase, were evaluated in the preparation, which indicated normal divisions. Chiasmata results reveal a minimum of one chiasma per chromosome, obligatory for normal spermatogenesis. Extra chiasmata on long chromosomes could exert interference. Different factors are thought to affect the number of chiasmata on particular chromosomes: 1) Chromosome length. The number of chiasmata is correlated with the chromosome length. 2) Position of chiasmata. The position of the first chiasma exerts interference preventing additional chiasmata forming nearby. 3) The location of the centromere. It has been proposed that the presence of the centromere inhibits the crossover formation in close proximity (Anderson *et al.*, 1999). However, there is evidence of crossing over events occurring very close to the centromere in human acrocentric chromosomes e.g. human chromosome 15 (Saadallah and Hultèn, 1983). Different number of chiasmata were detected for the same chromosome in different nuclei, which could be due to the position of the first crossover on the chromosome and from the centromere. Different configurations of chromosomes were visualised, which were due to the number of the chiasmata and their locations. For example, rod shape indicating the presence of one chiasma in the chromosome distal part, cross shape reveal the presence of one chiasma in the chromosome interstitial part, while ring shape indicating the presence of two chiasmata in the metacentric chromosome arms.

The production of normal spermatozoa depends on proper meiosis-specific modifications to chromosome behaviour (Judis *et al.*, 2004). Studying the testicular samples, with different antibodies that recognize and localize different meiotic protein components at different stages, is important to examine the initiation and processing the intermediates of recombination, SCs formation and maintenance, chiasmata formation and gamete production (Judis *et al.*, 2004). Through using antibodies against recombination components, such as anti-SCP3, it became possible to directly monitor progression of germ cells during PI. Different stages of PI are identified and characterised. Thus, this indicates that the analysis of PI stages in horse primary spermatocytes by immunofluorescent using anti-SCP3 is reliable. In this respect, this finding is important in future assessFing idiopathic azoospermic cases. For instance, de Boer and colleagues (2004) reported that the succession of PI substages is not entirely normal in non-obstructive azospermic human males.

The overall mean of autosomal crossover events of 50.11 (mean 1.6 crossover per bivalent) detected in normal fertile male horse in present study is not substantially different from that noted for males of other mammals. There is a remarkable difference in crossover frequency within and among individuals which is linked to the difference in the length of the SC. So the physical structure of SC reflects the genetic distance not physical distance (Lynn *et al.*, 2002).

Comparison of the mean number and general locations of autosomal MLH1 foci measured in surface spread nuclei (50.11 ± 2.35) with the mean number and locations of autosomal chiasmata measured in air-dried nuclei (49.45 ± 2.07) reveals that the means show a remarkable coincidence. Thus, this provides strong evidence that MLH1 marks the sites of meiotic recombination in equine pachytene spermatocytes. No significant difference was observed between the two techniques for the average of the total count for the same individual. However, some individuals showed significant different for one or two crossovers. This little variation could be due to the technical bias or to the presence of very close neighboring crossovers that can mark and easily detected by anti-MLH1 but not as chiasma. Moreover, the autosomal genetic map length of horse males obtained from MLH1 foci analysis (2,505.5 cM) is close to the one obtained from chiasmata analysis (2,472.5 cM). Thus, MLH1 provides an easy and straight forward alternative to chiasma analysis for crossover events.

Traditional semen analysis, which is either quantitative such as volume and count or qualitative such as percentage of motility and abnormality of spermatozoa, is not

enough to evaluate the horse male fertility (Samper, 2009). Thus, multi-parametric functional analysis, including sperm viability testes, could give much clue by improving the prediction of stallion fertility (Phetudomsinsuk *et al.*, 2008). The viability evaluation can be done in combination with assessment of morphology. Thus, more informative classification of spermatozoa can be made. However, if this information is not enough, biopsies of the testes may be necessary to obtain further insight into the quality of spermatogenesis.

In this report, the main functional spermatozoa regions, the head, the midpiece and the tail, were assessed to evaluate the fertility of the stallions. Spermatozoa membrane permeability is an important factor for the spermatozoal heads and tails stability and viability. Chicago sky blue (CSB) stain method, which can bind to the spermatozoa proteins, was simply used and gave a reliable result through differentiating between live and dead of spermatozoa heads and tails. It showed results reproducibility and staining uniformity. FITC-*Pisum sativum agglutinin* (FITC-PSA) and MitoTracer green were used successfully to assess the spermatozoal acrosomal status as well as the mitochondrial function, respectively.

This is the first study to evaluate the average number of viable spermatozoa heads and tails (81.26%) as well as spermatozoal acrosome integrity (93.84%) status and mitochondria function (95.63%) for the stallion epididymal collected semen samples. Different factors should be taken in consideration during interpreting the viability results: 1) Nature of the sample: Present results, through using epididymal collected semen, could not give a clear idea about the fertility status of the stallion. Some spermatozoa may be immature as well as some abnormal cells could be destroyed during spermatozoa maturation and before ejaculation. 2) Date of sample collection: results here showed higher viability results from the samples collected during the breeding season, between May and June (Mckinnon & Voss, 1992). In addition, a significant difference was observed between the samples which collected during breeding season and the rest. 3) Age of the stallion at the collection date: The age of achieving sexual maturation, maximum reproductive capacity, is different from stallion to stallion, which might be influenced by breed and season of birth. For most stallions, puberty, production of first spermatozoa, starts at 14 months. Two to four years after that, they achieve their sexual maturation (Jones & Berndtson, 1986).

In this study, testicular sample were used from castrated horses; however, in future, testicular biopsy from infertile or subfertile horse is enough to assess the spermatogenesis process particularly meiosis abnormalities.

Conclusion and Future work

This is the first report to study the horse spermatogenesis in details from the first division of the germ cells until the releasing of mature spermatozoa. The knowledge of the molecular genetics of horse fertility is expanding. The genome-wide chiasmata and MLH1 foci frequency and distribution as well as detail chiasmata mapping in eight different autosomes, using combined air dry preparation with FISH techniques, were reported for the first time.

This result, from using fertile stallions and documentation of the normal range of recombination, could be the cornerstone in understanding the genetic basis of normal spermatogenesis. This could offer an excellent opportunity to increase the knowledge in this area. This could be the first step in understanding the meiotic disturbances observed in infertile stallions due to structural chromosome abnormalities, which could be undetected by mitotic chromosomal analysis. It is an essential prerequisite for the understanding of changes that are observed in abnormal situations such as chromosomal non-disjunction or rearrangement as well as its value in mapping and identifying diseases. This will provide important information that will enable equine practitioners and horse breeders to make the most informed decisions about the health and breeding of horses and possibly even reverse cases of idiopathic infertility in horses.

Further studies need to be carried out in order to establish a recombination map for all horse chromosomes as well as studying the recombination frequency in infertile cases. Both unusual numbers and an unusual distribution are expected to be observed in infertile horse males and translocation carriers. Also more studies are required to elucidate the frequency of recombination as well as their physical distribution in horse females. Many more recombination events are expected since the linkage analysis reveal that the genetic length of human females is approximately 60% longer than that of males (Dib *et al.*, 1996; Tease and Hultèn, 2004).

References

- Afshar, K., Barton, N.R., Hawley, R.S., and Goldstein, L.S.B. (1995). DNA binding and meiotic chromosomal localization of the *Drosophila* Nod kinesin-like protein. *Cell* 81: 129–138.
- Alani, E., Padmore, R., and Kleckner, N. (1990). Analysis of wildtype and *rad50* mutants of yeast suggests an intimate relationship between meiotic chromosome synapsis and recombination. *Cell* 61: 419–436.
- Alberts, B., Bray, D., Lewis, J., Raff, M., Roberts, K. and Watson, J. D. (1994). *Molecular Biology of the Cell*. 3rd Edition. pp 1011–1035.
- Albini, S.M. and Jones, G.H. (1987). Synaptonemal complex spreading in *Allium cepa* and *A. fistulosum*. I. The initiation and sequence of pairing. *Chromosoma* 95: 324–338.
- Alessandra, G., Michele, L.G., Angela, F., Flavia, P., Michele, N., Elena, D.A.M. and Fiorenza, M. (2010). Assessment of viability, chromatin structure, mitochondrial function and motility of stallion fresh sperm by using objective methodologies. *Journal of Cell and Animal Biology*. 4 (2): 34–41.
- Amann, R. P. (1981). A critical Review of Methods for Evaluation of Spermatogenesis from Seminal Characteristics. *Journal of Andrology*. 2: 37–58.
- Amann, R.P. (2005). Weakness in reports of “fertility” for horses and other species. *Theriogenology*. 63:698–715.
- Anderson, LK, Offenberg, HH, Verkuijlen, WMHC and Heyting, C. (1997). RecA-like proteins are components of early meiotic nodules in lily. *Proceeding the National Academy of Sciences USA*. 94:6868–6873.
- Anderson, L.K., Reeves, A., Webb, L.M. and Ashley, T. (1998). Distribution of crossing over on mouse synaptonemal complexes using immunofluorescent localization of MLH1 protein. *Genetics*. 151: 1569–1579.
- Anderson, L.K. and Stack, S.M. (2002). Meiotic recombination in plants. *Current Genomics*. 3: 507–526
- Anderson, L. K. and Stack, S. M. (2005). Recombination Nodules in Plants. *Cytogenetic and Genome Research*. 109: 198–204.

- Ashley T. (1994). Mammalian meiotic recombination: A reexamination. *Human Genetics*. 94: 587–593.
- Ashley, T., Plug, A.W., Xu, J., Solari, A., Reddy, G., Golub, E.I., and Ward, D.C. (1995). Dynamic changes in Rad51 distribution on chromatin during meiosis in male and female vertebrates. *Chromosoma*. 104: 19–28.
- Bahler, J., Wyler, T., Loidl, J., and Kohli, J. (1993). Unusual nuclear structures in meiotic prophase of fission yeast: A cytological analysis. *Journal of Cell Biology*. 121: 241–256.
- Baker, B.S., Carpenter, A.T., Esposito, M.S., Esposito, R.E. and Sandler, L. (1976). The Genetic Control of Meiosis. *Annual Review of Genetics*. 10: 53–134.
- Baker, S.M., Bronner, C.E., Zhang, L., Plug, A.W., Robatzek, M., Warren, G., Elliott, E.A., Yu, J., Ashley, T., Arnheim, N., Flavell, R.A., and Liskay, R.M. (1995). Male mice defective in the DNA mismatch repair gene *PMS2* exhibit abnormal chromosome synapsis in meiosis. *Cell*. 82: 309–319.
- Baker, S.M., Plug, A.W., Prolla, T.A., Bronner, C.E., Harris, A.C., Yao, X., Christie, D.M., Monell, C., Arnheim, N., Bradley, A., Ashley, T. and Liskay, R.M. (1996). Involvement of Mouse MLH1 in DNA Mismatch Repair and Meiotic Crossing Over. *Nature Genetics*. 13: 336–342.
- Barlow, A.L. & Hultèn, M.A. (1996). Combined Immunocytogenetic and Molecular Cytogenetic Analysis of Meiosis I Human Spermatocytes. *Chromosome Research*. 4: 562–573.
- Barlow, A.L., Benson, F.H., West, S.C. and Hultèn, M.A. (1997). Distribution of the Rad51 recombinase in human and mouse spermatocytes. *EMBO Journal*. 16: 5207–5215.
- Barlow, A.L. and Hultèn, M.A. (1998). Crossing over analysis at pachytene in man. *European Journal of Human Genetics*. 6: 350–358.
- Barnes, T.M., Kohara, Y., Coulson, A., and Hekimi, S. (1995). Meiotic recombination, noncoding DNA and genomic organization in *Caenorhabditis elegans*. *Genetics*. 141: 159–179.
- Bascom-Slack, C., Ross, L. and Dawson, D. (1997). Chiasmata, crossovers, and meiotic chromosome segregation. *Advances in Genetics*. 35: 253–283.
- Baudat, F. and de Massy, B. (2007). Regulating double-stranded DNA break repair towards crossover or non-crossover during mammalian meiosis. *Chromosome research*. 15: 565–577.

- Bickel, S.E., Wyman, D.W., and Orr-Weaver, T.L. (1997). Mutational analysis of the *Drosophila* sister-chromatid cohesion protein ORD and its role in the maintenance of centromeric cohesion. *Genetics*. 146: 1319–1331.
- Bishop, D., Park, D., Xu, L., and Kleckner, N. (1992). *DMC1*: A meiosis-specific yeast homolog of *E. coli recA* required for recombination, synaptonemal complex formation, and cell cycle progression. *Cell*. 69: 439–456.
- Bishop, DK. (1994). RecA homologs Dmc1 and Rad51 interact to form multiple nuclear complexes prior to meiotic chromosome synapsis. *Cell*. 79:1081–1092.
- Borde, V. (2007). The Multiple Roles of the Mre11 Complex for Meiotic Recombination. *Chromosome Research*. 15:551–563.
- Borodin, P.M., Karamysheva, T.V. and Rubtsov, N.B. (2007). Immunofluorescent analysis of meiotic recombination in the domestic cat. *Cell and Tissue Biology*. 1 (6): 503–507.
- Bowling, A.T., Breen, M., Chowdhary, B.P., Hirota, K., Lear, T., Millon, L.V., Ponce, de Loen, F.A., Raudsepp, T. and Stranzinger, G. (1997). International system for cytogenetic nomenclature of the domestic horse. *Chromosome Research*. 5: 433–443.
- Braekeleer, M.De and Dao, T.N. (1991). Cytogenetic Studies in Male Infertility. *Human Reproduction*. 6: 245–250.
- Brown, P.W., Judis, L., Chan, E.R., Schwartz, S., Seftel, A., Thomas, A. and Hassold, T.J. (2005). Meiotic synapsis proceeds from a limited number of subtelomeric sites in the human male. *American Journal of Human Genetics*. 77: 556–566.
- Bruce, A., Dennis, B., Julian, L., Martin, R., Keith, R. and James, D.E. (1994). *Molecular Biology of the Cell*. (3rd ed). Grand Publishing, Inc. New York & London, pp 1011–135.
- Bullard, S.A., Kim, S., Galbraith, A.M. and Malone, R.E. (1996). Double strand breaks at the *HIS2* recombination hot spot in *Saccaromyces cerevisiae*. *Proceeding National Academy for Sciences of USA*. 93: 13054–13059.
- Buoen, L.C., Zhag, T.Q., Weber, A.F. and Ruth, G.R. (2000). SRY negative, XX intersex horses: the need for pedigree studies to examine the mode of inheritance of the condition. *Equine Veterinary Journal*. 32: 78–81.
- Cano, M.I., Jones, G.H. and Santos, J.L. (1987). Sex differences in chiasma frequency and distribution in natural populations of *Eypreocnemis plorans* containing B-chromosomes. *Heredity*. 59: 237–243.

- Carpenter, A.T.C. (1975). Electron microscopy of meiosis in *Drosophila melanogaster* females: II: The recombination nodule – a recombination-associated structure at pachytene? *Proceeding of the National Academy of Sciences of the USA*. 72:3186–3189.
- Carpenter, A.T.C. (1979). Recombination nodules and synaptonemal complex in recombination-defective females of *Drosophila melanogaster*. *Chromosoma* 75: 259–292.
- Carpenter, A.T.C. (2003). Normal synaptonemal complex and abnormal recombination nodules in two alleles of the *Drosophila* meiotic mutant meieW68. *Genetics*. 163:1337–1356.
- Casey, P.J., Hillman, R.B., Robertson, K.R., Yudin, A.I., Liu, I.K.M. and Drobnis, E.Z. (1993). Validation of acrosomal stain for equine sperm that differentiates between living and dead sperm. *Journal of Andrology*. 14(4): 289–297.
- Cha, R.S., Weiner, B.M., Keeney, S., Dekker, J. and Klechner, N. (2000). Progression of meiotic DNA replication is modulated by interchromosomal interaction proteins, negatively by Spo11p and positively by Rec8p. *Genes and Development*. 14: 493–503
- Chaganti, R.S., Jhanwar, S.C., Ehrenbard, L.T., Kourides, I.A. & Williams, J.J. (1980). Genetically Determined Asynapsis. Spermatogenic Degeneration and Infertility in Men. *American Journal of Human Geneics*. 32: 833–848.
- Chandley, A.C. (1986). A model for effective pairing and recombination at meiosis based on early replicating sites (R-bands) along chromosomes. *Human Genetics*. 72: 50–57.
- Cheng, F.P., Fezeli, A., Voorhoiu, W.F., Marks, A., Bevers, M.M. and Colenbrander, B. (1996). Use of Peanut Agglutinin to assess the acrosomal status and the zona pellucid-induced acrosome reaction in stallion spermatozoa. *Journal of Andrology*. 17 (6): 674–682.
- Chikashige, Y., Tsutsumi, C., Yamane, M., Okamasa, K., Haraguchi, T. and Hiraoka, Y. (2006). Meiotic proteins bqt1 and bqt2 tether telomeres to form the bouquet arrangement of chromosomes. *Cell*. 125(1): 59–69.
- Chowdhary, B.P. and Raudsepp, T. (2008). The horse derby: racing from map to whole genome sequence. *Chromosome Research*. 16: 109–127.

- Chua, P.R. and Roeder, G.S. (1997). Tam1, a telomere-associated meiotic protein, functions in chromosome synapsis and crossover interference. *Genes and Development*. 11: 1786–1800.
- Cobb, J. and Handel, M.A. (1998). Dynamic of Meiotic Prophase I During Spermatogenesis: from Pairing to Division. *Seminar in Cell and Developmental Biology*. 9: 445–450.
- Codina-Pascual, M., Kraus J., Speicher, M.R., Oliver-Bonet, M., Murcia, V., Sarqella, J., Egozcue, J., Navarro, J. and Benet, J. (2004). Characterization of all human male synaptonemal complexes by subtelomere multiplex-FISH. *Cytogenetic and Genome Research*. 107: 18–21.
- Cohen, P.E. and Pollard, J.W. (2001). Regulation of Meiotic Recombination and Prophase I in Mammals. *BioEssays*. 23: 996–1009.
- Comings, D.E. and Okada, T.A. (1972). Holocentric Chromosomes in *Oncopeltus*: Kinetochores are Present in Mitosis But Absent in Meiosis. *Chromosoma*. 37 (2):177–192.
- Cook, P.R. (1997). The Transcriptional of Chromosome Pairing. *Journal of Cell Science*. 110: 1033–1040.
- Costa, Y., Speed, R., Ollinger, R., Alsheimer, M., Semple, C.A., Gautier, P., Maratou, K., Novak, I., Höög, C., Benavente, R. and Cooke, H.J. (2005). Two novel proteins recruited by synaptonemal complex protein 1 (SYCP1) are at the centre of meiosis. *Journal of Cell Science*. 118: 2755–2762.
- Costa, Y., Speed, R.M., Gautier, P., Semple, C.A., Maratou, K., Turner, J.M. and Cooke, H.J. (2006). Mouse MAELSTROM: the link between meiotic silencing of unsynapsed chromatin and microRNA pathway? *Human Molecular Genetics*. 15: 2324–2334.
- Costa, Y. And Cooke, H.J. (2007). Dissecting the mammalian synaptonemal complex using targeted mutations. *Chromosome Research*. 15: 579–589.
- Critchlow, H.M., Payne, A. and Griffin, D.K. (2004) Genes and Proteins Involved in the Control of Meiosis. *Cytogenetic Genome Research*. 105: 4–10.
- Cross, N.L., Meizel, S. (1989). Methods for evaluating the acrosomal status of mammalian sperm. *Biology of Reproduction*. 41:635–641.

- de Boer, P., Giele, M., Lock, M.T.W.T., de Rooij, D.G., Giltay, J., Hochstenbach, R. and te Velde, E.R. (2004). Kinetics of meiosis in azoospermic males: a joint histological and cytological approach. *Cytogenetic and Genome Research*. 105: 36–46.
- de Jonge, C. and Barratt, C. (2006). *Sperm Cell: Production, Maturation, Fertilization, Regeneration*. Cambridge University Press, pp 1–25.
- Dib, C., Fauré, S., Fizames, C., Samson, D., Drouot, N., Vignal, A., Millasseau, P., Marc, S., Hazan, J., Seboun, E., Lathrop, M., Gyapay, G., Morissette, J. and Weissenbach, J. (1996). A comprehensive genetic map of the human genome based on 5,264 microsatellites. *Nature*. 380: 152–154.
- Dobson, M.J., Pearlman, R.E., Karaiskakis, A., Spyropoulos, B., and Moens, P.B. (1994). Synaptonemal complex proteins: occurrence, epitope mapping, and chromosome disjunction. *Journal of Cell Science*. 107: 2749–2760.
- Dolganov, G.M, Maser, R.S., Novikov, A., Tosto, L., Chong, S., Bressan, D.A. and Petrini, J.H. (1996). Human Rad50 is physically associated with human Mre11: identification of a conserved multiprotein complex implicated in recombinational DNA repair. *Molecular and Cellular Bioogyl*. 16(9): 4832–4841.
- Drabent, B., Kardalidou, E. and Doenecke, D. (1991). Structure and Expression of the Human Gene Encoding Testicular H1 Histone (H1t). *Gene*. 103: 263–268.
- Drabent, B., Bode, C. and Doenecke, D. (1993). Structure and Expression of the Mouse Testicular Hi Histone gene (H1t). *Biochimica et Biophysica Acta*. 1216: 311–313.
- Drabent, B., Bode, C., Bramlage, B. and Doenecke, D. (1996). Expression of the Mouse Testicular Histone gene H1t During Spermatogenesis. *Histochemistry and Cell Biology*. 106: 247–251.
- Egel, R. (1995). The synaptonemal complex and the distribution of meiotic recombination events. *Trends in Genetics*. 11: 206–208.
- Egel-Mitani, M., Olson, L.W., and Egel, R. (1982). Meiosis in *Aspergillus nidulans*: Another example for lacking synaptonemal complexes in the absence of crossover interference. *Hereditas* 97: 179–187.

- Egozcue, J., Templado, C., Vidal, F., Navarro, J., Morer-Fargas, F. and Marina, S. (1983). Meiotic Studies in Series of 1100 Infertile and Sterile Males. *Human Genetics*. 65: 185–188.
- Evans, J.W. (1992). *Horse Breeding & Management*. Elsevier Health Sciences. pp 41–45.
- Fang, J.S. and Jagiello, G.M. (1988). An analysis of the chromosome map and chiasmata characteristics of human diplotene spermatocytes. *Cytogenetics and Cell Genetics*. 47: 52–57.
- Farlin, M.E., Jasko, D.J., Graham, J.K. and Squires, E.L. (1992). Assessment of *Pisum sativum* agglutinin in identifying acrosomal damage in stallion spermatozoa. *Molecular Reproduction and Development*. 22: 23–27.
- Fawcett, D.W. (1956). The Fine Structure of Chromosomes in the Meiotic Prophase of Vertebrate Spermatocytes. *Journal of Cell Biology*. 2: 403–406.
- Froenicke, L., Anderson, L.K., Wienberg, J. and Ashley, T. (2002). Male Mouse Recombination Maps for Each Autosome Identified by Chromosome Pairing. *American Journal of Human Genetics*. 71: 1353–1368.
- Fuchs, J., Brandes, A. and Schubert, I. (1995). Telomere sequence localization and karyotype evolution in higher plants. *Plant Systematics and Evolution*. 1996: 227–241.
- Gadella, B.M., Colenbrander, B. and Lopes-Cardozo, M. (1991). Arylsulfatases are present in seminal plasma of several domestic mammals. *Biology of Reproduction*. 45: 381–384.
- Gamboa, S. and Ramalho-Santos, J. (2005). SNARE proteins and caveolin-1 in stallion spermatozoa: possible implication for fertility. *Theriogenology*. 64: 275–291.
- Gerton, J.F., DeRisi, J., Schroff, R., Lichten, M., Brown, P.O. and Petes, T.D. (2000). Global mapping of meiotic recombination hotspots and coldspots in the yeast *Saccharomyces cerevisiae*. *Proceeding the National Academy of Sciences of the USA*. 97: 11383–11390.
- Gilberson, L.A. and Stahl, F.W. (1996). A test of the double-strand break repair model for meiotic recombination in *Saccharomyces cerevisiae*. *Genetics*. 144:27–41.

- Gravance, C.G., Garner, D.L., Baumber, J. and Ball, B.A. (2000). Assessment of equine sperm mitochondrial function using JC-1. *Theriogenology*. 53: 1691–1703.
- Griffith, J.D., Comeau, L., Rosenfield, S., Stansel, R.M., Bianchi, A., Moss, H. and de Lange, T. (1999). Mammalian telomeres end in a large duplex loop. *Cell*. 97: 503–514.
- Hamer, G., Gell, K., Kouznetsova, A., Novak, I., Benavente, R. and Höög, C. (2006). Characterization of a novel meiosis-specific protein within the central element of the synaptonemal complex. *Journal of Cell Science*. 119: 4025–4032.
- Hargreave, T.B. (2000). Genetic basis of male fertility. *Br. Med. Bull.* 56: 650–671.
- Hart, E.J., pinton, A., Powell, A., Wall, R. and King, W.A. (2008). Meiotic recombination in normal and clone bulls and their offspring. *Cytogenetic and Genome Research*. 120: 97–101.
- Hassold, T.H., Abruzzo, M., Adkins, K., Griffin, D., Merrill, M., Millie, E., Saker, D., Shen, J., and Zaragoza, M. (1996). Human aneuploidy: Incidence, origin, and etiology. *Environmental and Molecular Mutagenesis*. 28: 167–175.
- Hassold, T., Sherman, S. and Hunt, P. (2000). Counting Cross-overs: Characterizing Meiotic Recombination in Mammals. *Human Molecular Genetics*. 9: 2409–2419.
- Hassold, T. and Hunt, P. (2001). The Genesis of Human Aneuploidy. *Macmillan Magazines*. 2: 280–291
- Hassold, T., Judis, L., Chan, E. R., Schwartz, S., Seftel, A. and Lynn, A. (2004). Cytological Studies of Meiotic Recombination in Human Males. *Cytogenetic Genome Research*. 107: 249–255.
- Hawley, R.S. and Theurkauf, W.E. (1993). Requiem for distributive segregation: Achiasmate segregation in *Drosophila* females. *Trends in Genetics*. 9: 310–317.
- Henderson, S.A. (1963). Chiasmata distribution at diplotene in a locust. *Heredity*. 18: 173–190.
- Heng, H.H.Q., Chamberlain, J.W., Shi, X.M., Spyropoulos, B., Tsui, L.C., and Moens, P.B. (1996). Regulation of meiotic chromatin loop size by chromosomal position. *Proceeding the National Academy of Sciences of the USA*. 93: 2795–2800.

- Herrera, E., Samper, E., Martin-Caballero, J., Flores, J.M., Lee, H-W and Blasco, M.A. (1999). Disease states associated with telomerase deficiency appear earlier in mice with short telomeres. *EMBO Journal*. 18: 2950–2960.
- Heyer, W.D. and Kohli, J. (1994). Homologous Recombination. *Experientia*. 50 (3): 189–191.
- Hollingsworth, N.M., Ponte, L., and Halsey, C. (1995). *MSH5*, a novel MutS homolog, facilitates meiotic reciprocal recombination between homologs in *Saccharomyces cerevisiae* but not mismatch repair. *Genes and Development*. 9: 1728–1739.
- Holloway, K., Lawson, V.E. and Jeffreys, A.J. (2006). Allelic recombination and de novo deletions in sperm in the human{beta}-globin gene region. *Human Molecular Genetics*. 15: 1099–1111.
- Holmes, R.J. and Cohen, P.E. (2007). Small RNAs and RNAi pathways in meiotic prophase I. *Chromosome Research*. 15: 653–665.
- Holstein, A. F., Schulze, W. and Davidoff, M. (2003). Understanding Spermatogenesis is a Prerequisite for Treatment. *Reproductive Biology and Endocrinology*. 1: 107–122.
- Hultèn, M. (1974). Chiasma distribution at diakinesis in the normal human male. *Hereditas*. 76: 55–78.
- Hultèn, M. (1994). Estimating Map Distances. *Trends in Genetics*. 10 (4):112–113.
- Hultèn, M., Baker, H. and Tankimanova, M. (2005). Meiosis and Meiotic Errors. Encyclopedia of Genetics, Genomics, Proteomics and Bioinformatics (online edition). John Wiley & Sons
- Hunt, P., Lemaire, R., Embury, P., Sheean, L. and Mroz, K. (1995). Analysis of chromosome behavior in intact mammalian oocytes: Monitoring the segregation of a univalent chromosome during female meiosis. *Human Molecular Genetics*. 4: 2007–2012.
- Hunter, N. and Borts, R.H. (1997). Mlh1 is unique among mismatch repair proteins in its ability to promote crossing over during meiosis. *Genes and Development*. 11: 1573–1582.
- Hunter, N. and Kleckner, N. (2001). The single-end invasion: An asymmetric intermediate at the double-strand break to double-Holliday junction transition of meiotic recombination. *Cell*. 106:59–70.

- Jankovičová, J., Simon, M., Antalíková, J. And Horovská, L. (2008). Acrosomal and viability status of bovine spermatozoa evaluated by two staining methods. *Acta Veterinaria Hungarica*. 56 (1): 133–137
- Jeffreys, A.J. and May, C.A. (2004). Intense and highly localized gene conversion in human meiotic crossover hot spots. *Nature Genetics*. 36: 151–156.
- Johnson, L. (1990). Spermatogenesis. In *Reproduction in Domestic Animals*. 4th Edition. New York , Academic Press. pp 173–219.
- Jones ,G.H. (1984). The control of chiasma distribution. *Symp Soc Exp Biol*. 38:293–320.
- Jones, G.H. and Albin, S. M. (1988). Recombination Nodules, Chiasmata and Crossing-Over in the Nucleolus Organizing Short Arm of *Allium fistulosum*. *Heredity*. 61: 217–224.
- Jones, L.S. and Berndtson, W.E. (1986). A quantitative Study of Sertoli Cell and Germ Cell Populations as Related to Sexual Development and Aging in the Stallion. *Biology of Reproduction*. 35: 138–148.
- Jonson, L. (1991). Seasonal Differentiation in Equine Spermatogenesis. *Biology of Reproduction*. 44: 284–291.
- Jordan, P. (2006). Initiation of homologous chromosome pairing during meiosis. *Biochemical Society Transactions*. 34 (4): 545–549.
- Judis, L., Chan, E.R, Schwartz, S., Seftel, A. and Hassold, T. (2004). Meiosis I arrest and azoospermia in an infertile male explained by failure of formation of a component of the synaptonemal complex. *Fertility and Sterility*. 81 (1): 205–209.
- Kaback, D.B., Guacci, V., Barber, D., and Mahon, J.W. (1992). Chromosome size-dependent control of meiotic recombination. *Science*. 256: 228–232.
- Karpen, G.H., Le, M.H. and Le, H. (1996). Centric heterochromatin and the efficiency of achiasmate disjunction in *Drosophila* female meiosis. *Science*. 273: 118–122.
- Keeney, S., Giroux, C.N. and Klechner, N. (1997). Meiosis-specific DNA double-strand breaks are catalysed by Spo11, a member of a widely conserved protein family. *Cell*. 88: 375–384.
- Kelly, W.G. and Aramayo, R. (2007). Meiotic silencing and the epigenetics of sex. *Chromosome Research*. 15: 633–651.

- Kemp, B., Boumil, R.M., Stewart, M.N. and Dawson, D.S. (2004). A role for centromere pairing in meiotic chromosome segregation. *Genes and Development*. 18: 1946–1951.
- Kerrebrock, A.W., Moore, D.P., Wu, J.S., and Orr-Weaver, T.L. (1995). Mei-S332, a *Drosophila* protein required for sisterchromatid cohesion, can localize to meiotic centromeric regions. *Cell*. 83: 247–256.
- Kilian, A., Stiff, C. and Kleinhofs, A. (1995). Barley telomeres shorten during differentiation but grow in callus culture. *Proceeding the National Academy of Sciences of the USA*. 92: 9555–9559.
- Klapholz, S., Waddell, C.S., and Esposito, R.E. (1985). The role of the *SPO11* gene in meiotic recombination in yeast. *Genetics*. 110: 187–216.
- Kleckner, N. and Weiner, B.M. (1993). Potential advantages of unstable interactions for pairing of chromosomes in meiotic, somatic, and premeiotic cells. *Cold Spring Harbor Symposia on Quantitative Biology*. 58: 553–565.
- Kleckner, N. (1996). Meiosis: How Could it Work. *Proceeding the National Academy of Sciences of the USA*. 93: 8167–8174.
- Klein, S., Zenvirth, D., Dror, V., Barton, A.B., Kaback, D.B. and Simchen, G. (1996). Patterns of meiotic double-strand breakage on native and artificial yeast chromosomes. *Chromosoma*. 105: 276–284.
- Kneitz, B., Cohen, P.E., Avdievich, E., Zhu, L., Kane, M.F., Hou, H.Jr., Kolodner, R.D., Kucherlapati, R., Pollard, J.W. and Edelman, W. (2000). MutS homolog 4 localization to meiotic chromosomes is required for chromosome pairing during meiosis in male and female mice. *Genes and Development*. 14(9): 1085–1097.
- Koehler, K.E., Boulton, C.L., Collins, H.E., French, R.L., Herman, K.C., Lacefield, S.M., Madden, L.D., Schuetz, C.D., and Hawley, R.S. (1996). Spontaneous X chromosome MI and MII nondisjunction events in *Drosophila melanogaster* oocytes have different recombinational histories. *Nature Genetics*. 14: 406–414.
- Kong, A., Gudbjartsson, D.F., Sainz, J., Jonsdottir, G.M., Gudjonsson, S.A., Richardsson, B., Sigurdardottir, S., Barnard, J., Hallbeck, B., Masson, G., Shlien, A., Palsson, S.T., Frigge, M.L., Thorgeirsson, T.E., Gulcher, J.R. and Stefansson, K. (2002). A High-Resolution Recombination Map of the Human Genome. *Nature Genetics*. 31:241–247

- Koppel, D.A., Wplfe, S.A., Fogelfeld, L.A., Merchant, P.S., Prouty, L. and Grimes, S.R. (1994). Primate Testicular Histone H1t Genes are Highly Conserved and the Human H1t Gene is Located on Chromosome 6. *Journal of Cellular Biochemistry*. 54: 219-230.
- Koulischer, L., Schoysman, R. and Gillerto, Y. (1982). Meiotic chromosome and masculine infertility: evaluation of Results. *Journal de Gènètique Humaine*. 30: 81–99.
- Kútvölgyi, G., Stefler, J. and Kovács, A. (2006). Viability and acrosome staining of stallion spermatozoa by Chicago sky blue and Giemsa. *Biotechnic and Histochemistry*. 81 (4-6): 109–117.
- Lamb, N.E., Feingold, E., Savage, A., Avramopoulos, D., Freeman, S., Gu, Y., Hallberg, A., Hersey J., Karadima, G. and Pettay, D. (1997). Characterization of susceptible chiasma configurations that increase the risk for maternal non-disjunction of chromosome 21. *Human Molecular Genetic*. 6: 1391–1399.
- Lamb, N.E., Freeman, S.B., Savage-Austin, A., Pettay, D., Taft, L., Hersey, J., Gu, Y., Shen, J., Saker, D., May, K.M., Avramopoulos, D., Petersen, M.B., Hallberg, A., Mikkelsen, M., Hassold, T.J., and Sherman, S.L. (1996). Susceptible chiasmate configurations of chromosome 21 predispose to non-disjunction in both maternal meiosis I and meiosis II. *Nature Genetics*. 14: 400–405.
- Lammers, J.H.M., Offenbergh, H.H., van Aalderen, M., Vink, A.C.G., Dietrich, A.J.J., and Heyting, C. (1994). The gene encoding a major component of the lateral elements of synaptonemal complexes of the rat is related to X-linked lymphocytoregulated genes. *Molecular and Cellular Biology*. 14: 1137–1146.
- Lange, R., Krause, W. and Engel, W. (1997). Analysis of meiotic chromosomes in testicular biopsies of infertile patients. *Human Reproduction*. 12: 2154–2158.
- Laurie, D. and Hultèn, M. (1985a). Further studies on chiasma distribution and interference in human male. *Annals of Human Genetics*. 49: 203–214.
- Laurie, D. and Hultèn, M. (1985b). Further studies on bivalent chiasma frequency in human males with normal karyotypes. *Annals of Human Genetics*. 49: 189–201.
- Lear, T.L. and Bailey, E. (2008). Equine clinical cytogenetics: the past and future. *Cytogenetic and Genome Research*. 120: 42–49.
- Li, X. and Heyer, W. (2008). Homologous recombination in DNA repair and DNA damage tolerance. *Cell Research*. 18: 99–113.

- Lichten, M., Borts, R.H., and Haber, J.E. (1987). Meiotic gene conversion and crossing over between dispersed homologous sequences occurs frequently in *Saccharomyces cerevisiae*. *Genetics*. 115: 233–246.
- Lichten, M. and Goldman, A.S.H. (1995). Meiotic recombination hotspots. *Annual Review of Genetics*. 29: 423–444.
- Lin, Y. and Smith, G.R. (1994). Transient, meiosis-induced expression of the *rec6* and *rec12* genes of *Schizosaccharomyces pombe*. *Genetics*. 136: 769–779.
- Loidl, J., Scherthan, H., Dunnen, J.T.D. and Klein, F. (1995). Morphology of a human-derived YAC in yeast meiosis. *Chromosoma*. 104: 183–188.
- Long, S.E. (1996). Tandem 1;30 translocation: a new structural abnormality in the horse (*Equus caballus*). *Cytogenetics and Cell Genetics*. 72: 162–163
- Lynn, A., Koehler, K.E., Judis, L., Chan, E.R., Cherry, J.P., Schwatz, S., Seftel, A., Hunt, P.A. and Hassold, T.J. (2002). Covariation of synaptonemal complex length and mammalian meiotic exchange rates. *Science*. 296(5576): 2222–2225.
- Lynn, A., Soucek, R. and Börner, G.V. (2007). ZMM proteins during meiosis: Crossover artists at work. *Chromosome Research*. 15: 591–605.
- Maguire, M.P. (1992). The Evolution of Meiosis. *Journal of Theoretical Biology*. 154: 43–55.
- Mahadevaiah, S.K., Turner, J.M.A., Baudat, F., Rogakou, E.P., de Boer, P., Blanco-Rodríguez, J., Jasin, M., Keeney, S., Bonner, W.M. and Burgone, B.S. (2001). Recombinational DNA double-strand breaks in mice precede synapsis. *Nature Genetics*. 27: 271–276.
- Mäkinen, A., Katila, T., Andersson, M. and Gustavsson, I. (2000). Two sterile stallions with XXY-syndrome. *Equine Veterinary Journal*. 32: 358–360.
- Marsischky, G.T., Filosi, N., Kane, M.F., and Kolodner, R. (1996). Redundancy of *Saccharomyces cerevisiae* *MSH3* and *MSH6* in *MSH2*-dependent mismatch repair. *Genes and Development*. 10: 407–420.
- Matsuoka, S., Ballif, B.A., Smogorzewska, A., McDonald, E.R., Hurov, K.E., Luo, J., Bakalarshi, C.E., Zhao, Z., Solimini, N., Lerenthal, Y., Shiloh, Y., Gygi, S.P. and Elledge, S.J. (2007). ATM and ATR substrate analysis reveals extensive protein networks responsive to DNA damage. *Science*. 316: 1160–1166.
- McDermott, A. (1973). The frequency and distribution of chiasmata in man. *Annals of Human Genetics*. 37: 13–20.

- McKee, A.H.Z. and Kleckner, N. (1997). Mutations in *Saccharomyces cerevisiae* that block meiotic prophase chromosome metabolism and confer cell cycle arrest at pachytene identify two new meiosis-specific genes *SAE1* and *SAE3*. *Genetics*. 146: 817–834.
- McKim, K.S., Green-Marroquin, B.L., Sekelsky, J.J., Chin, G., Steninberg, C., Khodosh, R. and Hawley, R.S. (1998). Meiotic synapsis in the absence of recombination. *Science*. 279 (5352):876–878.
- Mckinnon, A.O. and Voss, J.L., (1992). Equine Reproduction. Lea & Febiger. pp 645–685
- Menchini, G.F., Voliani, S., Olivieri, L. and Izzo, P.L. (1981). Meiosis in Infertile Men. In Frajese, G., Haefez, E.S.E., Conti, C. & Fabbrini, A. (eds). Oligozoospermia: Recent Progress in Andrology. Raven Press. New York. pp. 267–273.
- Miyazaki, W.Y. and Orr-Weaver, T.L. (1994). Sister-chromatid cohesion in mitosis and meiosis. *Annual Reviews of Genetics*. 28: 167–187.
- Moens, P. B., Heyting, C., dietrich, A. J., van Raamsdonk, W. and Chen, Q. (1987). Synaptonemal Complex Antigen Location and Conservation. *The Journal of Cell Biology*. 105 (1): 93–103.
- Moens, P.B. and Pearlman, R.E. (1988). Chromatin organization at meiosis. *BioEssays* 9: 151–153.
- Moens, P.B. (1994). Molecular perspectives of chromosome pairing at meiosis. *BioEssays*. 16: 101–106.
- Moens, P.B., Chen, D.J., Shen, Z., Kolas, N., Tarsounas, M., Heng, H.H.Q., and Spyropoulos, B. (1997). Rad51 immunocytology in rat and mouse spermatocytes and oocytes. *Chromosoma*. 106 (4): 207–215.
- Moens, P.B., Kolas, N.K, Tarsounas, M., Marcon, E., Cohen, P.E. and Spyropoulos, B. (2002). The time course and chromosomal localization of recombination-related proteins at meiosis in the mouse are compatible with models that can resolve the early DNA-DNA interactions without reciprocal recombination. *Journal of Cell Science*. 115:1611–1622.
- Morel, D. (1999). Equine Reproductive Physiology, Breeding and Stud management. CABI Publishing. pp 1–381.

- Morin, I., Ngo, H., Greenall, A., Zubko, M.K., Morrice, N. and Lydall, D. (2008). Checkpoint-dependent phosphorylation of Exo1 modulates the DNA damage response. *EMBO Journal*. 27: 2400–2410.
- Moses, M.J. (1956a). Chromosomal structures in Crayfish spermatocytes. *Journal of cell Biology*. 2: 215–218.
- Moses, M.J. (1956b). Studies on Nuclei Using Correlated Cytochemical Light and Electron Microscope Techniques. *Journal of Cell Biology*. 2 (Suppl.): 397–406.
- Moses, M.J. (1968). Synaptonemal Complex. *Annal. Review of Genetics*. 2: 363–412.
- Munz, P., (1994). An Analysis of Interference in the Fission Yeast *Schizosaccaromyces pombe*. *Genetics*. 137: 701–707.
- Myers, S., Bottolo, L., Freeman, C., McVean, G. and Donnelly, P. (2005). A fine-scale map of recombination rates and hotspots across the human genome. *Science*. 310: 321–324.
- Nasmyth, K. (2002). Segregating Sister Genomes: The Molecular Biology of Chromosome Separation. *Science*. 297: 559–565.
- Neild, D.N., Gadella, B.M., Agüero, A., Stout, T.A.E. and Colenbrander, B. (2005). Capacitation, acrosome function and chromatin structure in stallion sperm. *Animal Reproduction Science*. 89: 47–56.
- Nicklas, R. B. (1997). How Cells Get the Right Chromosomes. *Science*. 275 (5300): 632–637.
- Paget, S., Ducos, A., Mignotte, F., Raymond, I. and Pinton, A. (2001). 63,XO/65,XYY mosaicism in a case of equine male pseudohermaphroditism. *The Veterinary Record*. 148: 24–25.
- Parvinen, M., Soder, O., Mali, P., Froyasa, B. and Ritzen, E.M. (1991). In Vitro Stimulation of Stage-Specific Deoxyribonucleic Acid Synthesis in Rat Seminiferous Tubule Segments by Interleukin-I Alpha. *Endocrinology*. 129: 1614–1620.
- Pearlman, R.E., Tsao, N. and Moens, P.B. (1992). Synaptonemal complexes from DNase-treated rat pachytene chromosomes contain (GT)_n and LINE/SINE sequences. *Genetics*. 130: 865–872.

- Pellestor, F., Anahory, T. and Hamamah, S. (2005). Effect of maternal age on the frequency of cytogenetic abnormalities in human oocytes. *Cytogenetic and genome research*. 111: 206–212.
- Phetudomsinsuk, K., Sirinarumitr, K., Laikul, A. and Pinyopummin, A. (2008). Morphology and head morphometric characters of sperm in Thai native crossbred stallions. *Acta Veterinaria Scandinavica*. 50: 1–9.
- Pillips, C.M. and Dernburg, A.F. (2006). A family of zinc-finger proteins is required for chromosome-specific pairing and synapsis during meiosis in *C. elegans*. *Developmental Cell*. 11: 817–829.
- Prolla, T.A., Pang, Q., Alani, E., Kolodner, R.D., and Liskay, R.M. (1994). MLH1, PMS1, and MSH2 interactions during the initiation of DNA mismatch repair in yeast. *Science*. 265: 1091–1093.
- Pycock, J.F. (2010). Fertility, infertility in the stallion and AI. Equine Reproductive Services. (<http://www.ul.ie/~equines/Laboratory%207.htm>) 1–7
- Ramalho-Santos, J., Amaral, A., Sousa, A.P., Rodrigues, A.S., Martins, L., Baptista, M., Mota, P.C., Tavares, R., Amaral, S. and Gamboa, S. (2007). Probing the structure and function of mammalian sperm using optical and fluorescence microscopy. *Modern Research and Educational Topics in Microscopy*: 394–402.
- Rappold, G.A. (1993). The pseudoautosomal regions of the human sex chromosomes. *Human Genetics*. 92: 315–324.
- Rockmill, B., Sym, M., Scherthan, H., and Roeder, G.S. (1995). Roles for two RecA homologs in promoting meiotic chromosome synapsis. *Genes and Development*. 9: 2684–2695.
- Roeder, G.S. (1997). Meiotic Chromosomes: It Takes Two to Tango. *Genes and Development*. 11: 2600–2621.
- Ross, L.O., Maxfield, R., and Dawson, D. (1996). Exchanges are not equally able to enhance meiotic chromosome segregation in yeast *Proceeding the National Academy of Sciences of the USA*. 93: 4979–4983.
- Roth, L.E. (1960). Observations on cells of the Ovotestis of a Pulmonate Snail. Springer-Verlag. pp 238–241
- Russell, N. (2007). Like Engend'ring like: Heredity and Animal Breeding in Early Modern England. Cambridge University Press. pp 58–111

- Saadallah, N. and Hultèn, M. (1983). Chiasma distribution, genetic lengths, and recombination fractions: a comparison between chromosomes 15 and 16. *Journal of Medical Genetics*. 20: 290–299.
- Samper, J. (2009). Equine breeding management and artificial insemination. Saunders Elsevier. pp 47–74
- Scherthan, H., Bähler J. and Kohli J. (1994). Dynamics of chromosome organization and pairing during meiotic prophase in fission yeast. *Cell Biology*. 127: 273–285.
- Scherthan, H., Weich, S., Schwegler, H., Heyting, C., Harle, M., and Cremer, T. (1996). Centromere and telomere movements during early meiotic prophase of mouse and man are associated with the onset of chromosome pairing. *Journal of Cell Biology*. 134: 1109–1125.
- Schwacha, A. and Kleckner, N. (1994). Identification of joint molecules that form frequently between homologs but rarely between sister chromatids during yeast meiosis. *Cell*. 76: 51–63.
- Schwacha, A. and Kleckner, N. (1997). Interhomolog bias during meiotic recombination: Meiotic functions promote a highly differentiated interhomolog-only pathway. *Cell*. 90(6):1123–1135.
- Schwazacher, T. (2003). Meiosis, recombination and chromosomes: a review of gene isolation and fluorescent in situ hybridization data in plants. *Journal of Experimental Botany*. 54 (380): 11–23.
- Scott, I.S. and Long, S.E. (1980). An examination of chromosomes in stallion (*Equus caballus*) during meiosis. *Cytogenetic and Cell Genetics*. 26: 7–13.
- Segatelli, T.M., Franc, L.R., Pinheiro, P.F., Almeida, C.C, Martinz, M. and Martinez, A.E. (2004). Spermatogenic cycle length and spermatogenic efficiency in Gerbil (*Meriones unguiculatus*). *Journal of Andrology*. 25 (6): 872–880
- Seshagiri, P.B. (2001). Molecular insights into the causes of male infertility. *Journal of Biosciences*. 26: 429–435.
- Sharples, G.J. and Leach, D.R.F. (1995). Structural and functional similarities between the SbcCD proteins of *Escherichia coli* and the RAD50 and MRE11 (RAD32) recombination and repair proteins of yeast. *Molecular Microbiology*. 17: 1215–1217.

- Shinohara, A., Ogawa, H., and Ogawa, T. (1992). Rad51 protein involved in repair and recombination in *S. cerevisiae* is a RecA-like protein. *Cell*. 69: 457–470.
- Siderakis, M. and Tarsounas, M. (2007). Telomere regulation and function during meiosis. *Chromosome Research*. 15: 667–679.
- Smith, A.V. and Roeder, G.S. (1997). The yeast Red1 protein localizes to the cores of meiotic chromosomes. *Journal of Cell Biology*. 136: 957–967.
- Smith, K.N. and Nicolas, A. (1998). Recombination at Work for Meiosis. *Current Opinion in Genetics and Development*. 8: 200–211.
- Sotelo, J.R. and Trujillo-Cenòz, O.T. (1958). Submicroscopic structure of meiotic chromosomes during prophase. *Experimental Cell Research*. 14: 1–8.
- Speed, R.M. (1988). The possible role of meiotic pairing anomalies in the atresia of human fetal oocytes. *Human Genetics*. 78: 260–266.
- Stack, S. and Anderson, L. (1986). Two-dimensional spreads of synaptonemal complexes from solanaceous plants. III. Recombination nodules and crossing over in *Lycopersicon esculentum* (tomato). *Chromosoma*. 94: 253–258.
- Sukardi, S., Curry, M.R. and Watson, P.F. (1997). Simultaneous detection of acrosomal status and viability of incubated ram spermatozoa using fluorescent markers. *Animal Reproduction Science*. 46: 89–96.
- Sun, F., Oliver-Bonet, M., Liehr, T., Stark, H., Ko, E., Rademaker, A., Navarro, J., Benet, J., and Martin, R.H. (2004). Human Male Recombination Maps for Individual Chromosomes. *American Journal of Genetics*. 74: 521–531.
- Sun, F., Oliver-Bonet, M., Liehr, T., Starke, H., Turek, P., Ko, E., Rademaker, A. and Martin R.H. (2006). Variation in MLH1 distribution in recombination maps for individual chromosomes from human males. *Human Molecular Genetics*. 15(15): 2376–2391.
- Sung, P. (1997). Yeast Rad55 and Rad57 proteins form a heterodimer that functions with replication protein A to promote DNA strand exchange by Rad51 recombinase. *Genes and Development*. 11: 1111–1121.
- Swierstra, E.E., Pickett, B.W. and Gebauer, M.R. (1975). Spermatogenesis and Duration of Transit Spermatozoa Through the Excurrent ducts of Stallions. *Journal of Reproduction and Fertility. Suppl.* 23: 53–57.
- Swinburne, J.E., Bournsnel, M., Hill, G., Pettitt, L., Allen, T., Chowdhary, B., Hasegawa, T., Kurosawa, M., Leeb, T., Mashima, S., Mickelson, J.R.,

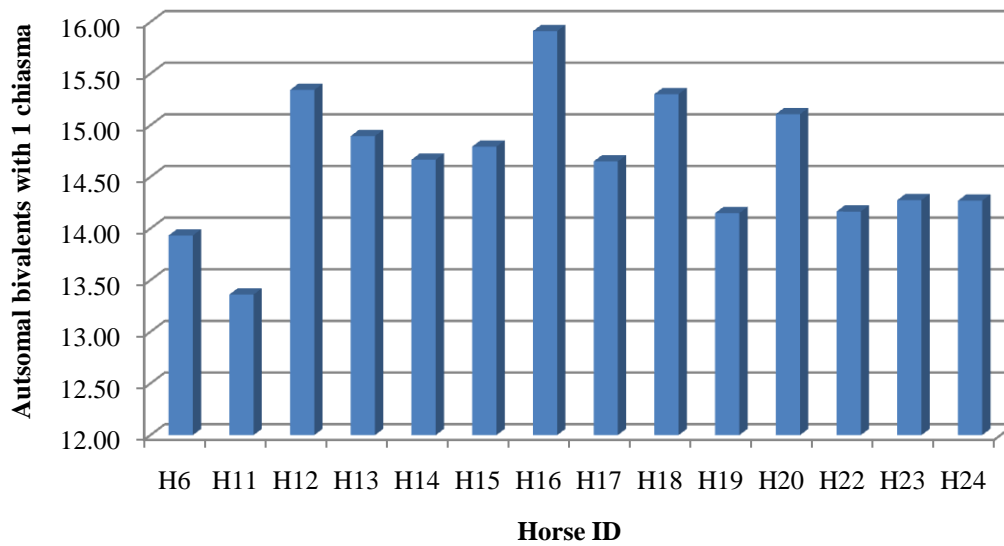
- Raudsepp, T., Tozaki, T. and Binns, M. (2006). Single linkage group per chromosome genetic linkage map for the horse, based on two three-generation, full-sibling, crossbred horse reference families. *Genomics*. 87: 1–29.
- Sybenga, J. (1996). Recombination and chiasmata: few but intriguing discrepancies. *Genome*. 39: 473–484.
- Sybenga, J. (1999). What makes homologous chromosomes find each other in meiosis? A review and hypothesis. *Chromosoma*. 108: 209–219.
- Sym, M., Engebrecht, J., and Roeder, G.S. (1993). ZIP1 is a synaptonemal complex protein required for meiotic chromosome synapsis. *Cell*. 72: 365–378.
- Sym, M. and Roeder, G.S. (1994). Crossover interference is abolished in the absence of a synaptonemal complex protein. *Cell*. 79: 283–292.
- Tapper, W.J., Ke, X., Morton, N.E. and Collins, A. (2002). Recombination, Interference and Sequence: Comparison of Chromosomes 21 and 22. *Annals of Human Genetics*. 66:75–86
- Tavassoli, M., Shayeghi, M., Nasium, A., and Watts, F.Z. (1995). Cloning and characterization of the *Schizosaccharomyces pombe rad32* gene: A gene required for repair of doublestrand breaks and recombination. *Nucleic Acids Research*. 23: 383–388.
- Tease, C., Hartshorne, G., Hultèn, M. (2002). Patterns of Meiotic Recombination in Human Fetal Oocytes. *American Journal of Human Genetics*. 70:1469–1479.
- Tease, C. and Hultèn, M. (2004). Inter-sex variation in synaptonemal complex length largely determine the different recombination rates in male and female germ cells. *Cytogenetic and Genome Research*. 107: 208-215
- Theurkauf, W.E. and Hawley, R.S. (1992). Meiotic spindle assembly in *Drosophila* females: Behavior of nonexchange chromosomes and the effects of mutations in the *nod* kinesinlike protein. *Journal of Cell Biology*. 116: 1167–1180.
- Thomas, H.S. (2001). Infertility in Stallions: Evaluation of semen and sperm. *Horse Care*. (<http://archive.ctba.com/01magazine/aug01/thomas.pdf>). 118–119.
- Thomas, S.E., Soltani-Bejnood, M., Roth, P., Dorn, P., Logsdon, J.J.M. and McKee, B.D. (2005). *Cell*. 123: 555–568.
- Trelles-Sticken, E., Dresser, M.E. and Scherthan, H. (2000). Meiotic telomere protein Ndj1p is required for meiosis-specific telomere distribution, bouquet formation and efficient homologue pairing. *Journal of Cell Biology*. 151: 95–106.

- Tsubouchi, T. and Roeder, G.S. (2005). A synaptonemal complex protein promotes homology-independent centromere coupling. *Science*. 308(5723): 870–873.
- Tsubouchi, T., Zhao, H. and Roeder, G.S. (2006). The meiosis-specific Zip4 protein regulates crossover distribution by promoting synaptonemal complex formation together with Zip2. *Developmental Cell*. 10: 809–819.
- Turner, J.M., Aprelikova, O., Xu X., Wang, R., Kim, S., Chandramouli, G.V.R., Barrett, J.C., Burgoyne, P.S. and Deng, C. (2004). BRCA1, Histone H2AX phosphorylation, and male meiotic sex chromosome inactivation. *Current Biology*. 14: 2135–2142.
- Turner, J.M.A. (2007). Meiosis 2007-Where have we got to and where are we going? *Chromosome Research*. 15: 517–521.
- Uhlmann, F. (2001). Chromosome Cohesion and Segregation in Mitosis and Meiosis. *Current Opinion in Cell Biology*. 13: 754–761.
- van der Heijden, G.W., Derijck, A.A., Pósfai, E., Giele, M., Pelczar, P., Ramos, L., Wansink, D.G., van der Vlag, J., Peters, A.H, and de Boer, P. (2007). Chromosome-wide nucleosome replacement and H3.3 incorporation during mammalian meiotic sex chromosome inactivation. *Nature Genetics*. 39(2): 251–258.
- Varner, D.D., Schumacher, J., Blanchard, T.L. and Johnson, L. (1991). Management of the breeding stallion. In: Prat, P.W., Thornwood, D.R. (Eds.), *Diseases and Management of Breeding Stallions*. American Veterinary Publications, Goleta, CA, Chapter 3, pp. 97–115.
- Villagómez, D.A.F. and Pinton, A. (2008). Chromosomal abnormalities, meiotic behavior and fertility in domestic animals. *Cytogenetic and Genome Research*. 120: 69–80.
- Vincent, J.E. and Jones, G.H. (1993). Meiosis in autopolyploid *Crepis capillaris*. *Chromosoma*. 102: 195–206.
- von Wettstein, D., Rasmussen, S.W. and Holm, P.B. (1984). The Synaptonemal Complex in Genetic Segregation. *Annual Review of Genetics*. 18: 331–413.
- Weiner, B.M. and Kleckner, N. (1994). Chromosome Pairing Via Multiple Interstitial Interactions Before and During Meiosis in Yeast. *Cell*. 77: 977–991

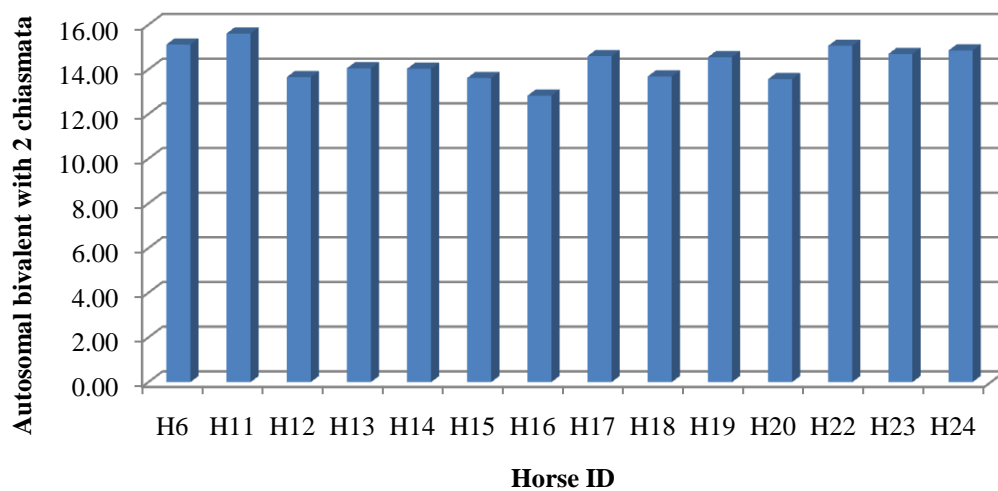
- White, M.A., Detloff, P., Strand, M., and Petes, T.D. (1992). A promoter deletion reduces the rate of mitotic, but not meiotic, recombination at the *HIS4* locus in yeast. *Current Genetics*. 21: 109–116.
- Willard, H.F. (1985). Chromosome specific organization of human alpha satellite DNA. *American Journal of Human Genetics*. 37: 524–532.
- Wolfe, S.A. and Grimes, S.R. (1999). Binding of Nuclear Proteins to an Upstream Element Involved in Transcriptional Regulation of the Testis-Specific Histone H1t gene. *Journal of Cellular Biochemistry*. 75: 555–565.
- Wolgemuth, D.J., Laurion, E. and Lele, K.M. (2002). Regulation of the Mitotic and Meiotic Cell Cycles in the Male Germ Line. *Recent Progress in Hormone Research*. 57: 75–101.
- Wright, W.E., Piatyszek, M.A., Rainey, W.E., Byrd, W. and Shay, J.W. (1996). Telomerase activity in human germline and embryonic tissues and cells. *Developmental Genetics*. 18: 173–179.
- Xu, L. and Kleckner, N. (1995). Sequence non-specific doublestrand breaks and interhomolog interactions prior to doublestrand break formation at a meiotic recombination hot spot in yeast. *EMBO Journal*. 14: 5115–5128.
- Zakian, V. (1995). Telomeres: beginning to understand the end. *Science*. 270: 1601–1607.
- Zetka, M. and Rose, A. (1995). The genetics of meiosis in *Caenorhabditis elegans*. *Trends in Genetics*. 11: 27–31.

Appendices

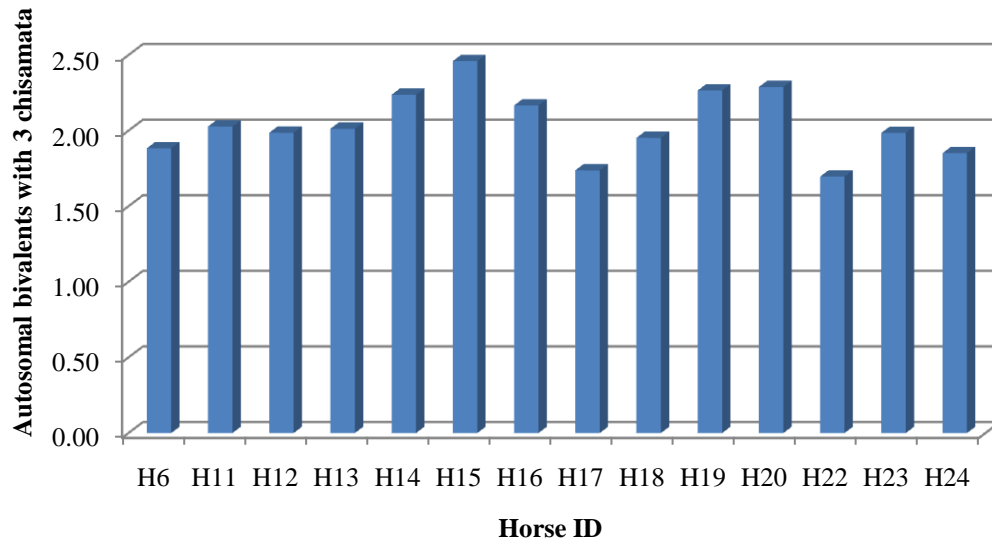
Appendix 1: Mean autosoma bivalents with 1 chiasma among 14 stallions



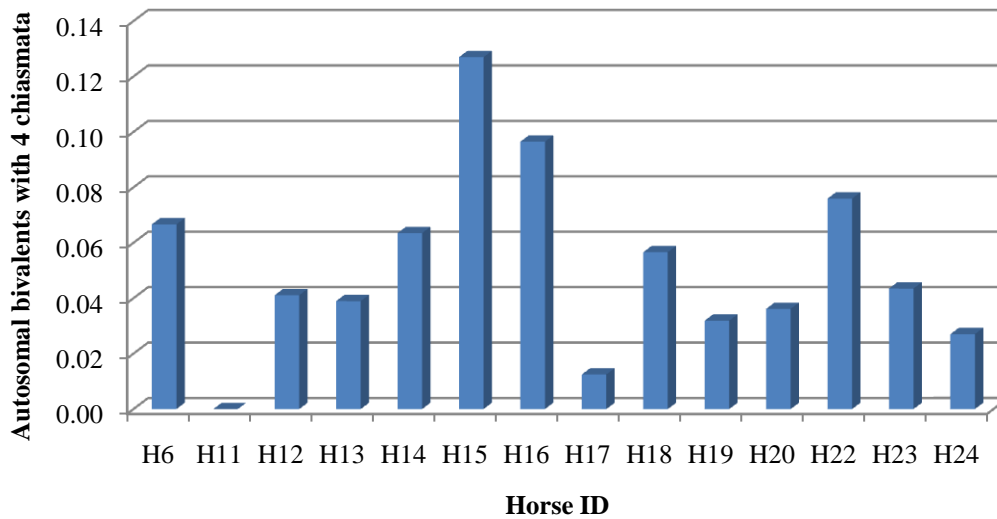
Appendix 2: Mean autosoma bivalents with 2 chiasmata among 14 stallions



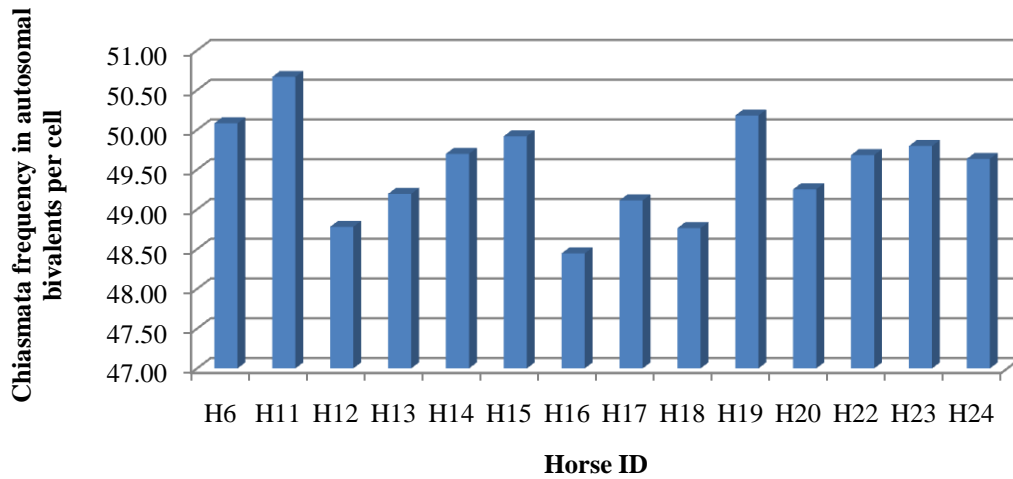
Appendix 3: Mean autosoma bivalents with 3 chiasmata among 14 stallions



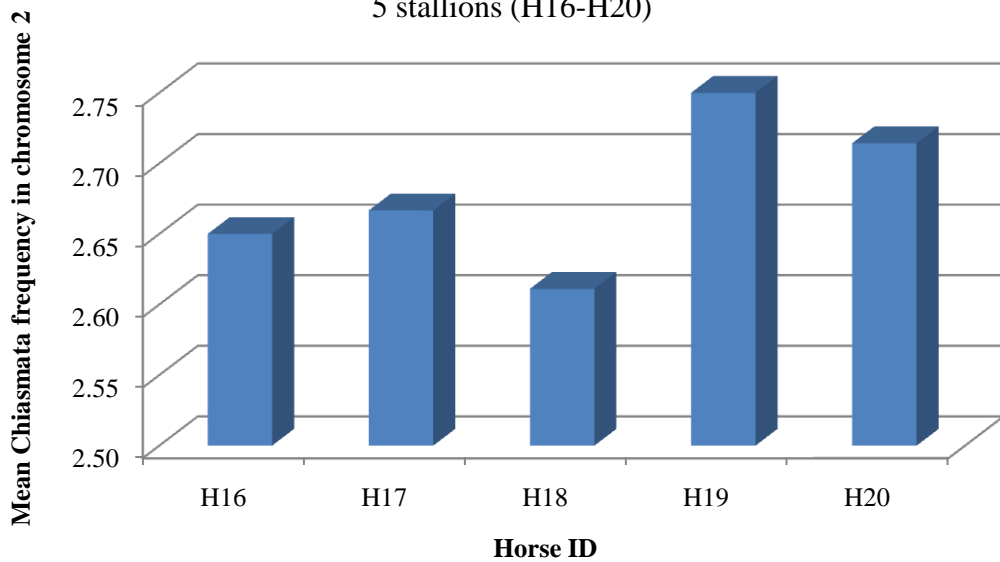
Appendix 4: Mean autosoma bivalents with 4 chiasma among 14 stallions



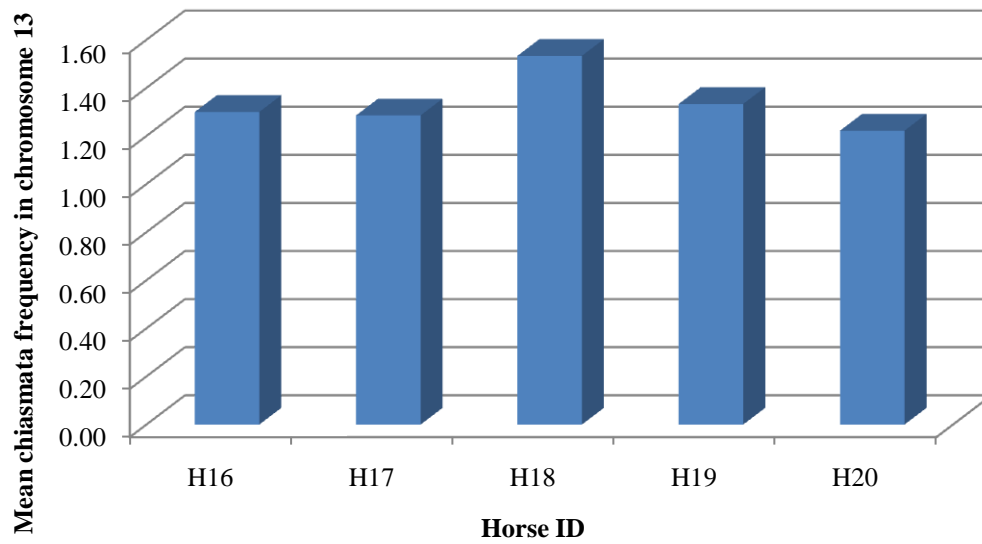
Appendix 5: Chiasmata Frequency in autosomal bivalents per cell among 14 Stallions



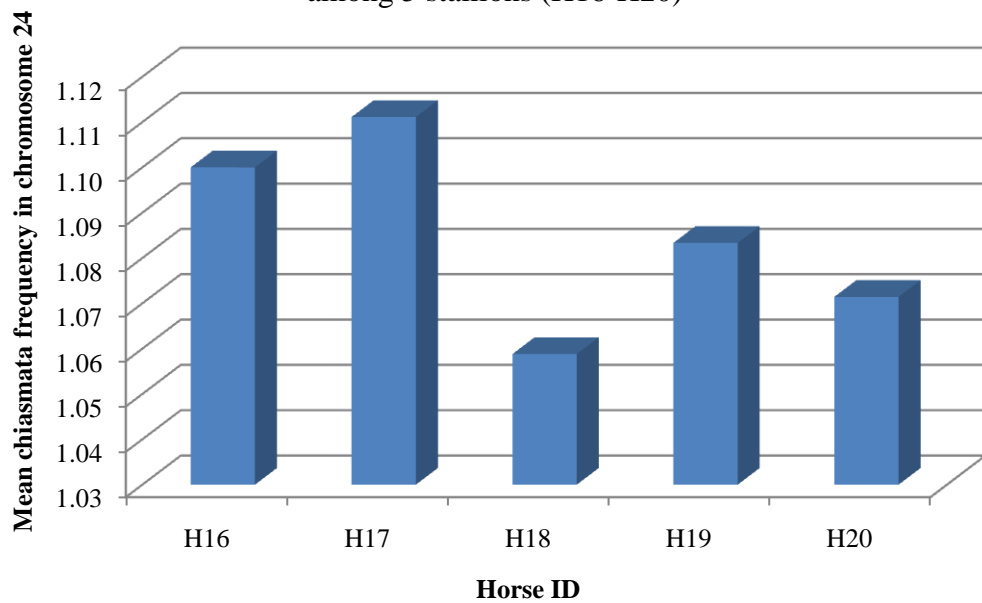
Appendix 6: Mean chiasmata frequency in chromosome 2 among 5 stallions (H16-H20)



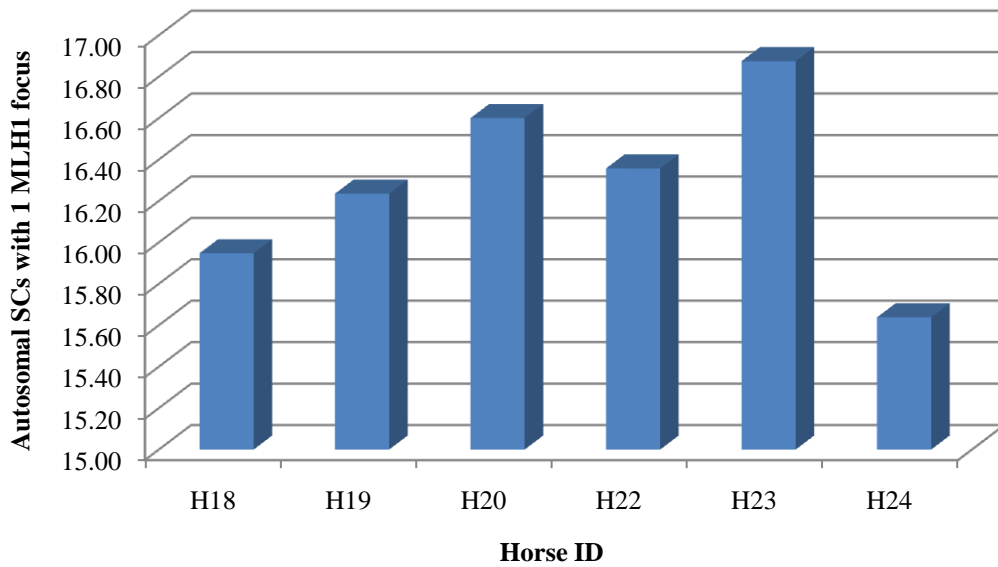
Appendix 7: Mean chiasmata frequency in chromosome 13 among 5 stallions (H16-H20)



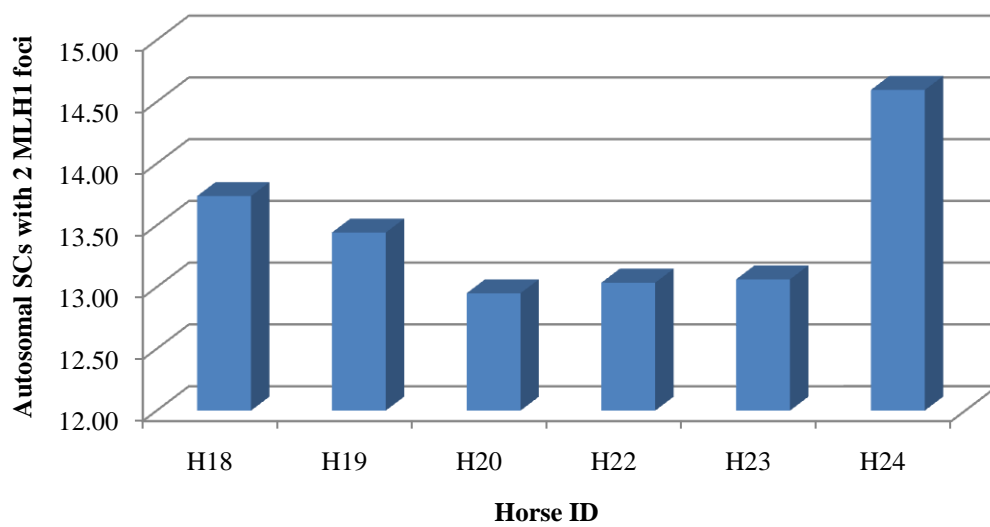
Appendix 8: Mean chiasmata frequency in chromosome 24 among 5 stallions (H16-H20)



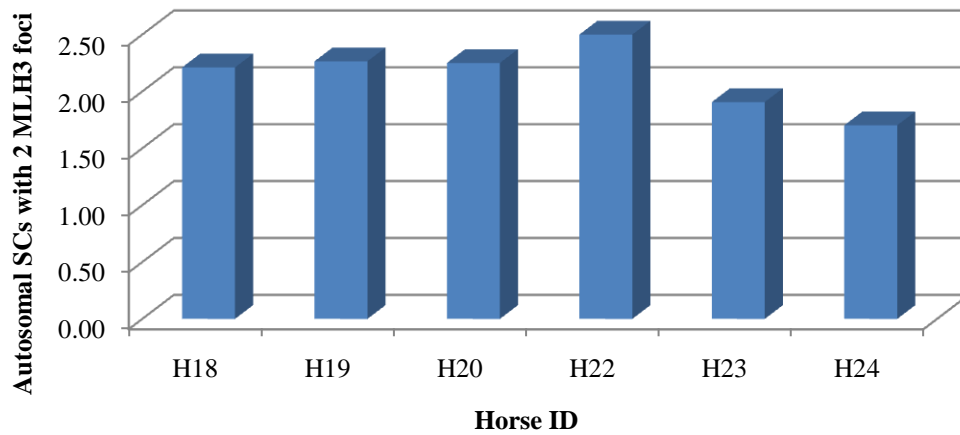
Appendix 9: Mean autosomal SCs with 1 MLH focus among 6 stallions (n=180)



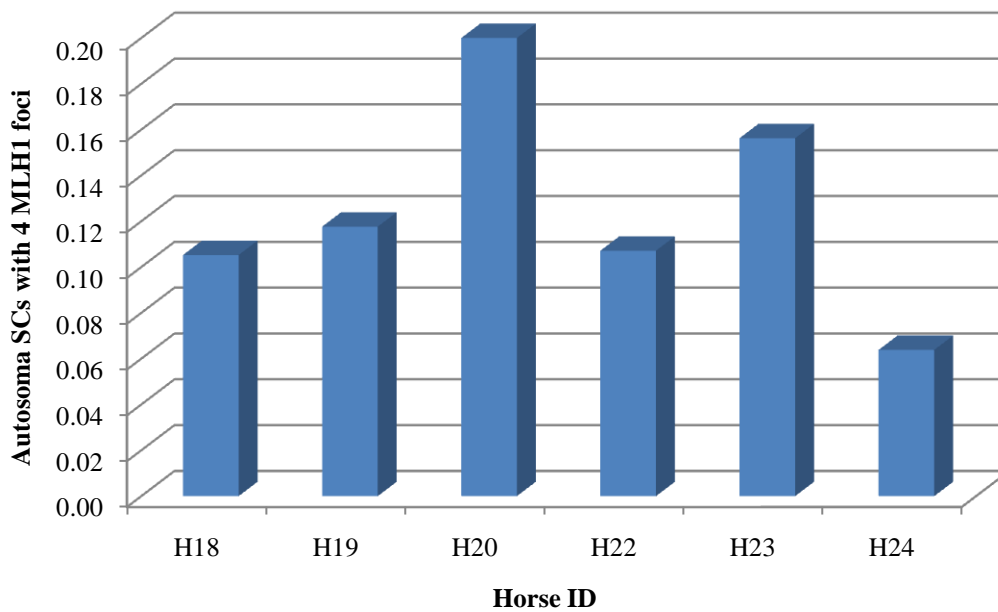
Appendix10: Mean autosomal SCs with 2 MLH foci among 6 stallions (n=180)



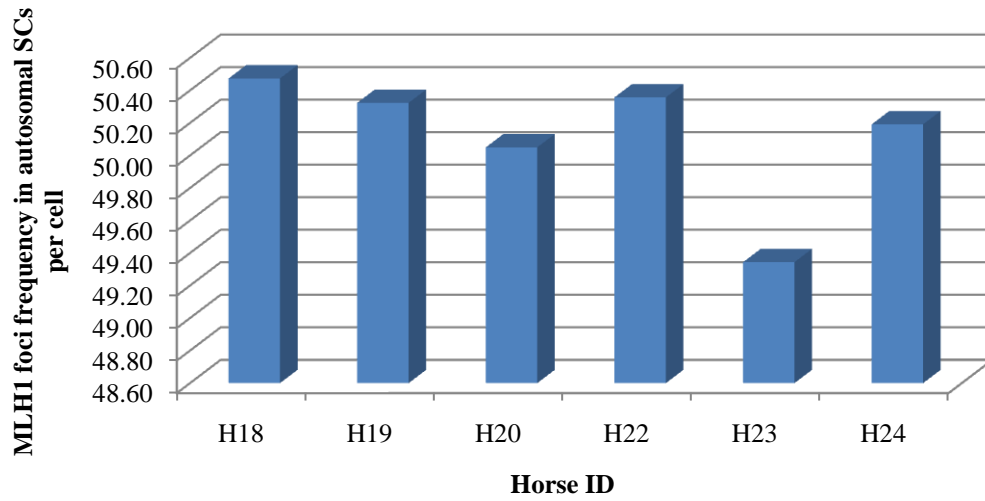
Appendix 11: Mean autosomal SCs with 3 MLH foci among 6 stallions (n=180)



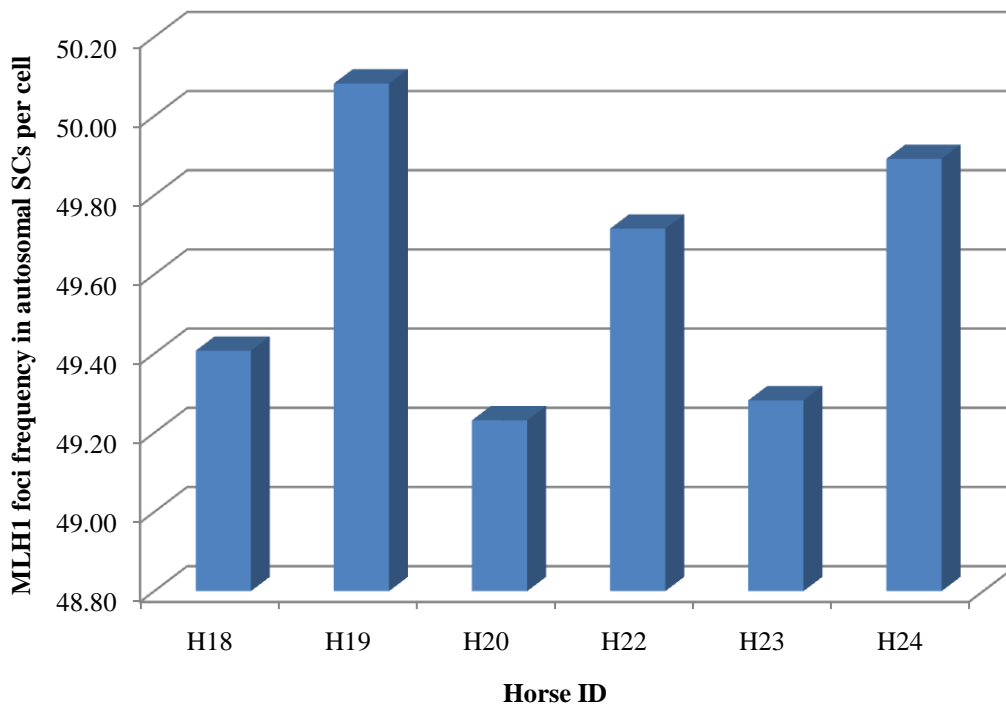
Appendix 12: Mean autosomal SCs with 4 MLH foci among 6 stallions (n=180)



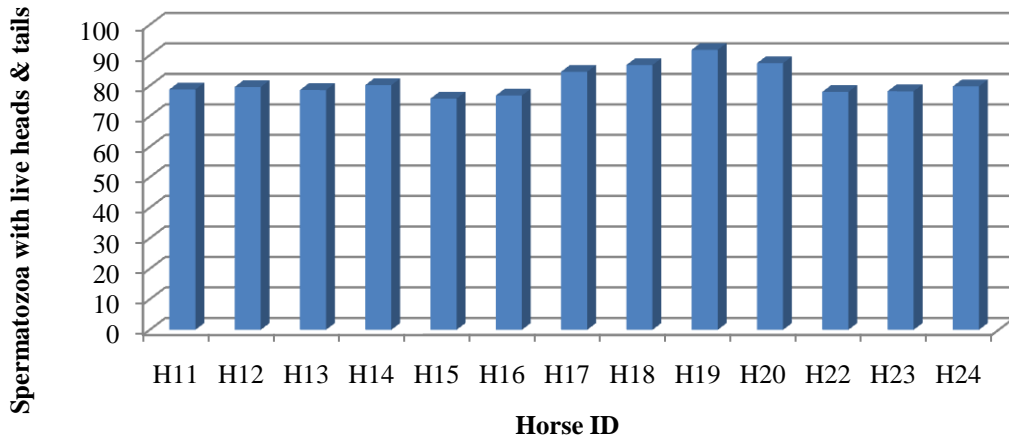
Appendix 13: MLH1 foci frequency in autosomal SCs per cell among 6 stallions (n=180)



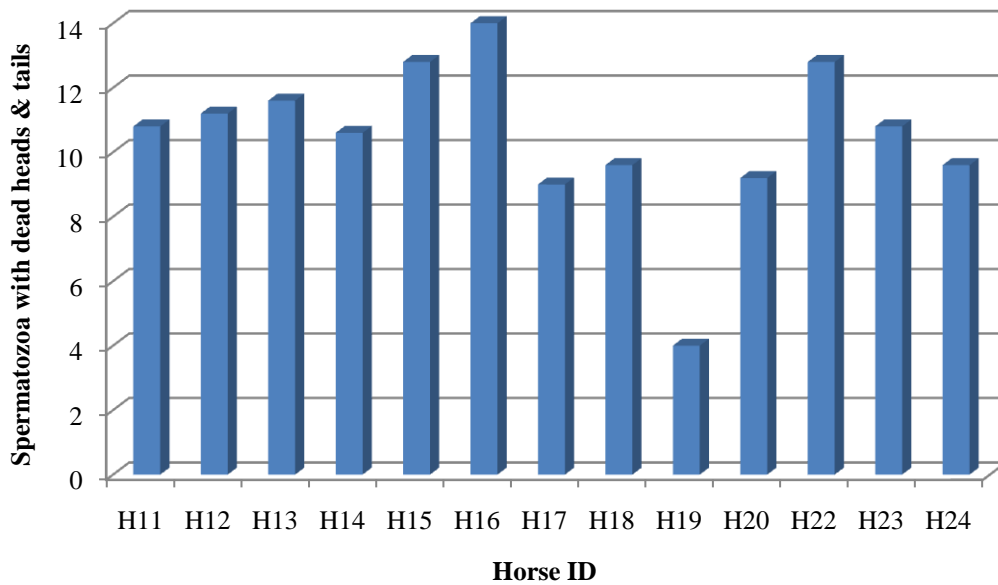
Appendix 14: MLH1 foci frequency in autosomal SCs per cell among 6 stallions (n=523)



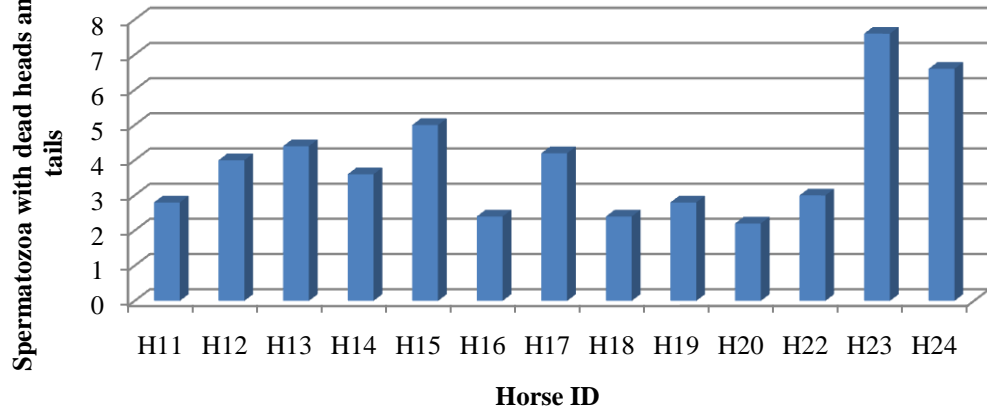
Appendix 15: Mean of spermatozoa with live heads and tails among 13 stallions (n=6500)



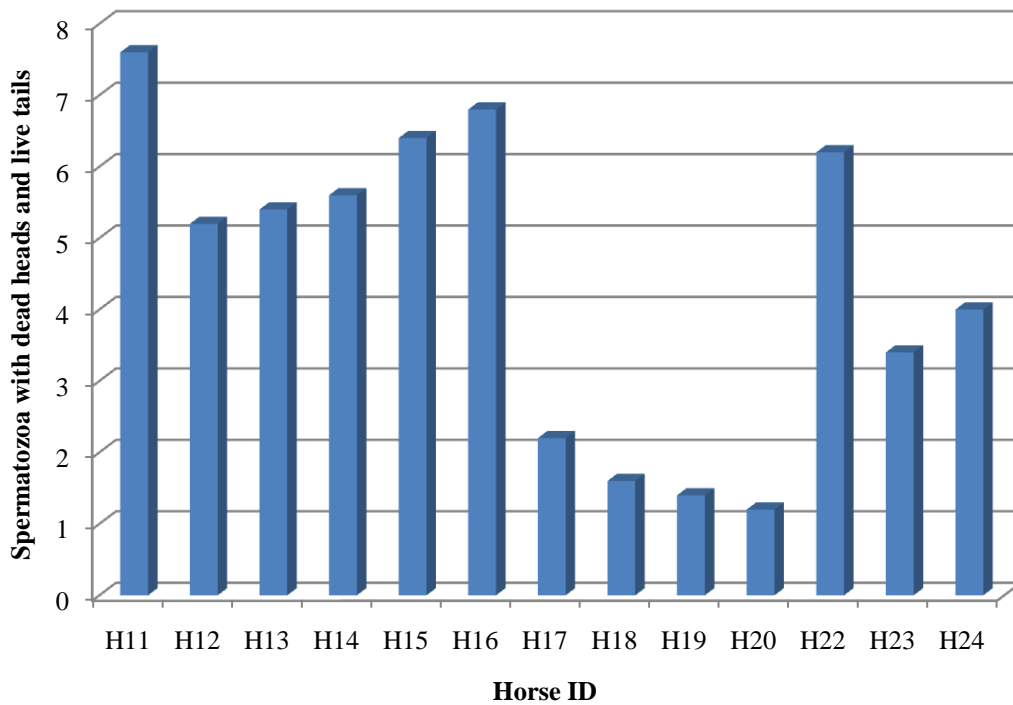
Appendix 16: Mean of Spermatozoa with dead heads and tails among 13 stallions (n=6500)



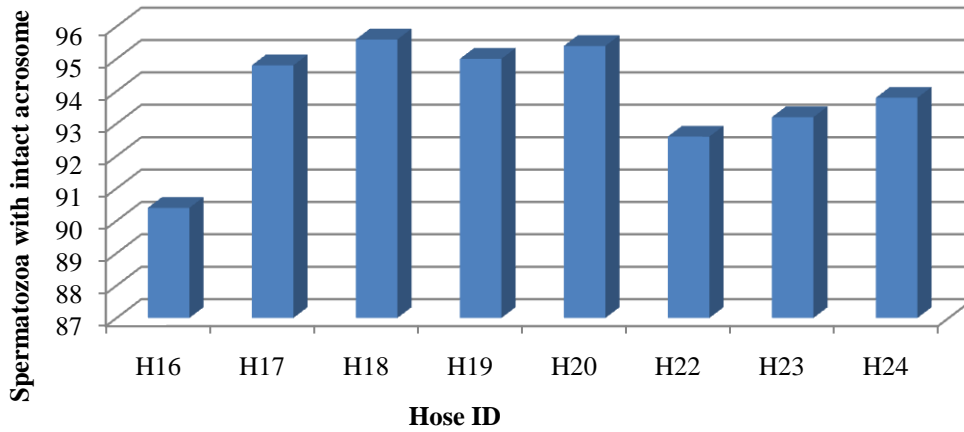
Appendix 17: Mean of spermatozoa with dead heads and live tails among 13 stallions (n=6500)



Appendix 18: Mean of spermatozoa with dead tails and live heads among 13 stallions (n=6500)



Appendix 19: Mean of spermatozoa with intact acrosome among 8 stallions (n=4000)



Appendix 20: Mean of spermatozoa with functional mitochondria among 8 stallions (n=4000)

